Republic of Iraq
Ministry of Higher Education
& Scientific Research University
of Kerbala/College of Science
Department of Chemistry

Preparation and Characterization of Ni/Al Nanohybrid with Folic Acid and Suggestion Equations to Evaluate the Diffusion of the Active Agent

A Thesis

Submitted to the Council of the College of Science-University of Kerbala as Partial Fulfillment of the Requirements of the Degree of Master of Science in Chemistry

By

Mohammed Adnan Mezaal
B.Sc. in Chemistry 2009 Kerbala University

Supervised by

Prof. Dr. Salih Mahdi Haddawi

Assistant Prof. Dr. Abass Matrood bashi

1433 A. H. *2012 A. D.*

Dedication

To my dear mother, who has spared no effort to raise me and guide me
I present this work.

To raison d'être... My beloved father's

You all the respect and Transfiguration

Mohammed

Acknowledgments

Firstly in the name of Allah SWT, The Most Merciful and Most compassionate, thanks to Allah SWT for the strength he gave to me in completing my project. The work I have completed this semester towards this fulfillment of the requirements for the Degree of Master of Sciences of Chemistry would not have been possible without the assistance of the various people and I would like to express my thanks to all those who offered advice, gave encouragement or shared some of their knowledge.

I would like to express my sincere thanks and my appreciation to my supervisors Prof. Dr. **Salih Mahdi Haddawi** and Dr. **Abass Matrood Bashi** for their kind interest, encouragement and guidance throughout the course of this work. Also my deep grateful thanks to Prof. Dr. **Lixu Lei** continuous help and faithful support and advice during my study.

Also my grateful thanks are extended to the staff members of the College of science/department of Chemistry/Kerbala University. I would like to thank the staff members of the School of Chemistry and Chemical Engineering, Southeast University (**China**).

With affection and deep appreciation I acknowledge my indebtedness to my wonderful family: parents, brother and sister for their patience, support and enthusiastic encouragement during doing the research.

Mohammed

Certification

We certify that, this thesis was prepared under our supervision at the Department of Chemistry, College of Science, and University of Kerbala in partial requirements for the **Degree of Master in Chemistry**.

Signature:

Supervisor: Dr. Salih Mahdi Haddawi

Professor

Date: / / 2012

Signature:

Supervisor: Dr. Abass Matrood Bashi

Assistant Professor

Date: / / 2012

In view of the available recommendations. I forward this thesis for debate by the examining committee.

Signature:

Dr. Ashour Haommoud

Assistant Professor

Head of the Chemistry Department

Date: / /2012

Examination Committee Certificate

We, the examination committee, after reading this thesis and examining the student **Mohammed Adnan Mezaal**, in its content, have found that it meets the standard and requirements as a thesis in fulfilling for the Degree of MSc. in Chemistry. Date / / 2012.

(Chairman(

Signature:

Name: Dr. Falah Hasan Hussein

Title: Professor

Address: Department of Chemistry,

College of Science, University of Babylon.

Date: / / 2012

(Member)

Signature:

Name: Dr. Musa Imran

Title: Assistant Professor

Address: Department of Chemistry,

College of Education for Girls, University of Kufa.

Date: / / 2012

.

(Member)

Signature:

Name: Dr. Iman Talib Kareem

Title: Assistant Professor

Address: Department of Chemistry,
College of Science, University of Kerbala.

Date: / / 2012

(Member& Supervisor)

Signature:

Name: Dr. Salih Mahdi Hadawi

Title: Professor

Address: Department of Chemistry,
College of Science, University of Kerbala.

Date: / / 2012

(Member& Supervisor)

Signature:

Name: Dr. Abass M. Bashi

Title: Assistant Professor

Address: College of Applied Medical Sciences, University of Kerbala.

Date: / / 2012

Approved by the council of the college of science in it's session No. in / /2012

Signature:

Name: Dr. Ahmed Mahmood

Title: Professor

Address: Dean of the College of Science, University of Kerbala.

Date: / / 2012

Report of Linguistic Evaluator

I certify that the linguistic evaluation of this thesis was carried out by me and it is accepted linguistically and in expression.

Signature:

Name: Dr. Sabah Wajid Ali

Title: Assistant Professor

Address: Kerbala University, College of Education for Humanity Studies, Department of the English Language

Date: / / 2012

Report of Scientific Evaluator

I certify that the scientific evaluation of this thesis was carried out by me and it is accepted scientifically.

Signature:

Name: Dr. Hameda Edan Salman

Title: Assistant Professor

Address: Kerbala University, College of Education for Pure Sciences, Department of Chemistry.

Date: / / 2012

Summary

For fully controlled drug release, it is important to understand the microstructure and nature of the layered double hydroxide that ultimately controls drug release properties. Ni/Al-Folic acid-Layered double hydroxide with the molar ratio of (R = 3, 4, 5 and 6) were prepared by two different approaches by direct (co-precipitation) and indirect of an ion-exchange method from aqueous solution by hydrothermal treatment for the formation of new nanohybrid compound as reported.

Layered double hydroxides of nickel and aluminum compounds were prepared under the hydrothermal treatment at 70, 120 and 180˚C. Characterization of LDH using X-Ray Diffractogram showed the presence of sharp and intense peaks with the d-spacing 7.9 Å which signify high crystallinity at 180˚C and it is regarded as the most convenient at this temperature degree. While, the XRD pattern of Folic acid-LDH showed the presence of sharp and intense peaks with the d-spacing 17.3 Å.

The comparison of the FTIR spectra of FA together with Ni-Al-NO_3-LDH and Ni-Al-FA-LDH reveals that the FTIR absorption bands for the nanocomposite resemble a mixture of the FA and LDH absorption characteristics, which indicates that the FA was successfully intercalated into the Ni-Al interlayer.

The release of Folic acid (FA) from the nanohybrid into the release media wasaccomplished using various aqueous solutions: carbonate, phosphate and sulphate. It is observed that carbonate dominated the accumulated release percentage.

Release kinetics of FA has been evaluated with various models such as zeroth order, first order and pseudo-second order as well as Bhaskar equation. It is observed that the release profiles of FA were governed by pseudo-second order.

Additionally, in this study, novel equations were innovated that were used for predicting the diffusion of guest anion through LDHs nanohybrid particles and applied it for the folic acid released. These equations were more suitable for diffusion than the previous equations like Bhaskar equation and it is the most convenient.

An Artificial Neural Network (ANN) based on the Quick Propagation (QP) algorithm was used in this study to predict the concentration of folic acid released (Ct) at the time t.

Contents

List of Tables

List of Figures

1. Introduction

1.1. Nanotechnology

Nanotechnology is almost a household word now-a-days, or at least some word with „„nano"" in it, such as nanoscale, nanoparticle, nanomaterials, nanophase, nanocrystal, or nanomachine [1]. In the past few years nanotechnology has grown by leaps and bounds, and this multidisciplinary scientific field is undergoing explosive development and considered as a key technology of molecular or atomic engineering that might have the potential to produce sweeping changes to almost all aspects of human society beyond the scope of conventional technologies [2]. Today, more than 60 countries have started national nanotechnology programs to explore ways to create novel re-engineered nanomaterials in areas as diverse as healthcare, energy efficiency, agriculture, environmental protection, and security [3].

According to the United States National Nanotechnology Initiative, Nanotechnology can be defined as the science and engineering involved in the design, synthesis, characterization and application of materials and devices whose smallest functional organization in at least one dimension is on the nanometer scale. [4,5], or it can be defined as (i) research and technology at the atomic, molecular or macromolecular levels, i.e. a length scale below 100 nm; (ii) creating and employing structures, devices and systems with novel properties and functions, (iii) the possibility to control and manipulate on the atomic scale, the purpose is the precise structurization for the production of extremely small devices or structures with prescribed properties. [6]. Nanotechnology, a field of applied science and technology, covers a broad range of topics and encompasses a variety of subjects such as biology, chemistry and physics. In a word, nanotechnology deals with nanoscale materials which are also called nanomaterials.

1.2. Nanomaterials

Nanomaterials used to describe materials with one or more components that have at least one dimension in the range of 1 to 100 nm [8]. The prefix “nano” derives from the (Greek:dwarf) [4,5].

Nanomaterials can be classified into nanocrystalline materials and nanoparticles. The former are polycrystalline bulk materials with grain sizes in the nanometer range, while the latter refers to ultrafine dispersive particles with diameters below 100 nm [9]. Nanomaterials differ significantly from the bulk materials by virtue of their small size. Where, the physical, chemical and biological properties of nanomaterials differ in fundamental and important ways from properties of individual atoms, molecules or larger sized bulk material [10].

In fact, the properties of materials can be different at the nanoscale for two main reasons. Firstly, nanomaterials have a relatively larger surface area when compared to the same mass of material produced in a larger form; in nanocrystalline solids, a large fraction of atoms (up to 49%) are boundary atoms [11]. It is attributable to the change of the bonding state of the atoms or the molecules constructing the particles. For example, as shown in “Figure 1” Imagine a chunk of metal with a side length of 1 cm is divided into a cube of 1μm, the particle number increases to 10^{12} and being divided into the one of 10 nm, then it amounts to 10^{18}, but when added together they make up the same amount of metal material that you started with. Where, the fraction of the atoms or the molecules located at the surface on the particles plays a great role, since they are more active than those inside the solid particles because of the free hand, which leads to easy bonding with the contacting materials and causes various changes in particle properties [12].

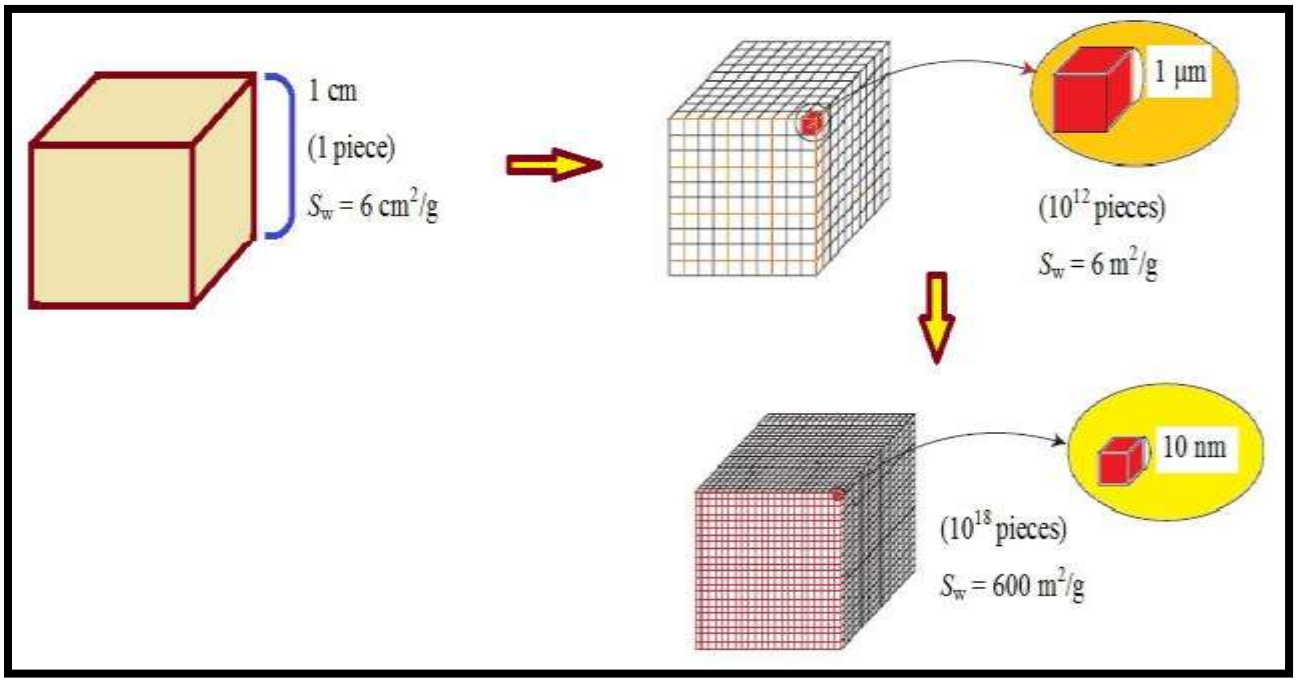

Figure 1. Change of specific surface area by miniaturization of a solid cube assuming the solid density of 1 g/cm3.

Secondly, the relative importance of physical laws shifts and quantum effects start to become more significant, especially for sizes less than 20 nm and begin to dominate the behavior of matter at the nanoscale particularly at the lower end affecting the optical, electrical and magnetic behavior of materials [11].

The advantages of nanomaterials are the large surface area/volume ratio exhibited by them, leading to a very high surface reactivity with the surrounding surface, ideal for catalysis or sensor applications, and the ability of varying their fundamental properties (e.g., magnetization, optical properties (color), melting point, hardness, etc.), relative to bulk materials without a change in chemical composition and the interface structure will plays an important role in determining the physical and mechanical properties of nanocrystalline materials [13]. In addition, Nanomaterials considered as the building blocks of nanotechnology, possess important physical properties such as particle aggregation, photoemission, electrical, increased strength,

solubility, heat conductivities, superior mechanical and chemical properties [14,15]. Such materials can be used for new applications in areas like information and communication technology, power engineering, industrial engineering, environmental engineering, chemical industry like (electronics, catalysis, ceramics, magnetic data storage, high current electrode materials for fuel cells, batteries, electrochromic displays, water, food and materials with new surface properties for paints, coatings for self-cleaning windows, stain-resistant textiles etc). Additionally, applications of nanotechnologies in medicine are especially promising, and areas such as disease diagnosis, drug delivery targeted at specific sites in the body and molecular imaging are being intensively investigated and some products are undergoing clinical trials [16,17].

1.3. Nanoparticles

Particles are considered to be nanoparticles if one of their dimensions is less than 100 nanometers (nm) across [18]. These particles are important to science and technology, as they are essentially a bridge between bulk materials and atomic or molecular structures. Colloidal inorganic nanometer-sized particles (nanoparticles, NPs) or nanocrystals (NCs) have proved to be useful as building blocks for the development of nanomaterials and biomaterials in nanoscience and biotechnology [19]. It may be amorphous, crystalline or of mixed character, with for instance amorphous surface layer and crystalline interior. In fact, the properties of a material start changing as its size approaches the nanoscale and as the percentage of atoms at its surfaces becomes significant [18,20].

1.4. Nanocomposite

Nanocomposites are composite materials in which nanoparticles are embedded in a host phase. This is part of the growing field of nanotechnology [21]. In chemistry, a

„composite" is defined as materials having two or more distinct components or phases and their components have significantly different physical properties and thus, the composite properties are noticeably different from the individual component properties. When there is the physical arrangement on a scale of 1 to 100 nanometers, it is said that this material is considered as "Nanocomposite". A composite material is a solid structure with multiple phases, which is a combination of two or more materials with different physical and chemical properties. One phase is usually called as matrix or a continuous phase (polymer, metal, ceramic, etc.), while the other was infamously known as reinforcement material a dispersed phase such as glass fibers, carbon particles, silica powder, clay minerals, etc.. [22, 23].

The presence of the natural interface between two different field of chemistry which is organic and an inorganic may be also called Hybrid composite. Hybrids are typically either homogeneous systems derived from monomers or miscible organic and inorganic components, or heterogeneous systems (nanocomposites) in which at least one of the components" domains has dimensions ranging from some Å to several nanometers. Hybrid inorganic–organic materials are not just physical mixtures of inorganic and organic moieties. They can be defined as nanocomposites with organic and inorganic components that are intimately mixed on a molecular level [24]. Intercalation of organic species into inorganic solids appears to offer a useful way of combining, at the nanometer level, both types of matter to provide well-defined organic–inorganic hybrids for the first time [25].

Generally, these materials preserve different electrical, mechanical, optical and catalytic properties than those in the individual component. This is because of the following three factors. First, the size of nanoparticles is comparable with the Bohr radius of an exaction; this determines their optical, luminescent and redox properties. Secondly, being small in size, surface tension effects are expected to increase. This

makes surface atoms very active and determines their considerable contribution to the thermodynamic characteristics of solids. Thirdly, the sizes of nanoparticles themselves are also comparable to those of molecules. These factors make the kinetics of chemical processes with nanoparticles specific [26].

1.5. Clay minerals

A great deal of attention has focused on clay minerals since the earliest days of civilization due to their abundance in nature and unlimited potentials. Clays may be divided into two broad groups: cationic clays, widespread in nature, and anionic clays, rarer in nature but relatively simple and inexpensive to synthesize [27]. Anionic clays can be considered as the opposite of cationic clays i.e. layers are either negatively (cationic) or positively (anionic) charged [28]. The interlayer region of clays consists of cations or anions to compensate for the layer charge, the free space also contains water molecules [29].

Clays are both versatile and have many beneficial features, such as low or null toxicity, good biocompatibility, and promise for controlled release, thus give rise to the incessant interest to their development for biological purposes, for example, pharmaceutical, cosmetic, and even medical ones [30], low cost, selectivity, coefficients of expansion, flammability resistance, mechanical, ion-exchange capacity, flexibility, catalytic properties, and a wide range of preparation and modification methods. In addition, organic modification of clay is performed to change the properties from hydrophobic to hydrophilic [27].

The properties which make clay minerals useful in pharmaceutical applications are the high adsorption ability, high internal surface area, high an ion exchange capacity, interlayer reactions, chemical inertness, and low or null toxicity. Lately, a new emerging class of nanocomposites, based on layered double hydroxides (LDHs), also known as anionic or hydrotalcite-like clays, has been investigated. The most

common type of LDHs is the hydrotalcite-type (HT) group of minerals. Hydrotalcite is a hydrated mineral containing magnesium, aluminum and carbonate with the general formula $Mg_6Al_2(OH)_{16}CO_3.4H_2O$ as shown in "figure 2" [31].

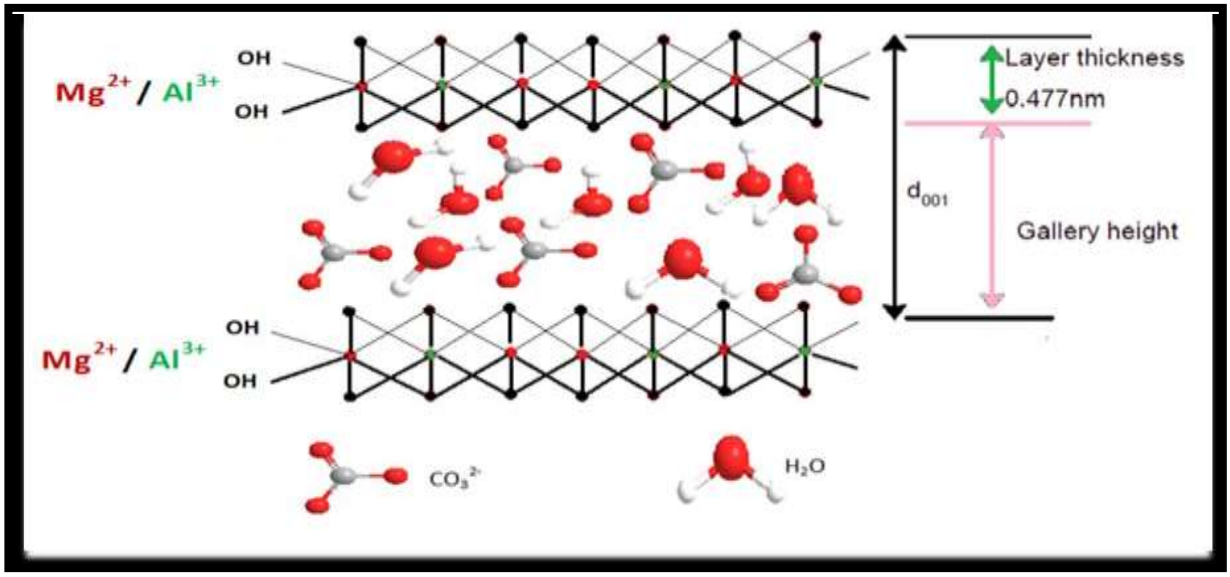

Figure 2. Hydrotalcite-type clays.

1.6. Layered Double Hydroxides (LDHs)

Layered double hydroxides (LDHs), also known as anionic or hydrotalcite-like clays, many LDHs such as *Hydrotalcite*, *Takovite*, *Carrboydite*, *Reevesite*, *Honessite*, *Pyroaurite*, and *Iowaite* occur in nature while others have been prepared synthetically in the laboratory[32, 33]. The first material discovered was *Hydrotalcite* which subsequently gave its name to the large mineral group of naturally occurring LDHs. The name is derived from the strong resemblance of the mineral to talc and its high water content. LDHs are a class of lamellar compounds that consist of positively charged brucite-like host layers and hydrated exchangeable anions located in the interlayer gallery for charge balance [34].

The structure of LDHs is derived from that of naturally occurring mineral brucite structure ($Mg(OH)_2$) in which, e.g. Al^{3+} substitutes for Mg^{2+}. In general any divalent cation could substitute for the Mg^{2+} having not too different a radius in the brucite-like

layer. In addition, any trivalent cation with similar radii may substitute for aluminum in the brucite layer [33, 35]. The isomorphous substitution of a part of the divalent metal ions with trivalent ones creates a positive layer charge on the hydroxide layers, which is compensated by interlayer anions or anionic complexes. This surface charge is dependent upon the degree of substitution. Claim that the formation of basic centers in hydrotalcite appears in the bridge oxygens between two magnesium atoms. These basic centers are due to the defects in oxygen linked to fully co-ordinated magnesium [36]. It also contains interlayer water which forms hydrogen bonds to the -OH groups on the surface of the LDHs or with the interlayer anions [37]. LDHs are represented by the general formula:

$$[M^{2+}_{1-x}M^{3+}_{x}(OH)_2]^{x+}[A^{n-}_{x/n}]^{x-}.mH_2O$$
$$_{-x}M_{x}(OH)_2]\ [A\ ]\ .mH_2O$$

Where M^{2+} is the divalent cation such as Mg^{2+}, Ca^{2+}, Zn^{2+}, Co^{2+}, Fe^{2+}, Cu^{2+}, Ni^{2+}, Mn^{2+} etc., and M^{3+} is the trivalent cation such as Al^{3+}, Cr^{3+}, Fe^{3+}, Co^{3+} etc., in the octahedral positions within the hydroxide layers, (A^{n-} is an interlayer anion such as Cl^{-}, CO_3^{2-}, NO_3^{-}, PO_4^{3-}, SO_4^{2-} and so on), with a negative charge n and m is the number of water molecules, x is the molar ratio and can be calculated as:

$$x = [M^{3+}/(M^{2+} + M^{3+})]$$

Which is normally between 0.1 and 0.5, it is possible to obtain pure hydrotalcite only for $0.2 \leq x \leq 0.33$. If x values lower than 0.33, the M^{3+} octahedral is not neighboring. For higher values of x the increase number of neighboring M^{3+} in brucite like sheet, acting as nuclei for the formation of $M(OH)_2$. [22, 27, 29, 38].

In comparison, the hydrotalcite-type anionic clays have a structure similar to that of brucite, $Mg(OH)_2$, where each Mg^{2+} ion is octahedrally surrounded by six OH^- ions “figure 3A”. These octahedral units form infinite layers by edge-sharing, with the hydroxide ions sitting perpendicular to the plane of the layers. The hydrotalcite

structure is obtained when some of the Mg^{2+} ions, in the brucite layer, are replaced by trivalent cations with a similar radius “figure 3B” [29].

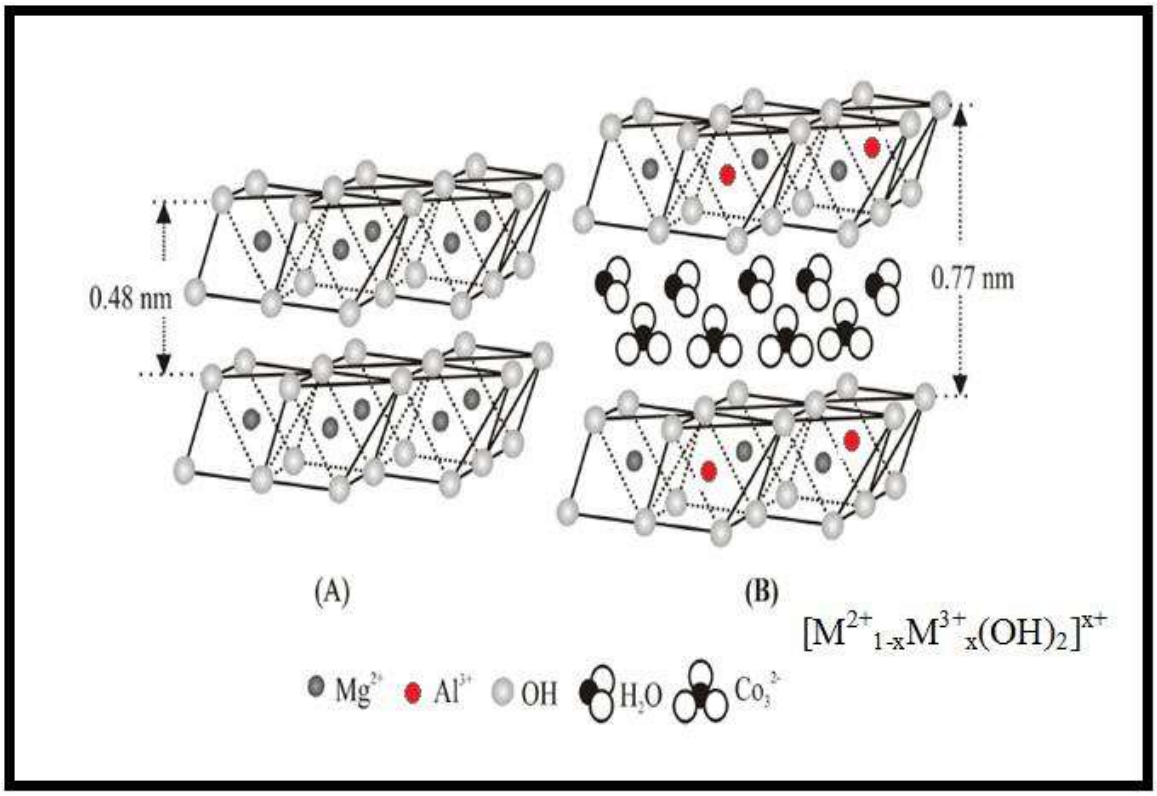

Figure 3. Schematic representation comparing the crystal structure of brucite (A) and LDH (B).

The higher charge of the cation imposes an overall positive charge in the brucite-type layer. These layers are maintained electrically neutral by the interlayer anions. These sheets are stacked on top of each other and are held together by hydrogen bonding to form the three-dimensional structure “figure 4” [27, 40]. Layered double hydroxides (LDHs), are two dimensional structures called nanosheets having approximate thicknesses of 1 nm and widths of 1 µm [41-42]. The main features of HT structures therefore are determined by the nature of the brucite-like sheet, by the position of anions and water in the interlayer region and by the type of stacking of the brucite-like sheets.

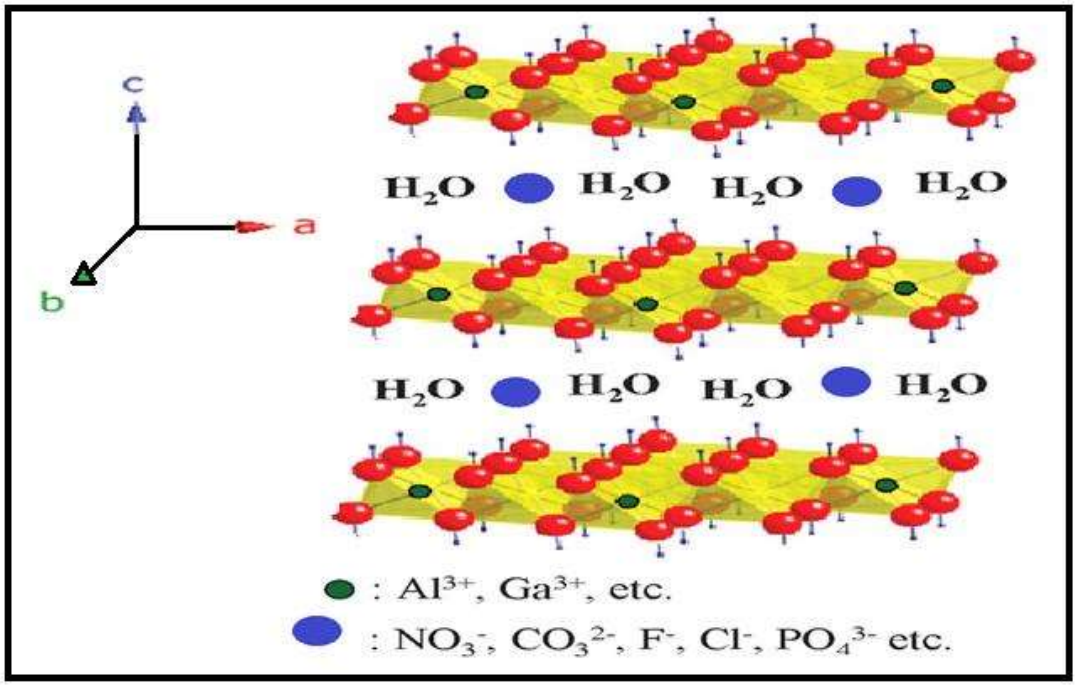

Figure 4. Schematic representation of the LDHs structure.

1.6.1. An ion nature

There is essentially no limitation on the nature of the anion which can compensate for the positive charge of the brucite-like sheet, and provided it doesn‟t form a complex with the cations [27, 29, 43].

The interlayer anions A^{n-} are exchangeable, giving rise to rich intercalation chemistry. The guest species may be organic or inorganic, simple or complex. Intercalation of a desired anionic guest is achieved by direct synthesis, ion-exchange, or by reconstruction of the layered structure [37, 43].

The intercalated molecules can only form monolayers or bilayers in the interlayer space of layered materials independent of molecular size, due to the interaction between the host layer plate and guest molecules [44]. In addition, the interlayer galleries of LDHs contain both interlayer anions and water molecules and there is a complex network of hydrogen bonds between layer hydroxyl groups, anions and water molecules. The interlayers are substantially disordered and hydrogen bonds are in a

continuous state of flux so that the precise nature of the interlayer is extremely complex [45]. Every anion has to satisfy excess positive charges on both of the sandwiching octahedral layers, which are electrically balanced by two neighboring interlayers; it has been suggested that charge compensation in LDHs has many of the characteristics of resonance effects [46].

1.6.2. Layered double hydroxide applications

Recently, LDHs are employed as the host material to synthesize a new organic–inorganic nanohybrid material and have received considerable attentions. The organic/LDHs nanohybrid materials have been investigated because the resulting intercalation compounds are expected to possess a novel nanostructure, new function such as high surface area, large anion exchange capacity, and good thermal stability. These materials offer many benefits across a wide range of industrial applications.

LDHs have been studied for their potential application to the removal of oxyanions such as arsenate/arsenite, chromate, selenate/selenite, borate, and nitrate from contaminated waters [47-54]. Owing to the intercalation property of LDHs, many LDHs compounds with intercalated beneficial organic anions, such as DNA [55-57], amino acid [58-61], vitamin [62-64], offered a safe preservation of the guest bioactivity without any deterioration of the structural integrity. In agriculture, LDHs nanocomposite formulations controlled the herbicidal efficiency of acid herbicides and also minimized the losses of plant pesticide [65-69]. Additionally, many of LDHs plant growth regulators [70] have been prepared.

On the other hand, Delivery of beneficial agents, such as drug in human body from controlled release formulation has lately attracted increasing interest. This is due to the advantages of controlled release formulation compared to its counterpart, such as prolonged duration of action of an active agent, minimized adverse reactions or maximized efficacy, with tailor-made properties and higher stability of the active

agents in the formulation. Therefore, in pharmacy, drug-LDH nanocomposites were formulated to control the amount of drug released [71-75].

In addition, Controlled release drug delivery systems offer great advantages over the conventional dosage forms. These include (a) dramatic decrease in dosing frequency and improved patient compliance, (b) minimized in vivo fluctuation of drug concentrations and maintenance of drug concentrations within a desired range, (c) localized drug delivery, and (d) reduced side effects. Thus, much attention has been focused on the organic-inorganic LDHs nanohybrid. Recently, Choy *et al* reported the folic acid intercalated LDH and thus modified LDH was used as a drug reservoir [76]. Lately, Wang *et al* said that the folic acid-LDH nanohybrids showed an enhanced thermal stability and a profound buffering property, which demonstrated that the hybrids could protect folic acid against heat degradation and prompt its available diffusion synthesized and their results suggested that the ternary folic acid-LDH nanohybrids may function as a useful nutritional tablet to promote the bioavailability of folic acid delivery [76].

Hence, it can envision that the strategy of using LDHs nanoformulation will hold promise as a versatile platform for folic acid low solubility, preservation, and controlled release properties as well as the folic acid biodegradation process.

1.7. Folic acid

Folic acid as shown in “Figure 5”, also known generically as folate or folacin, is a member of the vitamin B-Complex family which is required for new cell formation in particular in the growth period and pregnancy, its functions primarily as a methyl-group donor involved in many important body processes, including DNA synthesis, DNA repair. Therapeutically, folic acid is instrumental in reducing homocysteine levels; improve the total plasma antioxidant capacity in coronary artery disease and hemodialysis patients, and the occurrence of neural tube defects. It is especially

important in aiding rapid cell division and growth, such as in infancy and pregnancy, as well as in "feeding" some cancers. While a normal diet also high in natural folates may decrease the risk of cancer, there is diverse evidence that high folate intake from supplementation may actually promote some cancers as well as precancerous tumors and lesions. Children and adults both require folic acid to produce healthy red blood cells and prevent anemia. Folate deficiency may lead to glossitis, diarrhea, depression, confusion, anemia, and fetal neural tube defects and brain defects (during pregnancy) [71, 76].

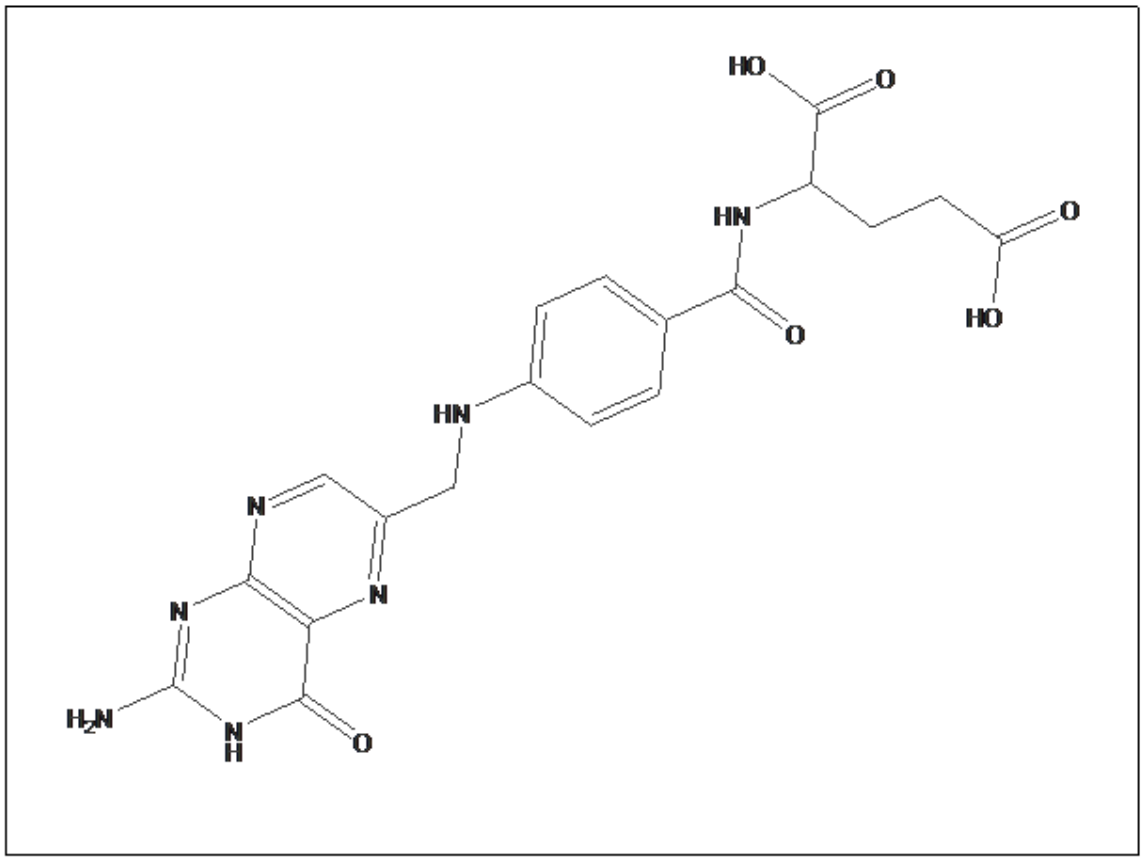

Figure 5. The chemical structure of folic acid.

In acid form, folic acid has very low aqueous solubility leading to low bioavailability when administered orally. Folic acid has many problems during formulation development due to photo labile, and sensitive upon light, temperature, pH

and oxygen exposure as well as in the presence of riboflavin which is often added in the liquid multivitamin dosage form. In addition, much drugs containing carboxyl groups like folic acid that cause highest acidity of stomach when dissolution it [73]. On the other hand, human body requires a specific amount of vitamin (FA) for the formation of new cells. Thus, both insufficient and excessive supplies of vitamin cause harmful effects on human body.

1.8. The Aims of this Work

The modification of layered double hydroxide (LDH) offers many advantages in a wide variety of applications. Because of the peculiar layered structure and interlayer anionic exchange capacity, layered double hydroxides have attracted considerable attention in biomedical fields. At the stage of strategy development to improve the solubility of such compound, it must be considered safety aspect instead of drug stability both chemically and physically, as well as the effectively of the method.

In general, additive used to improve the solubility are toxic or exhibit unwanted local irritation. To limit toxicity effect upon strategy development to improve solubility, particle reduction to a size in nanorange is the ideal choice. Thus, we must find out the approach that made the drug effective and not affect on the drug action. Hence, the aims of this study are to:

1. Synthesis and characterize of Ni/Al-folic acid-LDHs by two difference approaches which are co-precipitation method and an ion exchange method. In this regard, LDH could be an excellent candidate matrix due to high anion exchange capacity, biocompatibility, high surface area and good thermal stability..
2. Study the effect of the temperature on the LDH crystallite size.
3. Study the controlled release property by using the chemical kinetic field with zeroth, first and pseudo second order as well as Bhaskar equation.

4. Suggestion a new equations to evaluate the diffusion of the active agent through LDH particles.

2.1. **Chemical Kinetics**

2.1.1. Introduction

Kinetics is the study of the rates of chemical processes in an effort to understand what it is that influences these rates, the dependence of the rate of the reaction on concentration which is called the order of the reaction, the rate expression which is an equation which summarizes the dependence of the rate on the concentrations of substances which affect the rate of reaction, this expression involves the rate constant which is a constant of proportionality linking the rate with the various concentration terms, this rate constant collects in one quantity all the information needed to calculate the rate under specific conditions, the effect of temperature on the rate of reaction [78,79].

An understanding of chemical kinetics is important in providing essential evidence as to the mechanisms of chemical processes. Additionally, knowledge of reaction rates has many practical applications, for example in designing an industrial process, in understanding the complex dynamics of the atmosphere, in understanding the intricate interplay of the chemical reactions that are the basis of life and Drug action etc. [80].

In this study, we have used this field of study for predicting the kinetics related to drugs action, and diffusion-dissolution phenomena‟s in the human body from the LDHs nanohybrid beads by adapting it to several mathematical models. The study of chemical kinetics process in heterogeneous system such as anionic clays (LDHs) is greatly magnified. This is largely due to the complexity of these compounds which are made up of a mixture of inorganic and organic components [81].

2.1.2. In vitro drug release kinetics: mathematical models

Many drugs require to be released at a controlled rate so that sustained or prolonged action is obtained. The drug release based on drug–LDHs system could be

controlled either by dissolution of LDHs particles, or by diffusion through the LDHs nanohybrid particles [82]. To understand the release mechanism of the guest anion, it should be applied to the zeroth order together with first-order and pseudo-second order equation (equation 1, 2 and 3) respectively, which is normally used to describe the dissolution phenomena [83-84]:

$$X = k\,t + c \qquad (1)$$

$$-\ln\left(1 - \frac{C_t}{C_f}\right) = k\,t \qquad (2)$$

$$\frac{t}{C_t} = \frac{1}{k_2 C_f^2} + \left(\frac{1}{C_f}\right) t \qquad (3)$$

where X is the release percentage of folate anion (FA) at time t (min) and c is a constant. K is a rate constant, C_t the concentration of FA at the time t and C_f the final concentration of FA.

On the other hand, the release of active agent from a resinate particle can be controlled by the pore diffusion resistance (also called „particle diffusion control") or by the resistance of the film surrounding the particle [85]. Additionally, when the drug release fraction is slower than 0.85, Bhaskar (equation 4) was used to evaluate whether the diffusion through the particle is the rate-limiting step. i.e. which is also used to describe the diffusion phenomena

$$\ln\left(\frac{C_t}{C_f}\right) = -k\,t^{0.5} \qquad (4)$$

where, C_t is the concentration of FA at the time t, C_f the final concentration of FA and K is a rate constant [85].

In fact, there are inaccuracies when we say that the equations (1, 2 and 3) are used to describe the dissolution phenomena. Instead, they represent the dissolution as well as diffusion, because the time in these equations represent the total time.

2.1.3. Novel equations to evaluate diffusion through the LDHs nanohybrid particles

All the previous studies indicate that the release profiles of drug from the nanohybrid compounds were governed by the pseudo-second order (equation 3). Where, this equation refers to diffusion of drugs as well as dissolution as previously mentioned. All the equations used for this purpose including (the equation of Bhaskar, the parabolic diffusion model, the modified Freundlich model etc.) were the first order depending on the concentration. Unfortunately, they are not successful in that and could not use these equations for this purpose. Therefore, it must find out a mathematical model that represents the mechanism of drugs diffusion in order to be able to finally produce a good formulation.

In this study, it have innovated a novel equation to evaluate the diffusion through the LDHs particles. Because of, the time of diffusion is a part of the total time that included the diffusion and dissolution time. The precise expression for particle diffusion control obtained by solving the following equation as follows:

$$C_t \propto t^n \qquad (5)$$

where, Ct is the concentration of the active agent at the time t and n is the diffusional exponent.

$$C_t = Dt^n \qquad (6)$$

where D is the diffusion coefficient.

This may be integrated. The limits of integration are taken as $C_t = 0$ at t = 0 and $C_t = C_t$ at t = t, as follow:

$$\int_0^{C_t} \frac{dC_t}{(C_f - C_t)^2} = D \int_0^t t^n dt \qquad (7)$$

It can be integrate this equation as fellow:

$$\frac{t^{n-1}}{n-1} \qquad (8)\frac{1}{(C_f - C_t)} - \frac{1}{C_f} = D$$

$$\ln \frac{C_t}{C_f^2 - C_t C_f} = \ln \frac{\mathrm{D}}{\mathrm{n}-1} + (n-1)\ln t \qquad (9)$$

Let assume that:

$$\ln \frac{C_t}{C_f^2 - C_t C_f} = A \qquad (10)$$

$$\ln t = B \qquad (11)$$

According to (equation 10) the slope of the plot of A versus B will give the value of (n-1).

Let assume that: n-1=m, 0< m < 1

The n value calculating from (equation 9), can be substituted it in (equation 5) and integrate it to get the following equation:

$$\frac{t^m}{C_t} = \frac{m}{K C_f^2} + \frac{t^m}{C_f} \qquad (12)$$

where, K is the rate constant of diffusion.

Therefore, the (equation 12) represents the mathematical model which expresses the diffusion of the active agent through the LDHs nanohybrid particles.

2.1.4. Artificial Neural Networks (AANs)

An artificial intelligence (AI) has been established as the area of computer science dedicated to the production of software capable of sophisticated, intelligent, computations similar to those that the human brain routinely performs [86]. There are two main categories of AI developments. The first includes methods and systems that

simulate human experience and draw conclusions from a set of rules, such as expert systems. The second includes systems that model the way the brain works, for example, artificial neural networks (ANNs).

An artificial neural network (ANN) is a highly simplified model of the structure of a biological network. The fundamental processing element of ANN is an artificial neuron (or simply a neuron). A biological neuron receives inputs from other sources through synapses located on the dendrites or membrane of the neuron, combines them, performs generally a nonlinear operation on the result, and then outputs the final result, or this signal might be sent to another synapse, and might activate other neurons [87].

The main advantage of the ANN is that it does not need any mathematical model since an ANN learns from examples and recognizes patterns in a series of input and output data without any prior assumptions about their nature and interrelations, i.e. a significant difference between an ANN model and a statistical model is that the ANN can generalize the relationship between independent and dependant variables without a specific mathematical function. Such a model is easy to develop, yields satisfactory results when applied to complex systems which is poorly defined or implicitly understood. These are more tolerant to variable, incomplete or ambiguous input data. In addition, the ANN approach is faster compared to its conventional techniques, and can solve a wide range of problems. Hence, artificial neural networks (ANNs) are now the most popular artificial learning tool in biotechnology and have been used in numerous real time applications [87-91].

ANN based on the Quick Propagation (QP) algorithm was used in this study to predict the concentration of folic acid released (C_t) at the time t. In order to solve the forecasting model, a software program produced by Neuro Intelligence Company has been used. Alyuda Neuro Intelligence (AN) is ANN-based application software that achieves databases preprocessing and analysis, definition of the ANN with the best architecture, testing and optimizing the chosen ANN, application of ANN in solving

problems. This software allows the user to select the number of hidden layers, hidden layer nodes, iterations used during model training, learning algorithm and transfer functions. In the development of an application, both data and designed neural network pass through a sequence of stages, to achieve a maximum performance, ensuring a network error as small as possible. These stages are data analysis, data pre processing, neural network design, ANN training, ANN testing and ANN query.

To design an ANN, it is necessary to specify the network architecture (number of neurons in the hidden layer, number of hidden layers) and network properties (activation function, error), designed manually or automatically. In order to design the ANN for this application, several features have been activated: number of output neurons (1), activation function of hidden layer (Logistic), error function of output (sum of squares), and activation function of output (Logistic, number of neurons in the hidden layer (9) and number of hidden layer (5) as shown in “figure 6”.

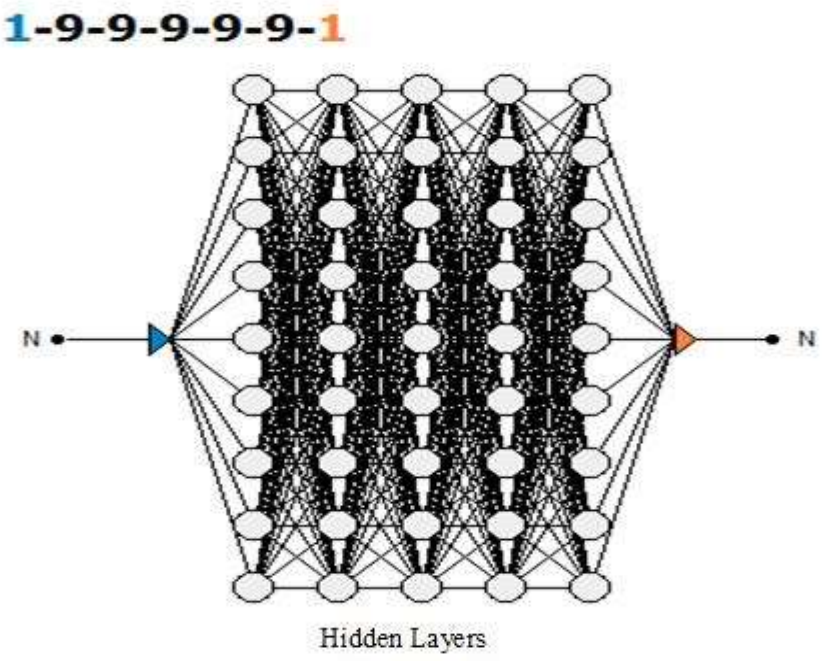

Figure 6. ANN architecture, N = the neuron.

2.2. **Materials and Methods**

2.2.1. Materials

Folic acid (99.0 %) was purchased from Enterprise Group Chemical Reagent Co., LTD, Al (NO3)3·9H2O (98%) was purchased from Xinbao Nice Chemical, NaOH and Ni (NO3)2·6H2O (98%) were purchased from Xilong Chemical. All chemicals were of analytical grade and used without further purification.

2.2.2. Preparation of Ni-Al–NO3-LDHs

A series of Ni/Al LDHs with nominal Ni^{2+}/Al^{3+} molar ratio of 3, 4 and 5 were prepared by hydrothermal reaction at 70, 120 and 180°C. The Ni-Al-NO_3-LDHs have been prepared by co-precipitation method from Ni and Al nitrate.

All of them were prepared as follows: a mixed aqueous solution containing 2.5M (7.27 g) Ni (II) and 0.82M (3.09g) Al (III) was titrated drop wise with NaOH (2M) solution. The pH was adjusted to 7 and the mixture was magnetically stirred at 100 ˚C for 1h under N_2 atmosphere to avoid or at least to minimize the contamination by atmospheric CO_2.

The suspension was transferred into a 500 ml stainless Teflon-lined autoclave and heated at appropriate temperature for 24h, and then left to room temperature. The resulting green precipitate was filtered, washed for several times with de-ionized water. The apple-green solid was collected and dried at 70°C for 24 h.

2.2.3. Preparation of Ni/Al-FA-LDHs by ion-exchange method

The green precipitated of Ni-Al-NO_3-LDHs (NAL) was dispersed in 50ml de-ionized water and then titrated drop wise with appropriate amount of folic acid. The mixture was magnetically stirred at 70°C for 18 h under N_2 atmosphere. The resulting green precipitate was filtered, washed for several times with de-ionized water to remove the excess amount of nitrate ion. The apple-green solid was collected and dried at 70°C for 24 h.

2.2.4. Preparation of Ni-Al-Folic acid-LDHs by co-precipitation method

A series of Ni/Al LDHs with nominal Ni^{2+}/Al^{3+} molar ratio of 3, 4, 5 and 6 were prepared by co-precipitation method from Ni and Al nitrate at 70°C. A mixed aqueous solution containing 2.5M (7.27g) Ni (II) and 0.82M (3.09g) Al (III) (molar ratio 3) was titrated drop wise with appropriate amount of folic acid and then with NaOH (2M) solution. The pH was adjusted to 7 and the mixture was magnetically stirred at room temperature for 18 h under N_2 atmosphere. The resulting green precipitate was filtered, washed with de-ionized water several time, and then dried at 70°C.

2.2.5. Release Study of Folic acid into Aqueous Solutions

The release of Folic acid (FA) from the nanohybrid into the release media was accomplished using various aqueous solutions: carbonate, phosphate and sulphate. The amount of intercalated folic acid was determined by using a (Cecil 1021) a UV spectrophotometer.

0.001 g of Ni-Al-Folic acid-LDHs nanohybrids was placed into a 3.5ml of the aqueous solution. The concentration of folic acid was determined by monitoring the absorbance at 285 nm with a UV–vis spectroscopy. The concentration was calculated according to an already obtained standard curve of folic acid (A = 0.031C - 0.046, r^2 = 0.997) as shown in "figure 7".

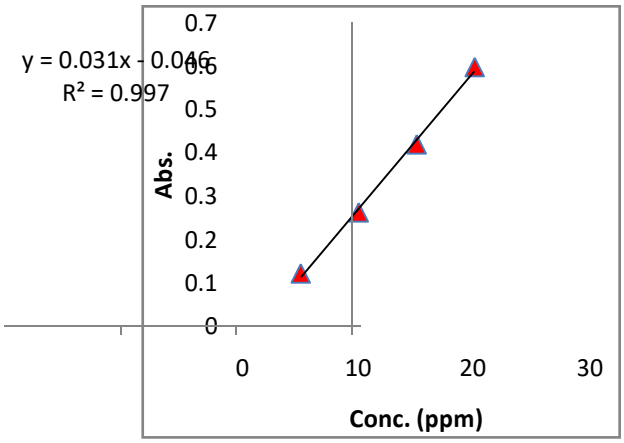

Figure 7. Folic acid calibration curve.

2.2.6. Instrumentations

Powder X-ray diffraction (XRD) was recorded on a Bruker-AXS Diffractometer Model D8 discover using Cu Kα source (k = 0.154060 nm) at 40 mA and 40 kV (Germany). Fourier Transform Infrared Spectra (FTIR) was recorded using SHIMADZU 8400S FT-IR (Japan). UV–visible measurements were recorded by (Cecil 1021) UV spectrophotometer (Japan). pH Meter WTW-720-ionlab (Germany). Thermostat Shaker water Bath GFL (D-3006) (Germany). Centrifuge / Megafuge 1.0 / Herouse Sepatech, (Germany). The materials were treated by stainless Teflon-lined autoclave.

3. Results and discussion

3.1. Powder X-ray Diffraction

Powder X-ray diffraction patterns of the solids obtained that indicate after hydrothermal treatment at 70, 120 and 180˚C a Ni-Al-NO_3-LDHs nanohybrids have been formed "Figure 8, 9 and 10" respectively. For sample Ni-Al-NO_3-LDHs at 70˚C, the basal reflections are recorded at 8.02 (003), 4.02 (006), and 2.57 Å (009), respectively. For the hydrothermally treated sample Ni-Al-NO_3-LDHs at 120˚C the basal reflections are recorded at 7.97, 3.91, and 2.56 Å respectively. On the other hand, the basal reflections of sample Ni-Al-NO_3-LDHs at 180˚C are recorded at 7.90, 3.93 and 2.59 Å respectively. Powder XRD patterns of the Ni-Al-NO_3-LDHs samples showed that the full width of half maximum (FWHM) value of (003) diffraction line decreased with increasing temperature of hydrothermal treatment, which indicated an increase of the LDH crystallite size. In addition, the intensity of (003) plane was increased with increased the temperature as can be seen in "Fig. 8, 9 and 10".

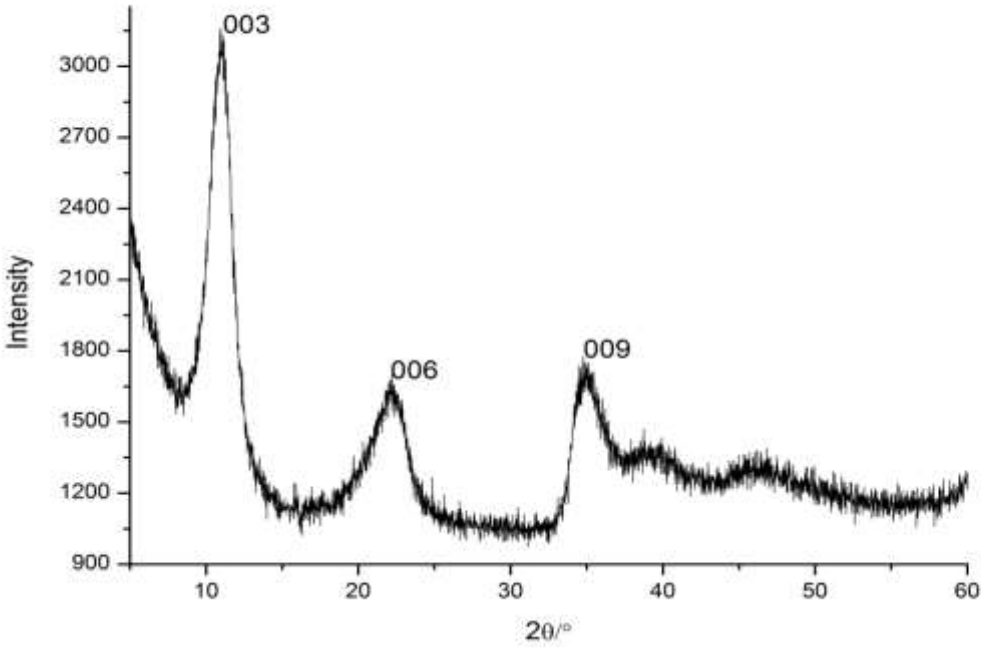

Figure 8. PXRD patterns of Ni-Al-NO_3-LDHS at 70˚C.

Intercalation of drugs leads to a significant increase in the interlayer space "Figure 10". For sample Ni-Al-FA-LDH, the basal reflections are recorded at 17.30 (003), 8.60 (006), and 5.64 Å (009) respectively.

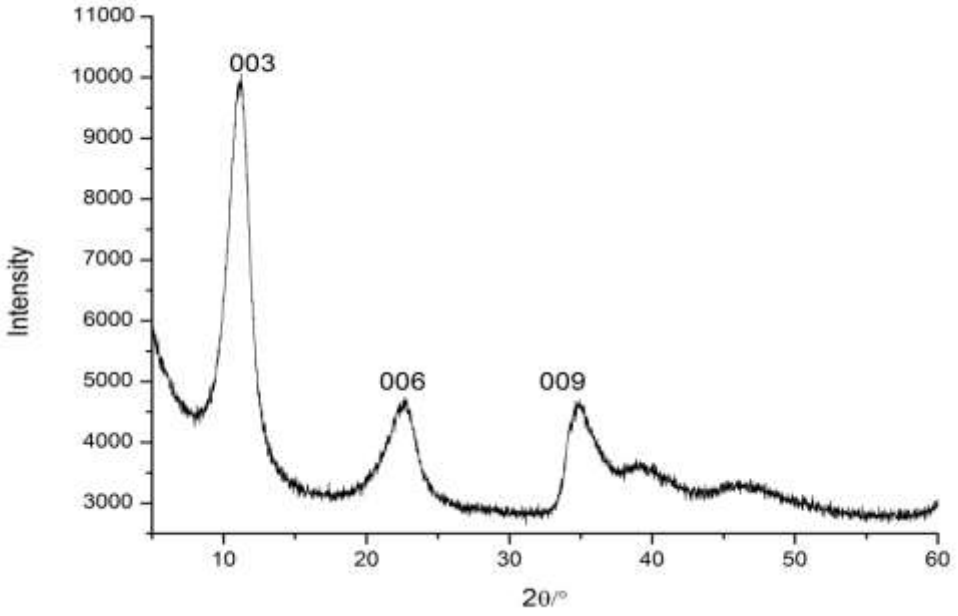

Figure 9. PXRD patterns of Ni-Al-NO3-LDHS at 120˚C.

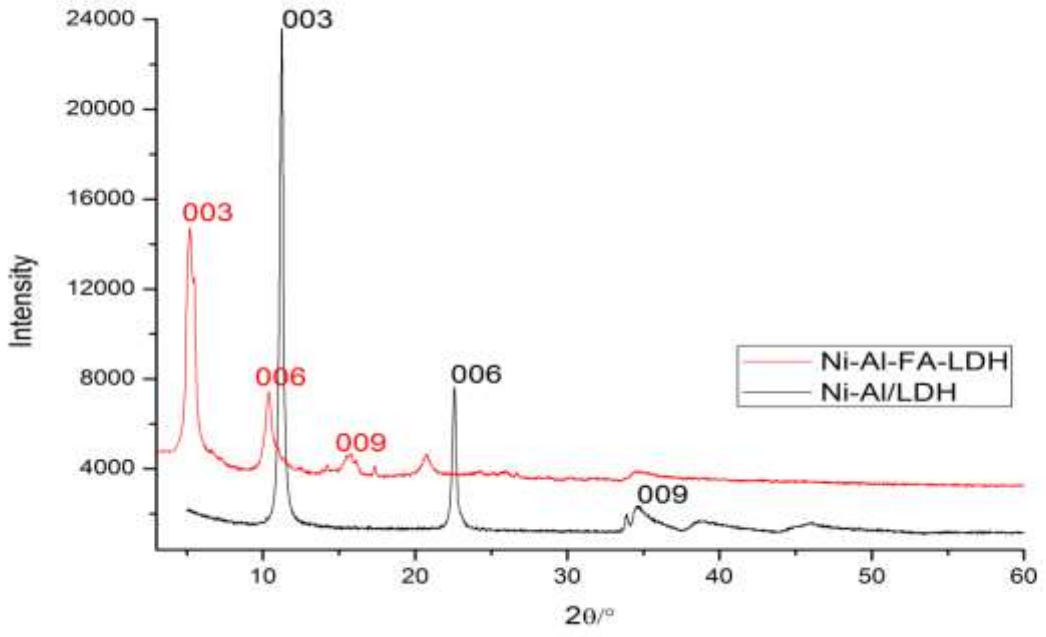

Figure 10. PXRD patterns of Ni-Al-NO_3-LDHS and Ni-Al-NO_3-LDHS at 180˚C.

3.2. Controlled Release of FA into Aqueous Media

The drug release properties of FA from the nanohybrid interlamellae into various aqueous media using (0.5, 0.05, 0.005) M of Na_2CO_3, Na_3PO_4 and Na_2SO_4 have been conducted. "Figure 11 to 17" show the release profiles of composite in different aqueous solutions. The effects of various aqueous systems on the release of FA were evaluated according to the maximum accumulated release and can be written as follows:

Carbonate > Phosphate > Sulphate

It was observed that carbonate dominated the accumulated release percentage as shown in (Table 1, 4) due to, carbonate was known to have the strongest affinity toward the interlayer of layered double hydroxides, also the release rate of FA in the carbonate solution was found to be the most rapid compared to those with phosphate and sulphate aqueous solution.

As can be seen in "Figure 11", a rapid release of FA occurs at the initial stage, which is followed by a slower release of FA. As shown in "Figure 11", FA is almost 88% replaced by CO_3^{2-}, resulting in the highest accumulated release among the media studied. The maximum release time shows that FA is exchange with PO_4^{3-} at 220 min followed by SO_4^{2-} with 385 min and CO_3^{2-} with 435 min. It is worth to note that even though CO_3^{2-} shows the highest accumulated release Table1, the replacement of FA by SO_4^{2-} was found to be slower when compared to PO_4^{3-}. In fact that the sulphate anion is known to have a resonance forms what made it more stable anion and reduce the net negative charge as well as the shape and it is considered as a big molecule compared with carbonate anion. All the previous discussions were about the 0.5M concentrations and the same discussion to the other concentrations. The effect of concentration of aqueous systems on the release of FA was investigated according to the maximum accumulated release and can be written as follows:

0.5 > 0.05 > 0.005

It was clear that the 0.5M aqueous system dominates the accumulated release percentage for all aqueous systems as shown in Table 1. It should be mentioned that the initial release rate of FA during the first 100 min in carbonate aqueous solution is much faster than that in the other aqueous systems, as shown in "Figure 11".

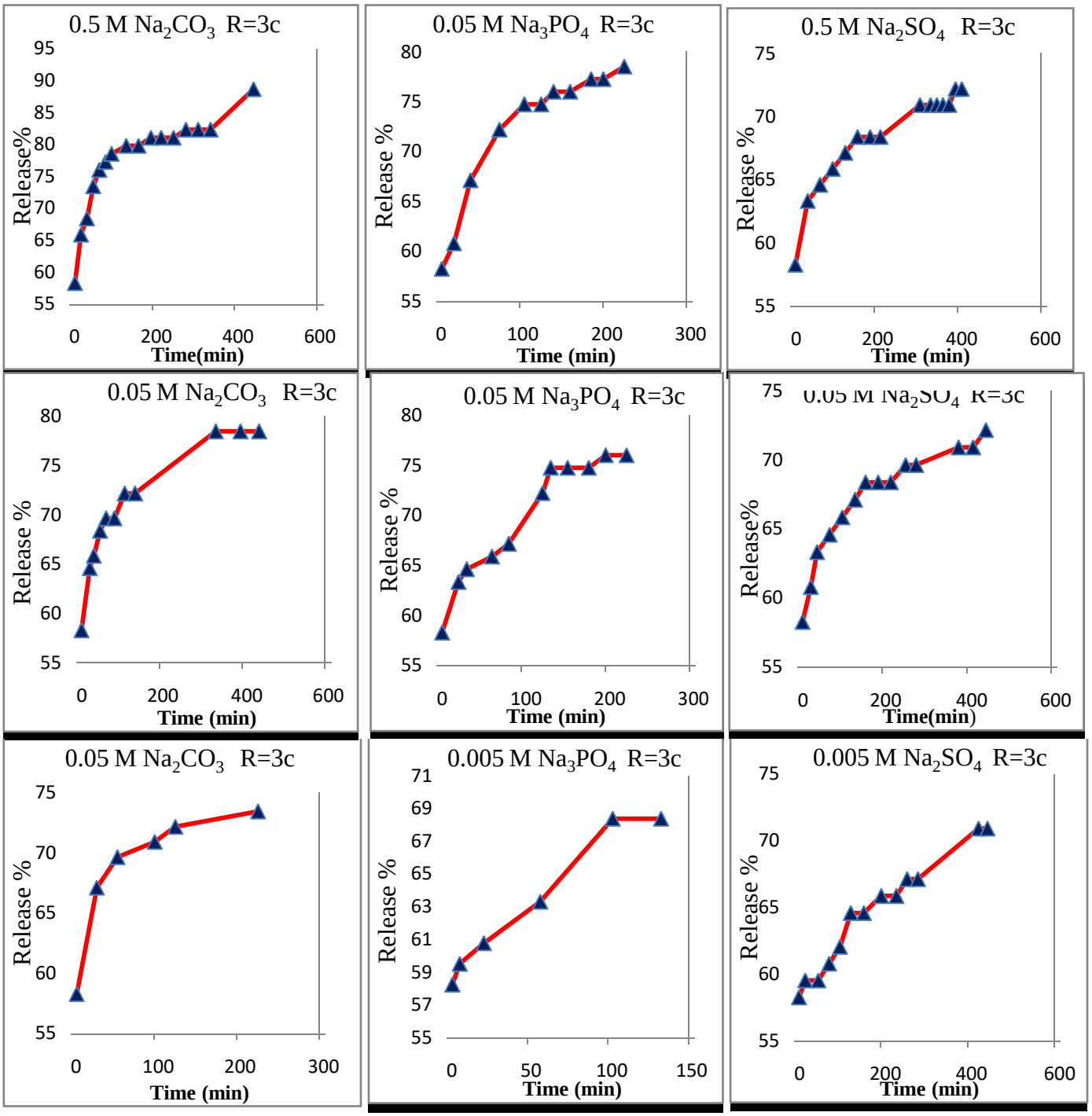

Figure 11. Release profiles of (FA) from the interlamellae of Ni-Al-FA-LDHs, the nanohybride into various aqueous solution systems with different concentrations were containing several anions of carbonate, phosphate and sulphate (Ni/Al=3 Co-precipitation).

Table 1. Percentage Release, Rate Constant (k), Half Life ($t_{1/2}$) and Correlation Coefficients (r^2) Obtained from Fitting of the Release Data of (FA) from Ni-Al-FA LDH Nanohybrids into various aqueous solution (Ni/Al=3 Co-precipitation).

Aqueous solution	Concentration (Mol.L^{-1})	Maximum Release %	Maximum Time (min)	Zeroth order	First order	Bhaskar equation	Pseudo-second order	Other parameters for pseudo-second order	
				r^2				K×10^{-4} (L.mg^{-1} min^{-1})	$t_{1/2}$ (min)
Na_2CO_3	0.500	88	435	0.696	0.818	0.914	0.997	370.000	10.366
	0.050	78	325	0.796	0.871	0.978	0.999	420.000	9.332
	0.005	73	220	0.613	0.675	0.884	0.999	1010.000	3.878
Na_3PO_4	0.500	78	220	0.841	0.889	0.972	0.999	650.000	5.963
	0.050	75	220	0.912	0.931	0.948	0.997	490.000	7.882
	0.005	68	130	0.963	0.964	0.948	0.998	1610.000	2.436
Na_2SO_4	0.500	72	385	0.855	0.893	0.982	0.999	390.000	9.982
	0.050	72	435	0.815	0.855	0.974	0.999	420.000	9.342
	0.005	70	415	0.954	0.970	0.946	0.997	260.000	14.938

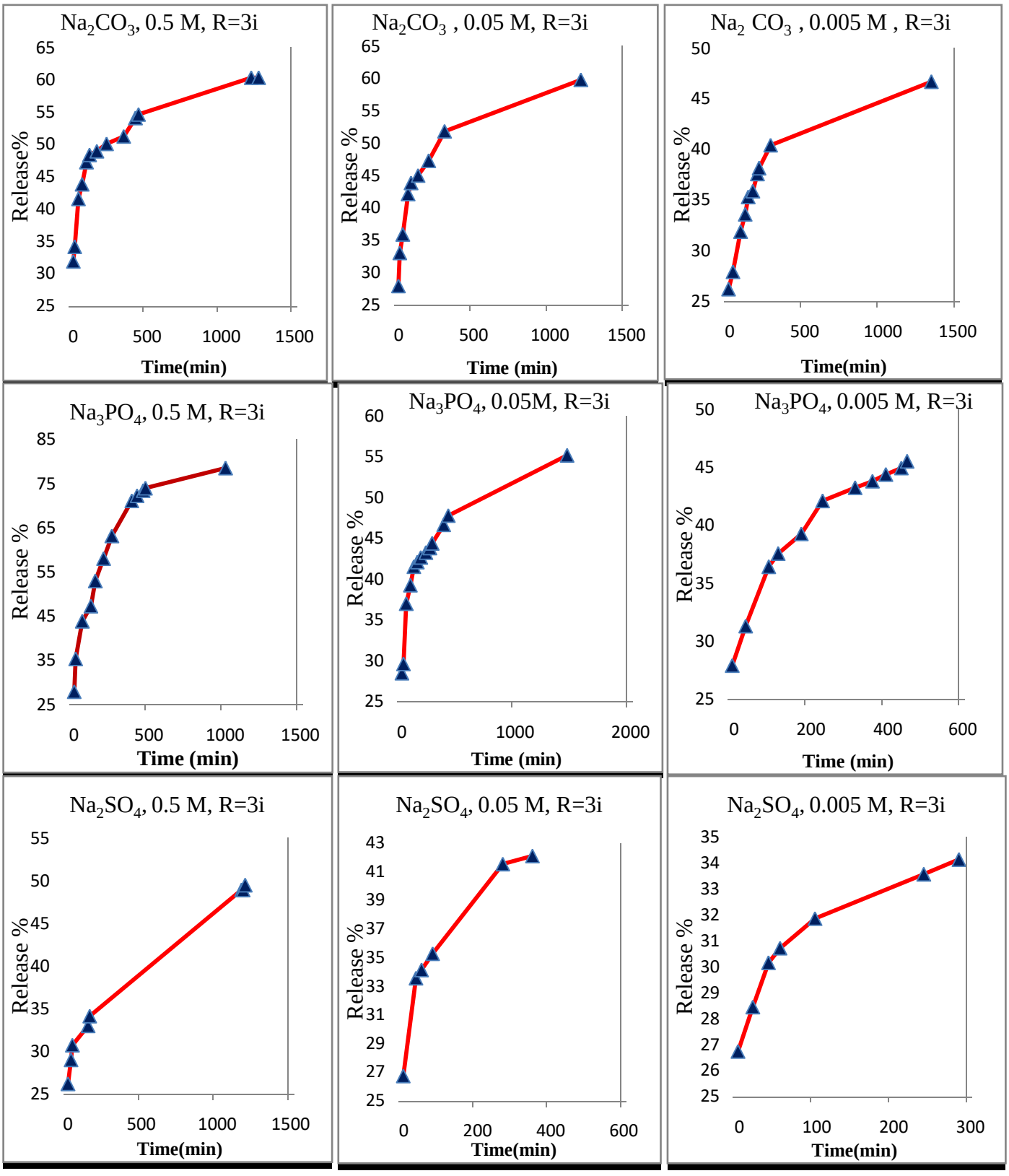

Figure 12. Release profiles of (FA) from the interlamellae of Ni-Al-FA-LDHs, the nanohybride into various aqueous solution systems with different concentrations were containing several anions of carbonate, phosphate and sulphate (Ni/Al=3 ion-exchange).

Comparing the release time, it is clear that the release time of compound (Ni/Al=3 Co-precipitation) is the shortest (Table 1). It was concluded that the electrostatic interaction between layer and FA molecule is strong and folic acid molecule has the highest affinity toward the layer. At the same time, the net negative charge of layer is higher than the net charge of other compound. While, the release time of compound (Ni/Al=4 Co-precipitation) is the longest (Table 3). It is mean prolong duration of action of this compound compared with other compounds.

Table 2. Percentage Release, Rate Constant (k), Half Life ($t_{1/2}$) and Correlation Coefficients (r^2) Obtained from Fitting of the Release Data of (FA) from Ni-Al-FA LDH Nanohybrids into various aqueous solution (Ni/Al=3 ion-exchange).

Other parameters for pseudo-second order		Pseudo-second order	Bhaskar equation	First order	Zeroth order	Maximum Time (min)	Maximum Release %	Concentration (Mol.L^{-1})	Aqueous solution $t_{1/2}$
t (min)	K×10^{-4} (L.mg^{-1} min^{-1})	r^2							
57.437	31.000	0.998	0.924	0.740	0.713	1250	60	0.500	Na_2CO_3
47.968	37.000	0.997	0.937	0.731	0.644	1200	59	0.050	
81.648	22.000	0.998	0.909	0.699	0.649	1325	46	0.005	
73.993	24.000	0.994	0.973	0.814	0.717	1000	78	0.500	Na_3PO_4
75.751	23.000	0.997	0.925	0.689	0.609	1440	55	0.050	
61.803	29.000	0.998	0.988	0.914	0.892	455	45	0.005	
85.106	21.000	0.998	0.995	0.982	0.972	1185	49	0.500	Na_2SO_4
22.237	79.000	0.998	0.980	0.864	0.835	350	42	0.050	
13.415	131.000	0.999	0.971	0.850	0.838	285	34	0.005	

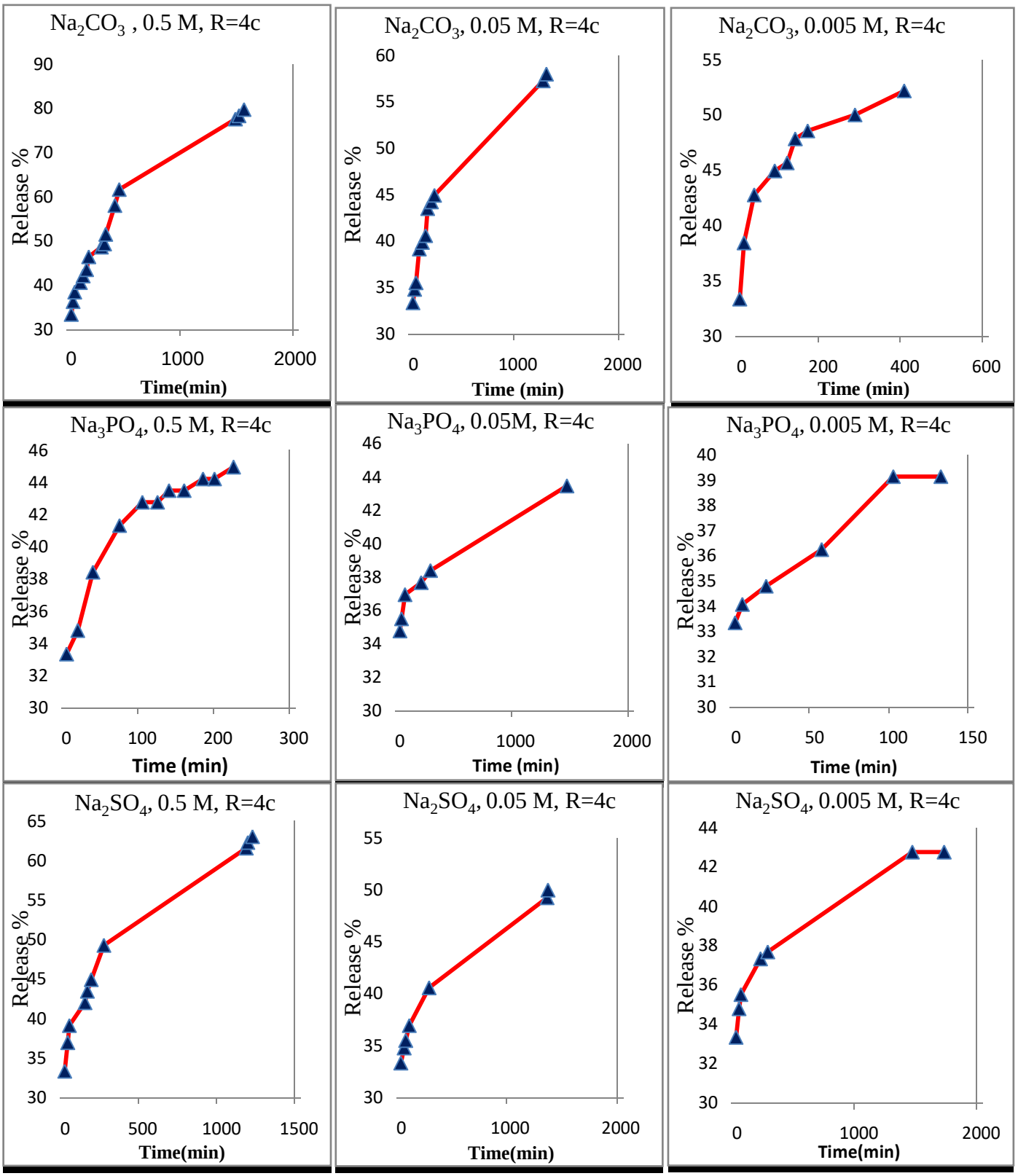

Figure 13. Release profiles of (FA) from the interlamellae of Ni-Al-FA-LDHs, the nanohybrid into various aqueous solution systems with different concentrations were containing several anions of carbonate, phosphate and sulphate (Ni/Al=4 Co-precipitation).

Table 3. Percentage Release, Rate Constant (k), Half Life ($t_{1/2}$) and Correlation Coefficients (r^2) Obtained from Fitting of the Release Data of (FA) from Ni-Al-FA-LDH Nanohybrids into various aqueous solution (Ni/Al=4 Co-precipitation).

Other parameters for pseudo-second order		Pseudo-second order	Bhaskar equation	First order	Zeroth order	Maximum Time (min)	Maximum Release %	Concentration ($Mol.L^{-1}$)	Aqueous solution
t (min)	$K\times10^{-4}$ ($L.mg^{-1}$ min^{-1})	r^2				r			$t_{1/2}$
147.295	15.000	0.989	0.974	0.977	0.923	1530	79	0.500	Na_2CO_3
69.509	32.000	0.998	0.989	0.922	0.884	1270	57	0.050	
16.954	133.000	0.997	0.959	0.771	0.730	400	52	0.005	
10.413	216.000	0.999	0.961	0.855	0.841	220	44	0.500	Na_3PO_4
33.152	68.000	0.999	0.989	0.933	0.922	1440	43	0.050	
4.254	528.000	0.998	0.956	0.963	0.963	130	39	0.005	
82.636	27.000	0.997	0.992	0.961	0.931	1200	63	0.500	Na_2SO_4
58.339	39.000	0.999	0.998	0.969	0.958	1335	50	0.050	
35.933	63.000	0.999	0.994	0.922	0.911	1700	42	0.005	

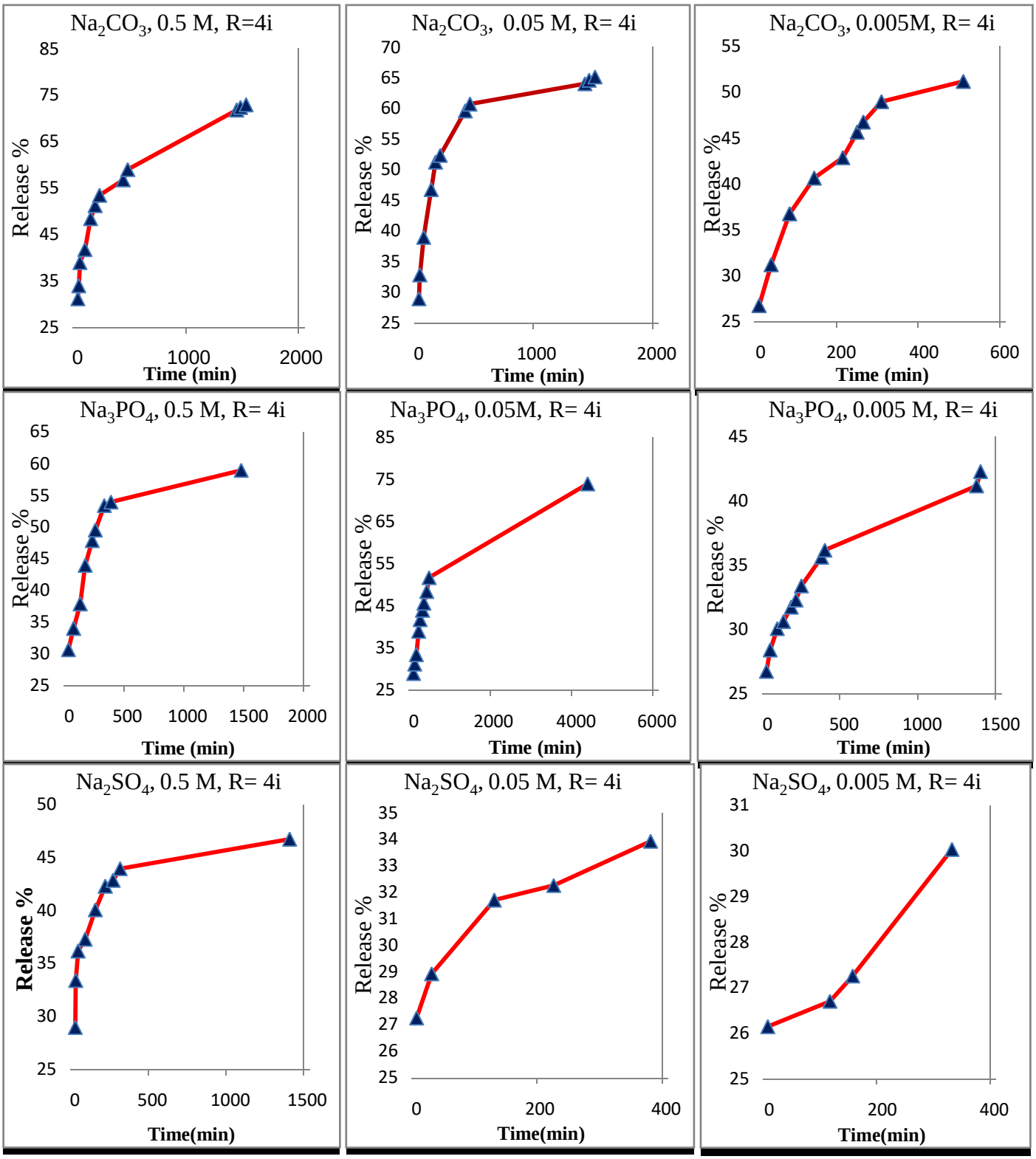

Figure 14. Release profiles of (FA) from the interlamellae of Ni-Al-FA-LDHs, the nanohybrid into various aqueous solution systems with different concentrations were containing several anions of carbonate, phosphate and sulphate (Ni/Al=4 ion-exchange).

The results indicate that the amount of folic acid intercalated depends on the structure and layer charge. According to the final concentration released C_f of all compounds, it can be seen that the compounds (Ni/Al=4 ion-exchange) (Table 4) and (Ni/Al=5 Co-precipitation) (Table 5) have the most amount of FA intercalated compared with their counterparts of ion-exchange and co-precipitation compounds respectively.

Table 4. Percentage Release, Rate Constant (k), Half Life ($t_{1/2}$) and Correlation Coefficients (r^2) Obtained from Fitting of the Release Data of (FA) from Ni-Al-FA-LDH Nanohybrid into various aqueous solution (Ni/Al=4 ion-exchange).

Other parameters for pseudo-second order		Pseudo-second order	Bhaskar equation	First order	Zeroth order	Maximum Time (min)	Maximum Release %	Concentration (Mol.L^{-1})	Aqueous solution
t (min)	K×10^{-4} (L.mg^{-1} min^{-1})	r^2				r			$t_{1/2}$
23.594	73.000	0.989	0.974	0.977	0.923	1530	79	0.500	Na_2CO_3
44.776	39.000	0.999	0.884	0.703	0.627	1480	65	0.050	
49.456	35.000	0.991	0.978	0.884	0.852	500	51	0.005	
81.606	21.000	0.999	0.821	0.576	0.516	1440	58	0.500	Na_3PO_4
178.524	10.000	0.999	0.978	0.878	0.754	4290	73	0.050	
118.204	15.000	0.998	0.985	0.893	0.871	1375	42	0.005	
34.046	51.000	0.999	0.829	0.507	0.472	1380	46	0.500	Na_2SO_4
14.268	121.000	0.998	0.988	0.891	0.883	375	33	0.050	
28.304	61.000	0.996	0.728	0.940	0.943	325	30	0.005	

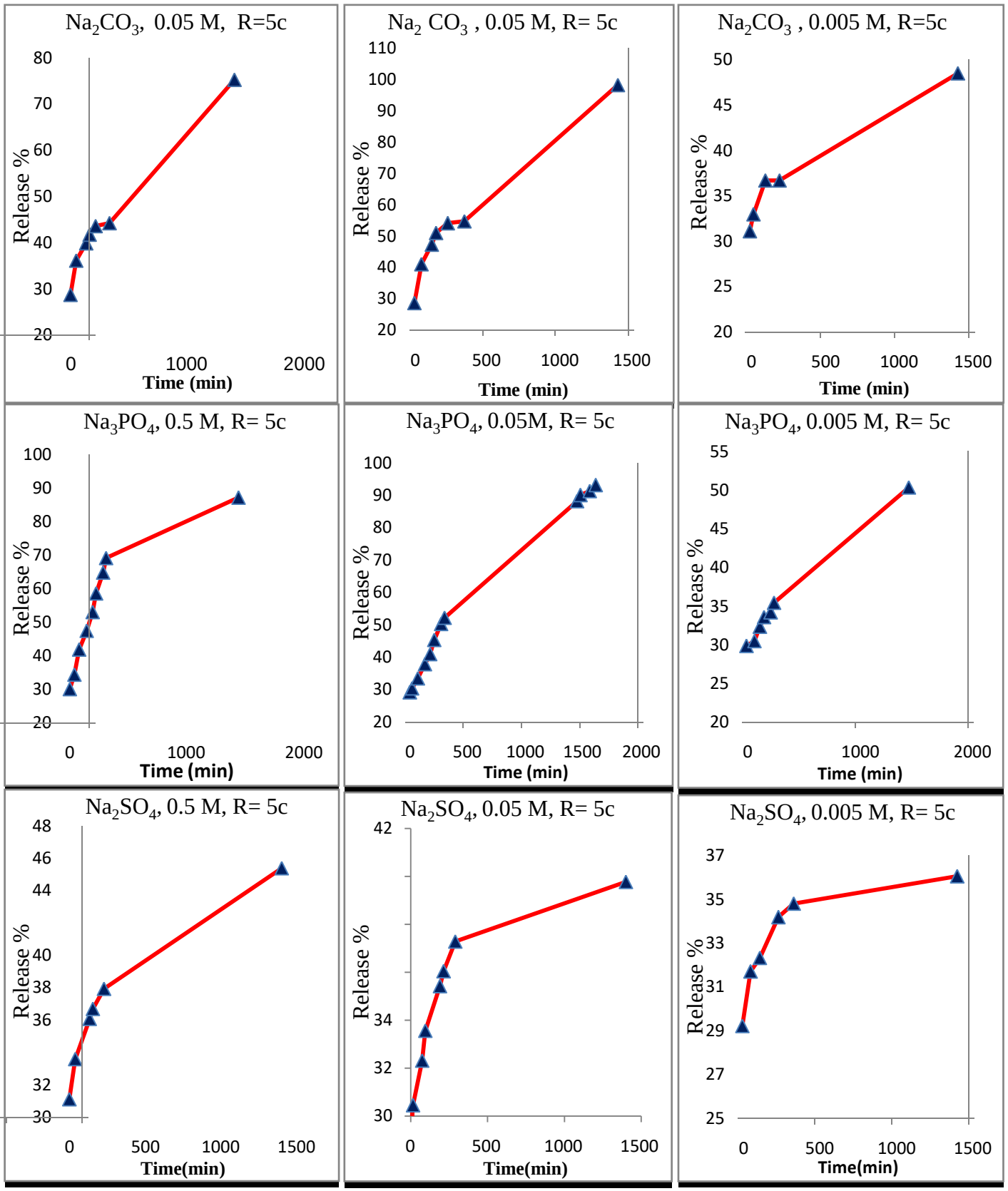

Figure 15. Release profiles of (FA) from the interlamellae of Ni-Al-FA-LDHs, the nanohybrid into various aqueous solution systems with different concentrations were containing several anions of carbonate, phosphate and sulphate (Ni/Al=5 Co-precipitation).

Finally, according to the release profiles and the amount of FA intercalated, it is observed that the compound (Ni/Al=4 ion-exchange) is more convenient "Figure 14".

Table 5. Percentage Release, Rate Constant (k), Half Life ($t_{1/2}$) and Correlation Coefficients (r^2) Obtained from Fitting of the Release Data of (FA) from Ni-Al-FA LDH Nanohybrids into various aqueous solution (Ni/Al=5 Co-precipitation).

Other parameters for pseudo-second order		Pseudo-second order	Bhaskar equation	First order	Zeroth order	Maximum Time (min)	Maximum Release %	Concentration (Mol.L^{-1})	Aqueous solution
$t_{1/2}$ (min)	$K\times10^{-4}$ (L.mg^{-1} min^{-1}	r^2							
200.645	10.000	0.978	0.928	0.899	0.888	1400	75	0.500	Na_2CO_3
171.270	11.000	0.977	0.911	0.821	0.752	1400	98	0.050	
56.467	34.000	0.998	0.990	0.953	0.936	500	51	0.005	
126.636	15.000	0.996	0.965	0.903	0.707	1440	87	0.500	Na_3PO_4
206.406	9.000	0.978	0.947	0.878	0.754	1400	75	0.050	
172.308	11.000	0.997	0.948	0.990	0.983	1440	50	0.005	
59.166	33.000	0.999	0.994	0.890	0.865	1400	45	0.500	Na_2SO_4
38.665	50.000	0.999	0.869	0.626	0.605	1400	39	0.050	
26.469	73.000	0.999	0.834	0.571	0.584	1400	36	0.005	

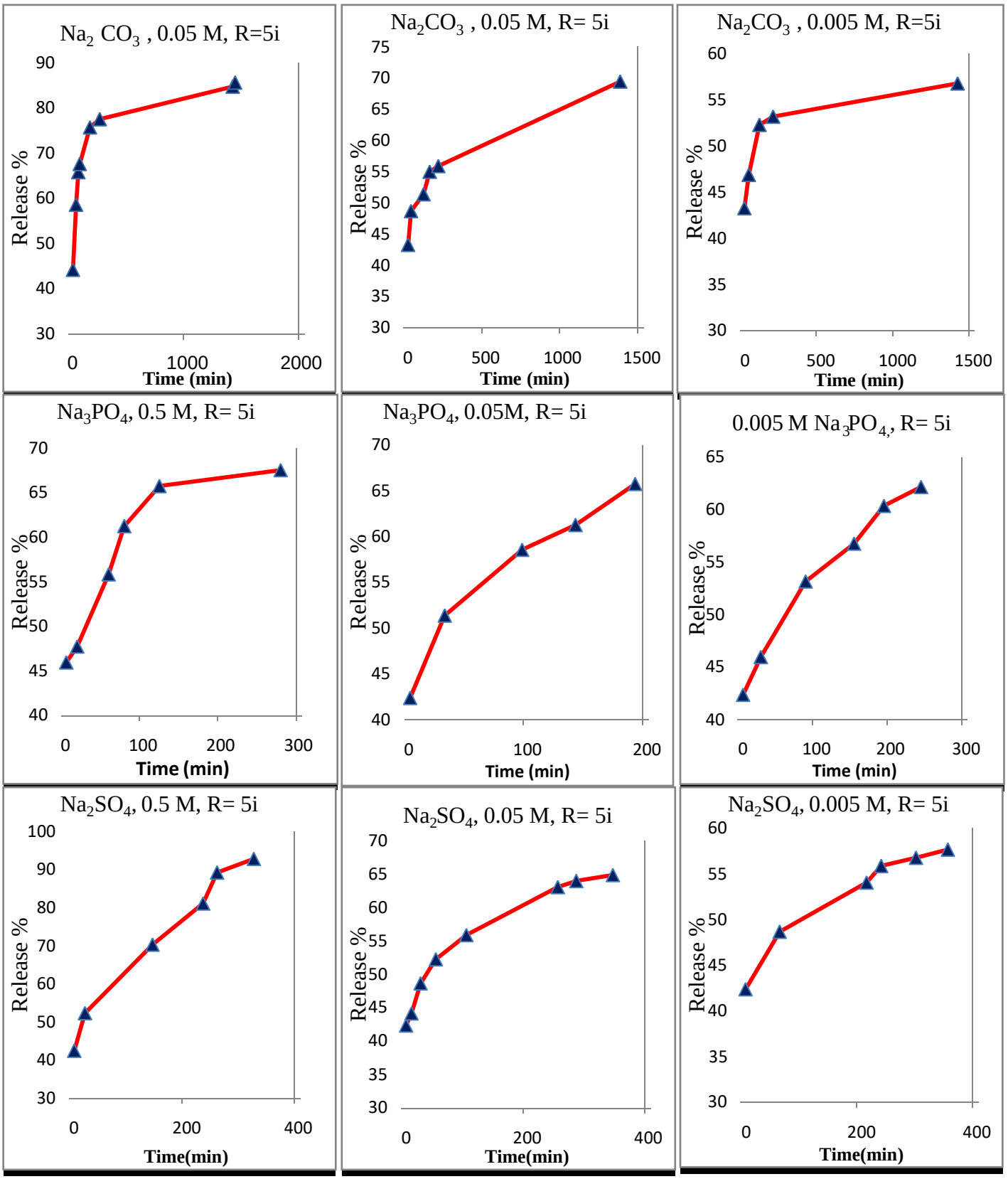

Figure 16. Release profiles of (FA) from the interlamellae of Ni-Al-FA-LDHs, the nanohybride into various aqueous solution systems with different concentrations were containing several anions of carbonate, phosphate and sulphate (Ni/Al=5 ion-exchange).

Table 6. Percentage Release, Rate Constant (k), Half Life ($t_{1/2}$) and Correlation Coefficients (r^2) Obtained from Fitting of the Release Data of (FA) from Ni-Al-FA LDH Nanohybrids into various aqueous solution (Ni/Al=5 ion-exchange).

Other parameters for pseudo-second order (Mol.L^{-1})		Pseudo-second order	Bhaskar equation	First order	Zeroth order	Maximum Time (min)	Maximum Release %	Concentration	Aqueous solution
t (min)	K×10^{-4} (L.mg^{-1} min^{-1}	r^2							$t_{1/2}$
17.570	159.000	0.999	0.881	0.735	0.551	1410	85	0.500	Na_2CO_3
37.375	75.000	0.998	0.990	0.903	0.837	1360	69	0.050	
12.530	223.000	0.999	0.782	0.953	0.936	1400	56	0.005	
9.666	289.000	0.998	0.908	0.759	0.720	275	67	0.500	Na_3PO_4
9.308	300.000	0.994	0.992	0.961	0.930	190	65	0.050	
12.888	217.000	0.995	0.980	0.980	0.965	1440	50	0.005	
18.974	147.000	0.981	0.875	0.899	0.900	320	92	0.500	Na_2SO_4
12.530	223.000	0.998	0.992	0.840	0.808	340	64	0.050	
12.601	222.000	0.998	0.995	0.845	0.828	350	57	0.005	

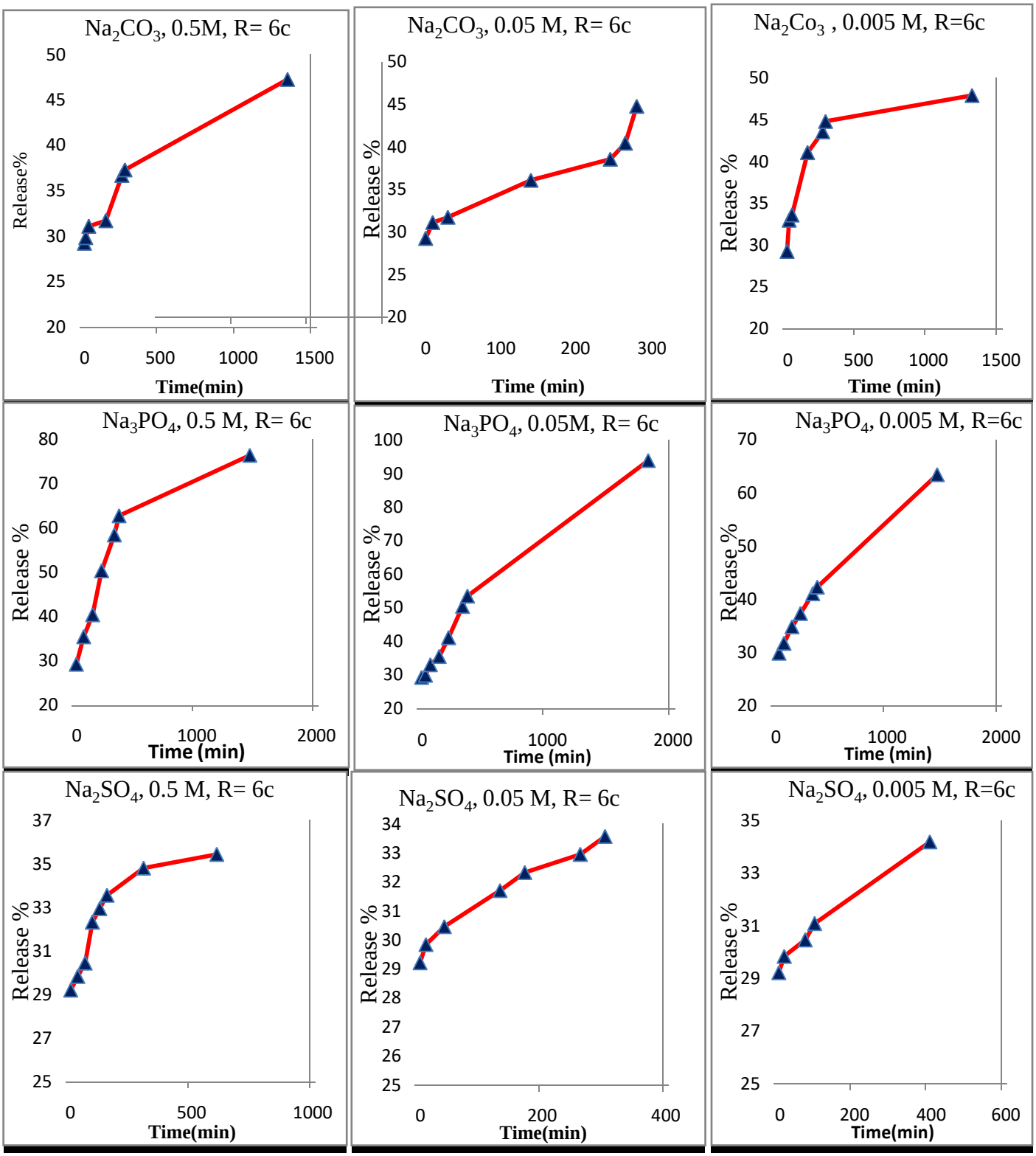

Figure 17. Release profiles of (FA) from the interlamellae of Ni-Al-FA-LDHs, the nanohybrid into various aqueous solution systems with different concentrations were containing several anions of carbonate, phosphate and sulphate (Ni/Al=6 Co-precipitation).

Table 7. Percentage Release, Rate Constant (k), Half Life ($t_{1/2}$) and Correlation Coefficients (r^2) obtained from Fitting of the release data of (FA) from Ni-Al-FA LDH Nanohybrid into various aqueous solution (Ni/Al=6 Co-precipitation).

Other parameters for pseudo-second order (Mol.L^{-1})		Pseudo-second order	Bhaskar equation	First order	Zeroth order	Maximum Time (min)	Maximum Release %	Concentration	Aqueous solution
$t_{1/2}$ (min)	K×10^{-4} (L.mg^{-1} min^{-1})	r^2							
99.648	19.000	0.995	0.966	0.834	0.812	1320	47	0.500	Na_2CO_3
50.602	38.000	0.995	0.844	0.620	0.597	1320	46	0.050	
31.762	61.000	0.999	0.830	0.568	0.537	1300	45	0.005	
140.130	14.000	0.998	0.952	0.852	0.726	1440	76	0.500	Na_3PO_4
233.550	8.000	0.977	0.902	0.961	0.930	1800	93	0.050	
212.790	9.000	0.998	0.986	0.987	0.965	1440	63	0.005	
23.355	82.000	0.999	0.942	0.724	0.715	600	35	0.500	Na_2SO_4
8.304	232.000	0.999	0.992	0.968	0.965	300	33	0.050	
14.532	133.000	0.999	0.995	0.779	0.762	400	34	0.005	

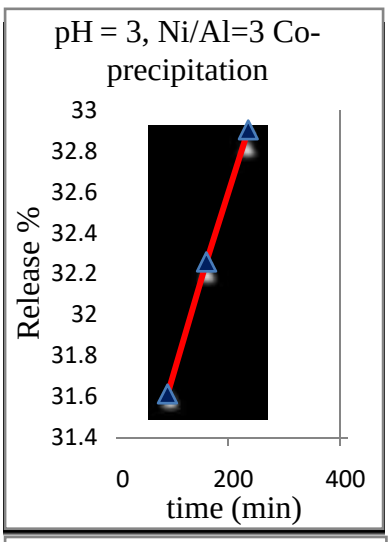
pH = 3, Ni/Al=3 Co-precipitation
Release %
33
32.8
32.6
32.4
32.2
32
31.8
31.6
31.4
0
200
400
time (min)

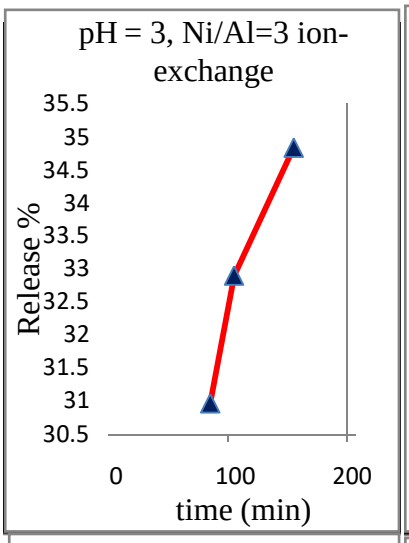
pH = 3, Ni/Al=3 ion-exchange
Release %
35.5
35
34.5
34
33.5
33
32.5
32
31.5
31
30.5
0
100
200
time (min)

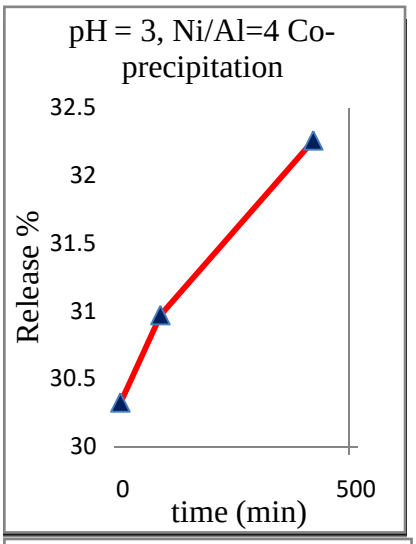
pH = 3, Ni/Al=4 Co-precipitation
Release %
32.5
32
31.5
31
30.5
30
0
500
time (min)

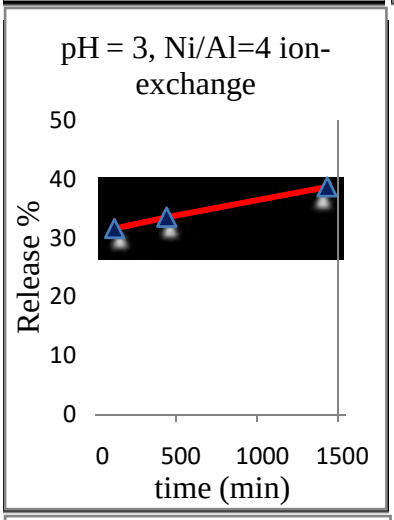
pH = 3, Ni/Al=4 ion-exchange
Release %
50
40
30
20
10
0
0
500
1000
1500
time (min)

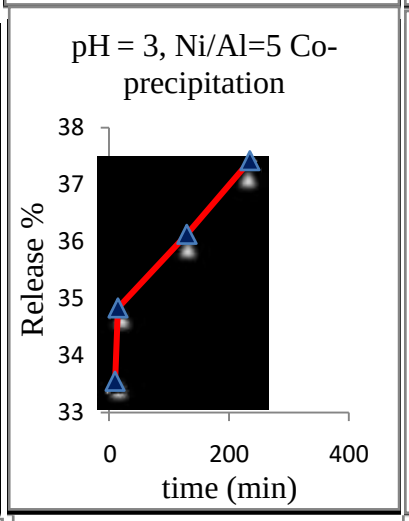
pH = 3, Ni/Al=5 Co-precipitation
Release %
38
37
36
35
34
33
0
200
400
time (min)

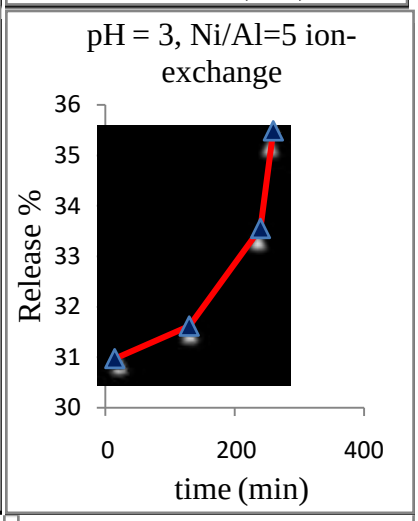
pH = 3, Ni/Al=5 ion-exchange
Release %
36
35
34
33
32
31
30
0
200
400
time (min)

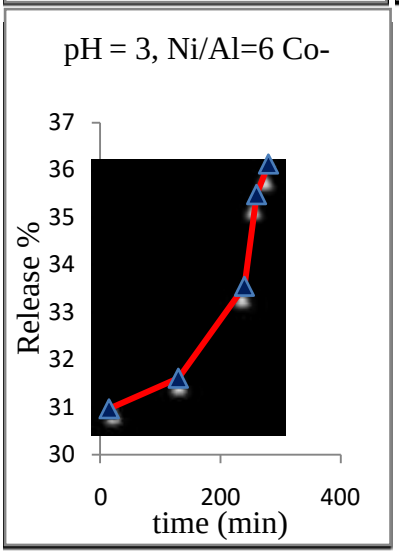
pH = 3, Ni/Al=6 Co-
Release %
37
36
35
34
33
32
31
30
0
200
400
time (min)

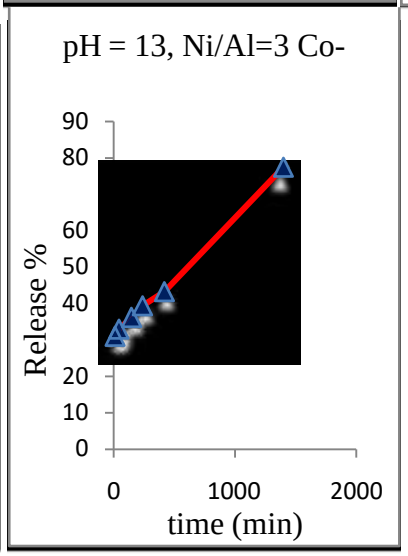
pH = 13, Ni/Al=3 Co-
Release %
90
80
60
50
40
20
10
0
0
1000
2000
time (min)

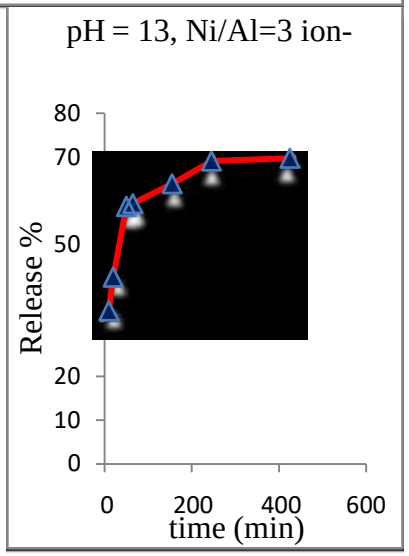
pH = 13, Ni/Al=3 ion-
Release %
80
70
50
20
10
0
0
200
400
600
time (min)

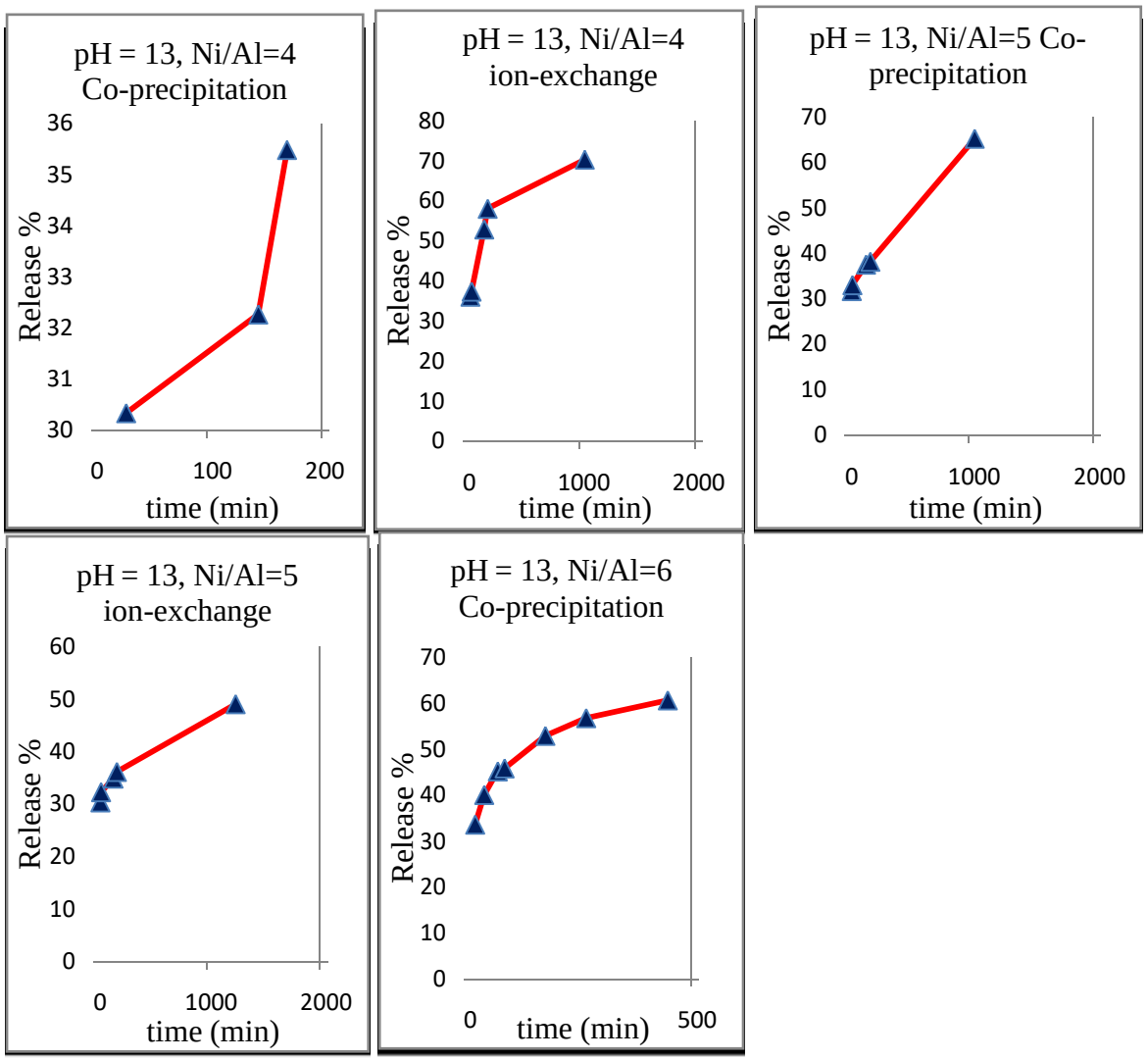

Figure 18. Release profiles of (FA) from the interlamellae of Ni-Al-FA-LDHs, the nanohybrid into various aqueous solution systems with different pH 3 and 13.

As shown in "Figure 18" the release profiles of folic acid from Ni/Al-LDH nanohybrid sheet. It was concluded that Ni/Al-FA-LDH is more stable in acidic media due to the lowest value of release percentages of folic acid compared with those obtain from basic media because of Al^{3+} ions can be readily dissolved into the alkaline media in forms of $Al(OH)^{4-}$ or its dehydrated form, AlO_2^- ions. Therefore, it is possible that $Al3^+$ in the brucite-type layers may be leached out and enters into the solution. It is well known that LDHs lose their stability without the presence of trivalent cations.

3.3. Release Kinetics

Release kinetics of FA has been evaluated with various models such as zeroth order, first order and pseudo-second order "Figure 19 - 25". Chemical kinetic study of the release behavior of FA was further elucidated by fitting the data to Bhaskar equation as shown in (Fig. 28 to 34) and (Table 1 - 7), as well as novel equations.

The corresponding rate constants together with the r^2 values obtained from the fittings are summarized in (Table 1 - 7). By comparing the correlation coefficient, r^2 values obtained from the fitting with those modules, it is clear that the release profile of FA from the nanohybrid was governed by the pseudo-second order kinetics modules. The rate constant k obtained from the pseudo-second order kinetic model was more pronounced in case of 0.05 M carbonate solution than in (0.5 and 0.005 M). While, phosphate solution has the highest value of rate constant (Table 1).

Furthermore, it could be seen that the rate constant and finally release rate depend on the molar ratio of Ni/Al, the nature of aqueous solution and the concentration of aqueous solution (Table 1 - 7). Generally, the phosphate anion has the highest value of rate constant, at the same time; it has the lowest value of release percentage.

Additionally, it can be seen from "Figure 19 - 25" that the aqueous solution of 0.5M concentration can be considered more convenient to present the release process due to it could be released much more amount of folic acid intercalated and it is too clockwork.

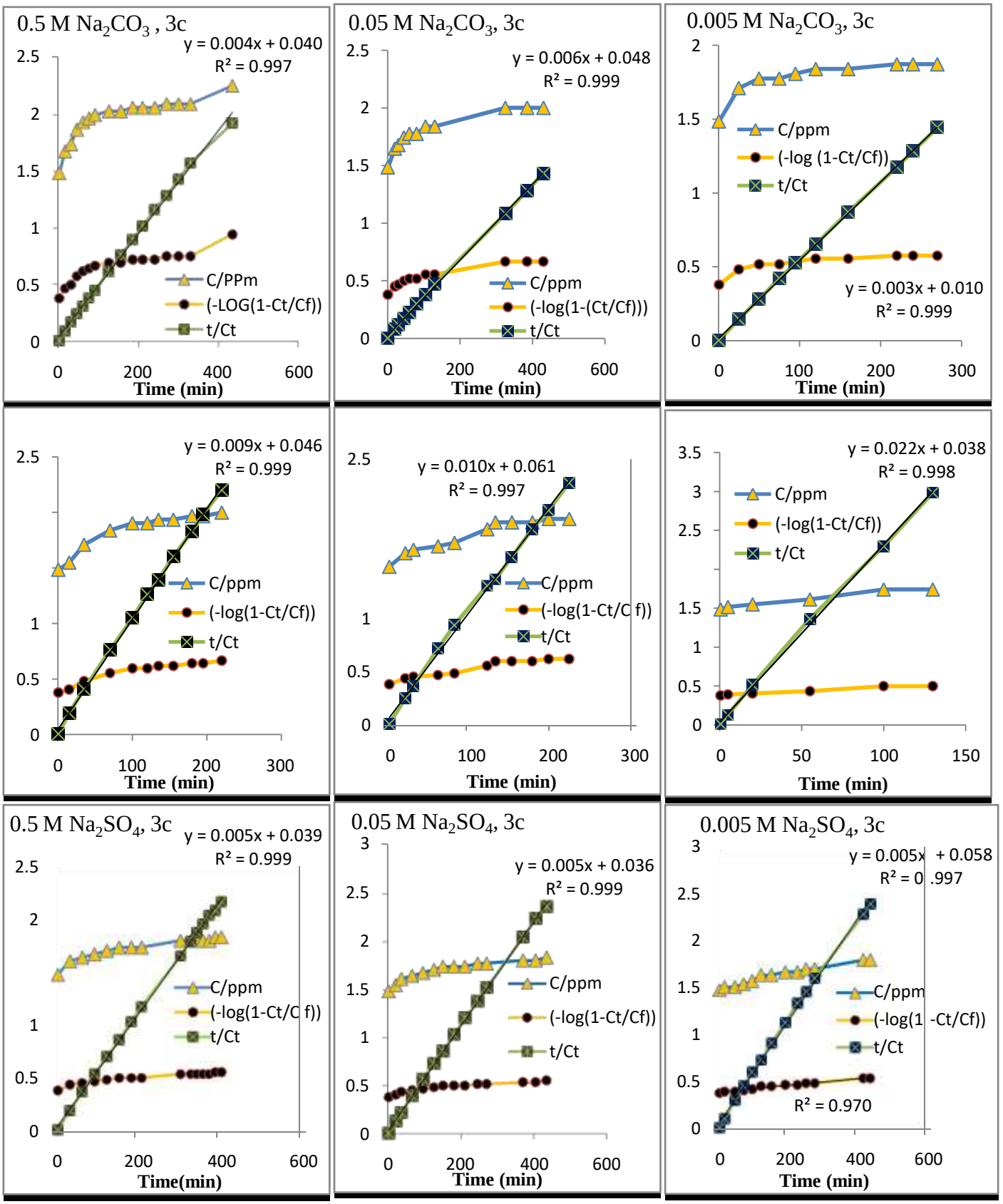

Figure 19. Fitting of the data to the zeroth, first and pseudo-second order kinetics for FA released into different aqueous solutions (Ni/Al=3 Co-precipitation).

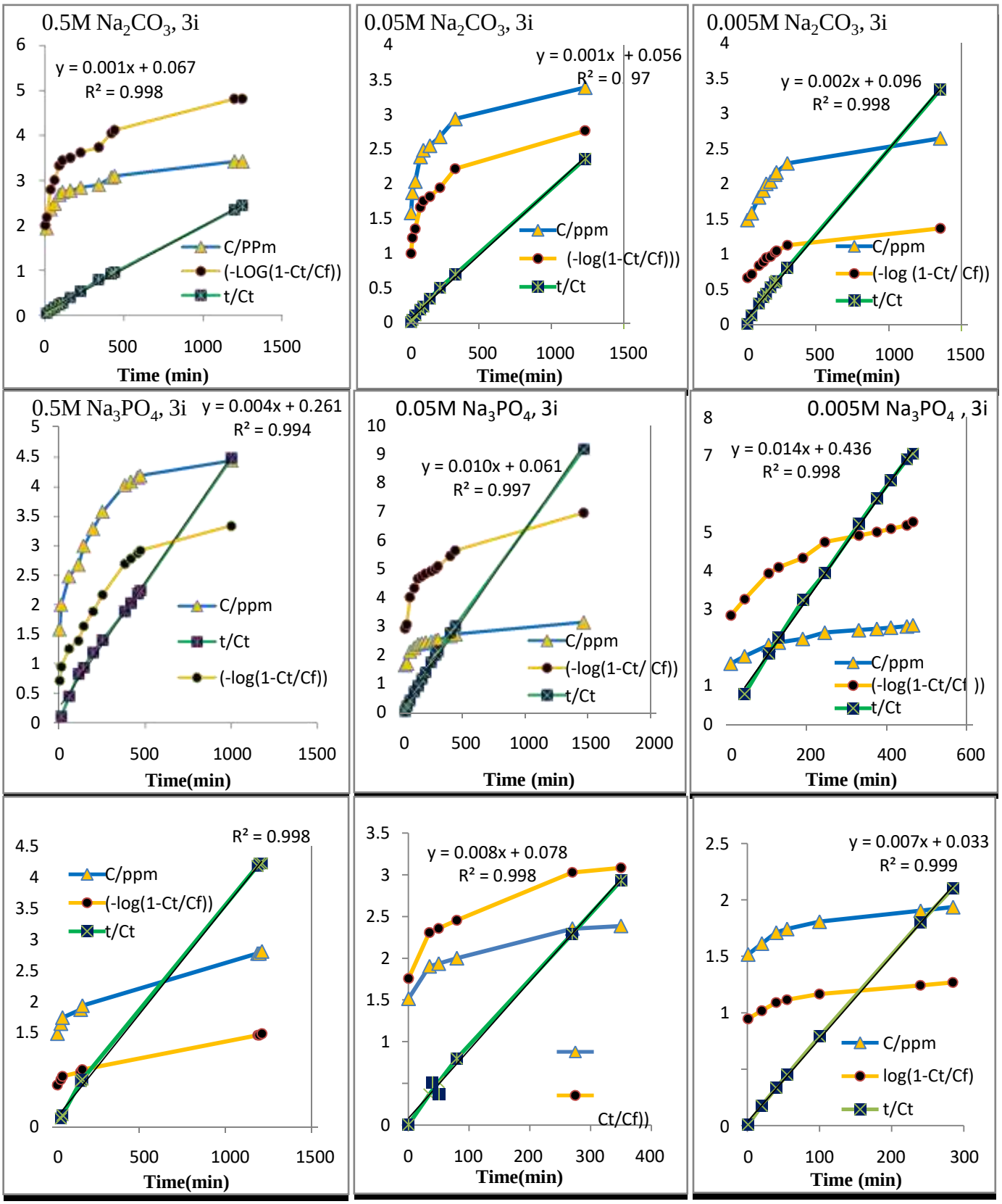

Figure 20. Fitting of the data to the zeroth, first and pseudo-second order kinetics for FA released into different aqueous solutions (Ni/Al=3 ion-exchange).

As shown in "Figure 21 – 23", the release kinetics of compounds (Ni/Al=4 Co-precipitation), (Ni/Al=4 ion-exchange) and (Ni/Al=5 Co-precipitation) in phosphate and sulphate aqueous solutions were not clear due to the release percentages value were too low. It is indicate that the reaction did not finish.

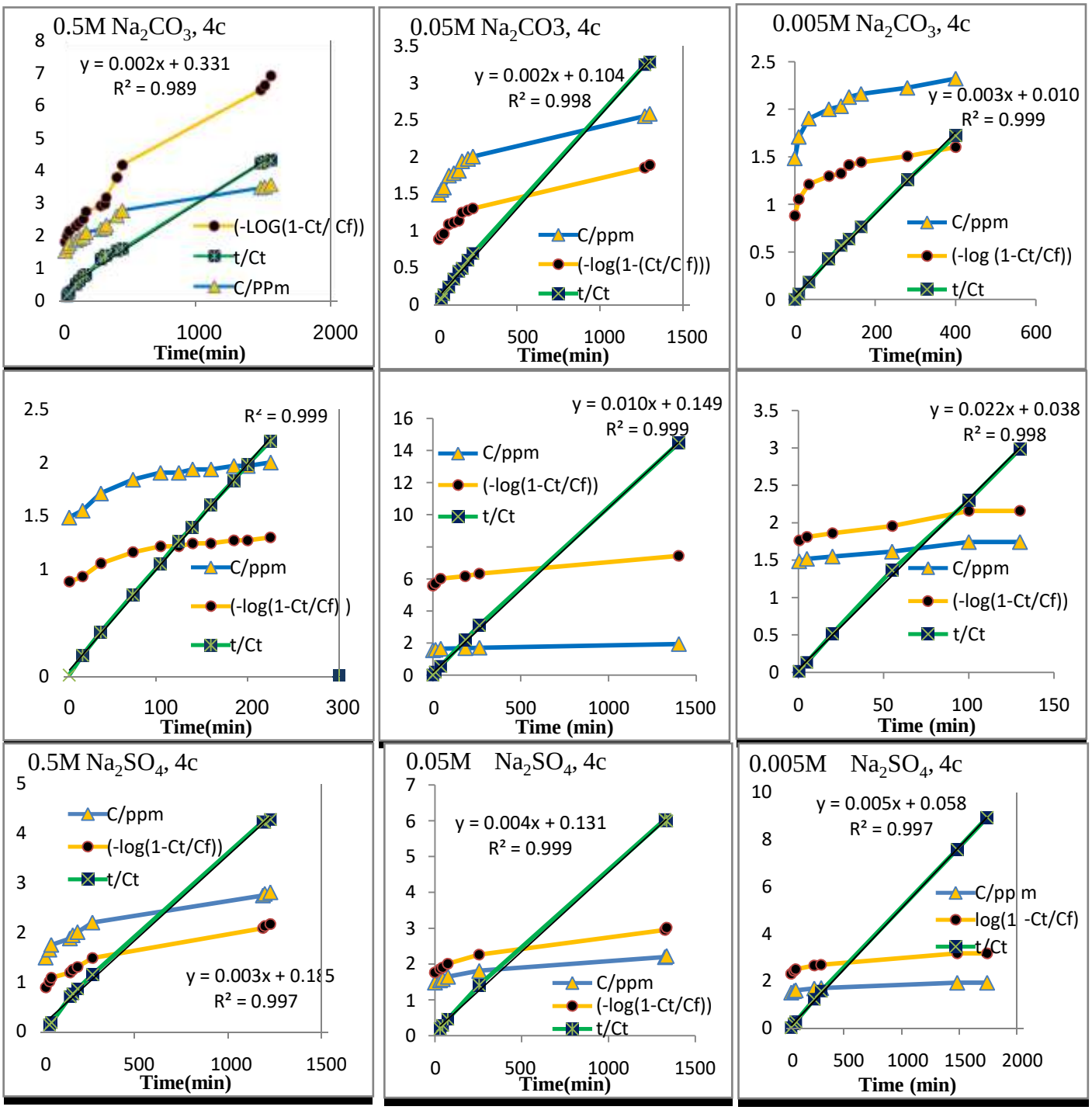

Figure 21. Fitting of the data to the zeroth, first and pseudo-second order kinetics for FA released into different aqueous solutions (Ni/Al=4 Co-precipitation).

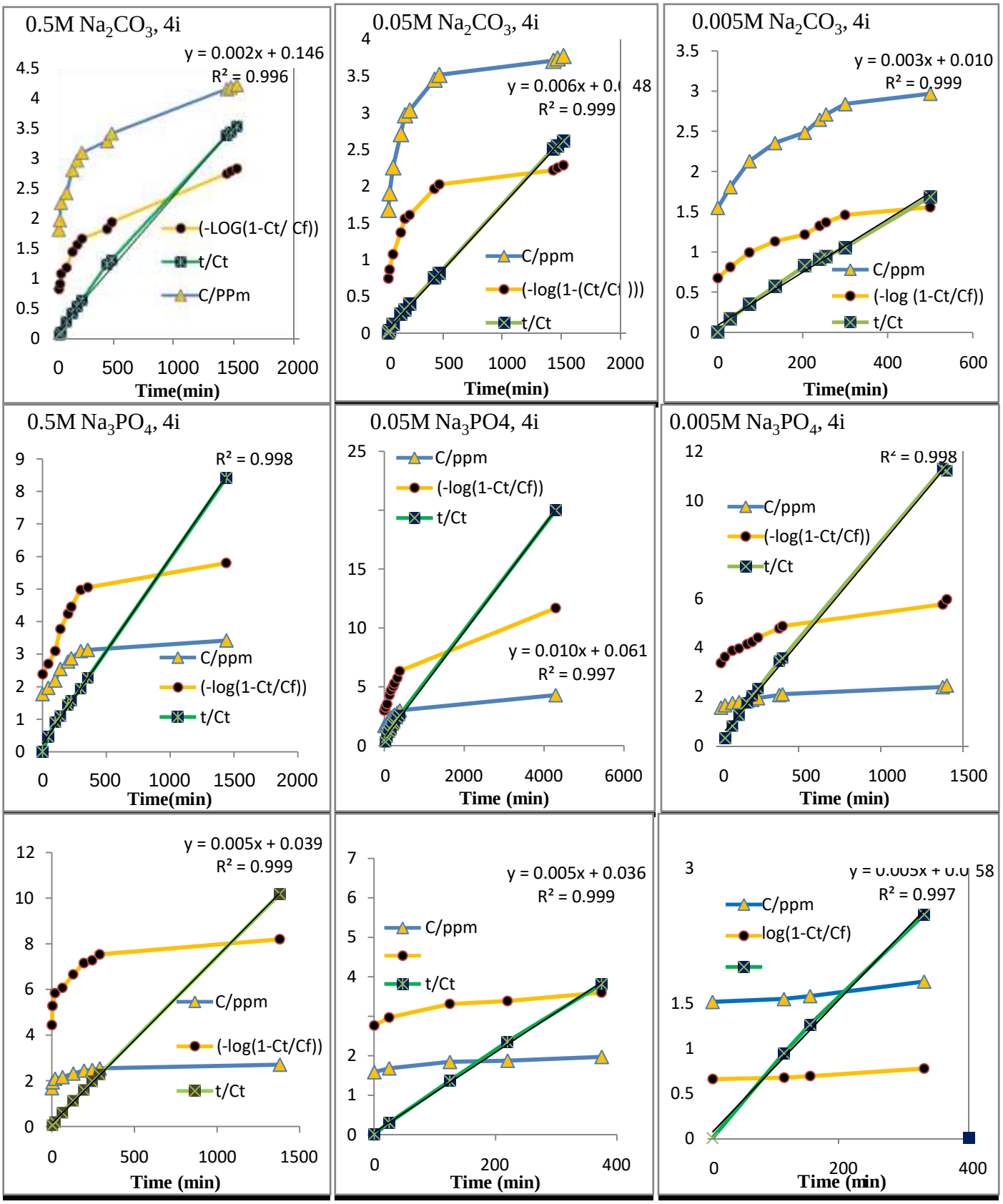

Figure 22. Fitting of the data to the zeroth, first and pseudo-second order kinetics for FA released into different aqueous solutions (Ni/Al=4 ion-exchange).

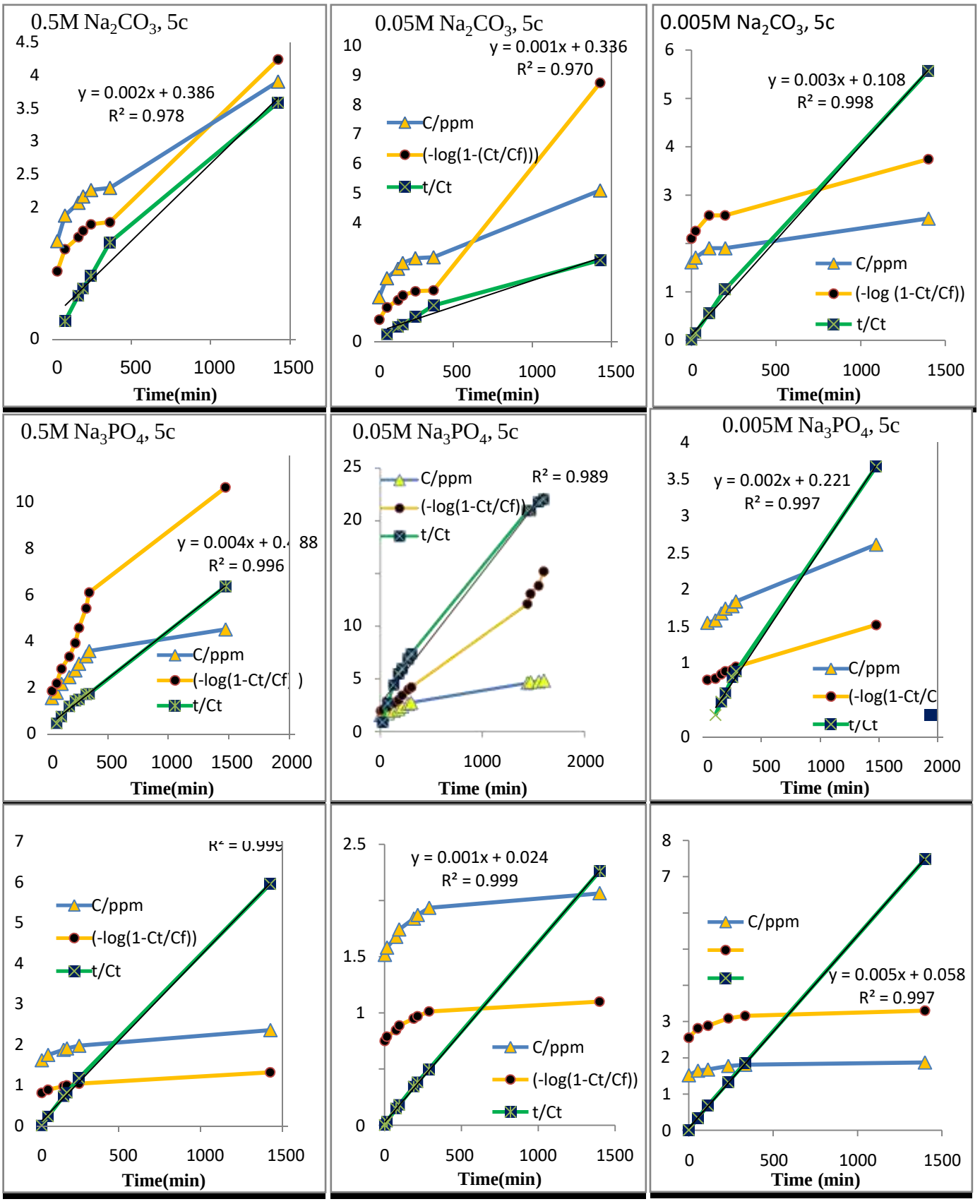

Figure 23. Fitting of the data to the zeroth, first and pseudo-second order kinetics for FA released into different aqueous solutions (Ni/Al=5 Co-precipitation).

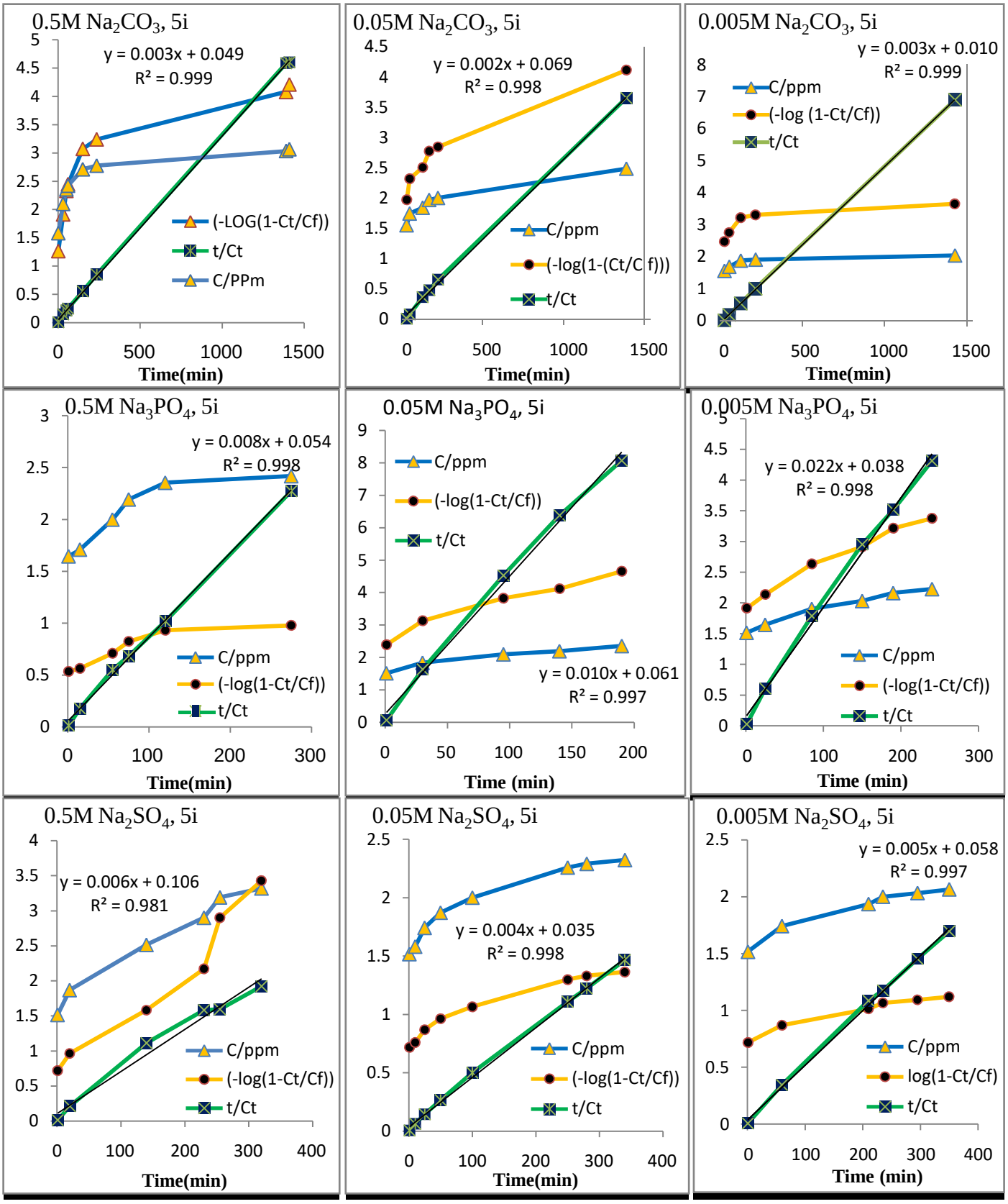

Figure 24. Fitting of the data to the zeroth, first and pseudo-second order kinetics for FA released into different aqueous solutions (Ni/Al=5 ion-exchange).

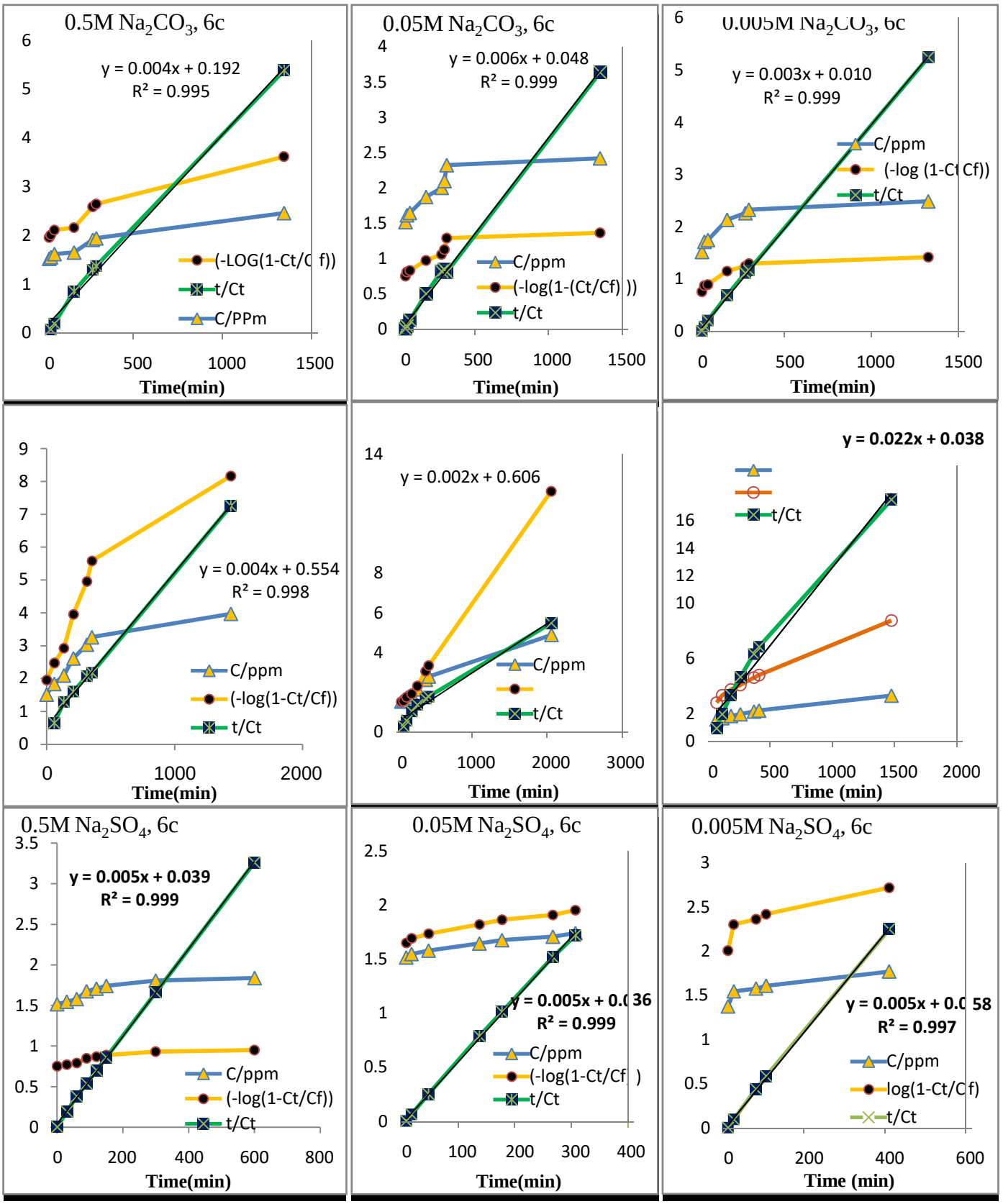

Figure 25. Fitting of the data to the zeroth, first and pseudo-second order kinetics for FA released into different aqueous solutions (Ni/Al=6 Co-precipitation).

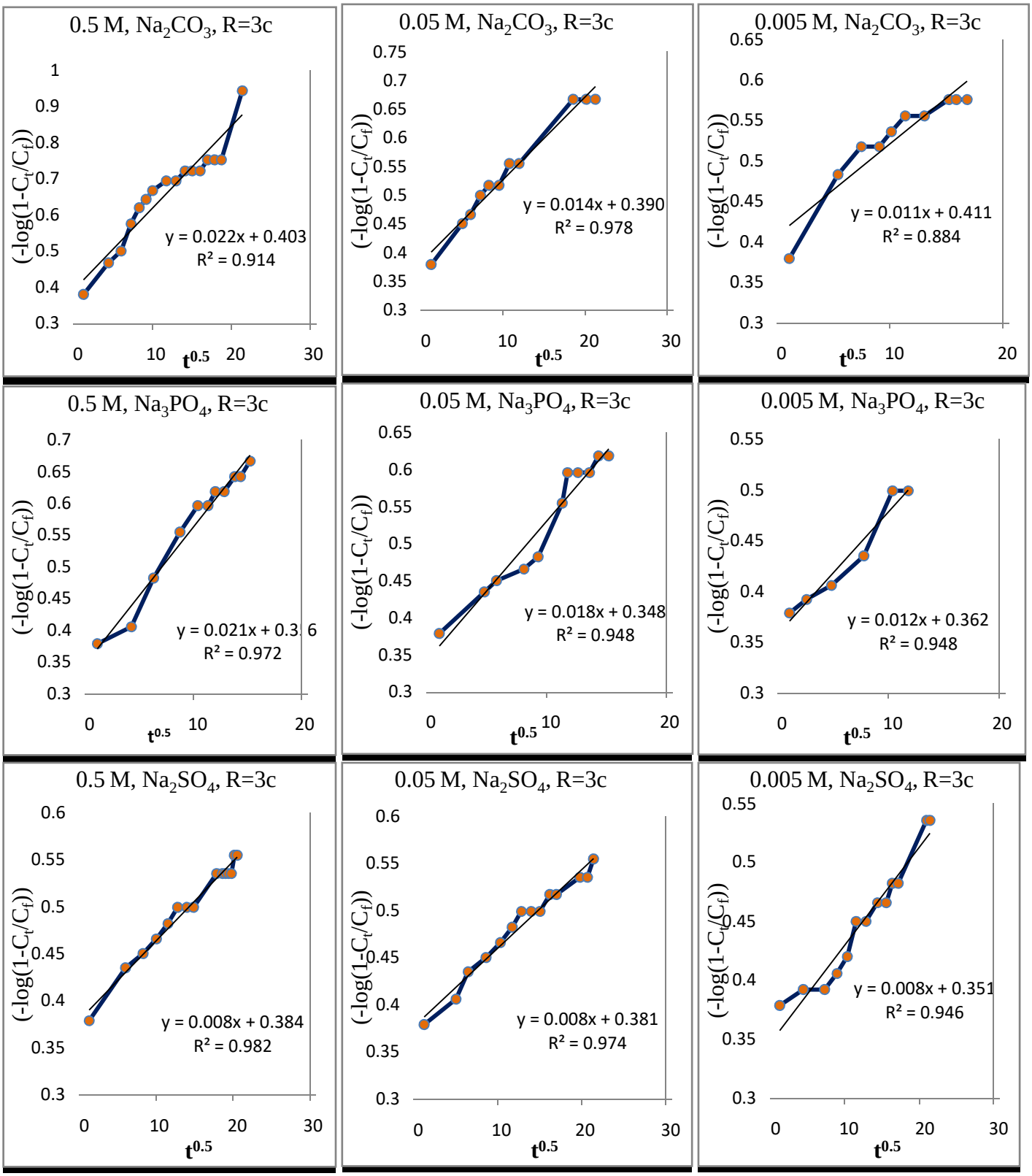

Figure 26. Fitting the data of the release of (FA) from the interlamellae of Ni-Al-FA-LDHs, the nanohybrid into various aqueous solution systems with different concentrations was containing several anions of carbonate, sulphate and phosphate using Bhaskar equation (Ni/Al=3 Co-precipitation).

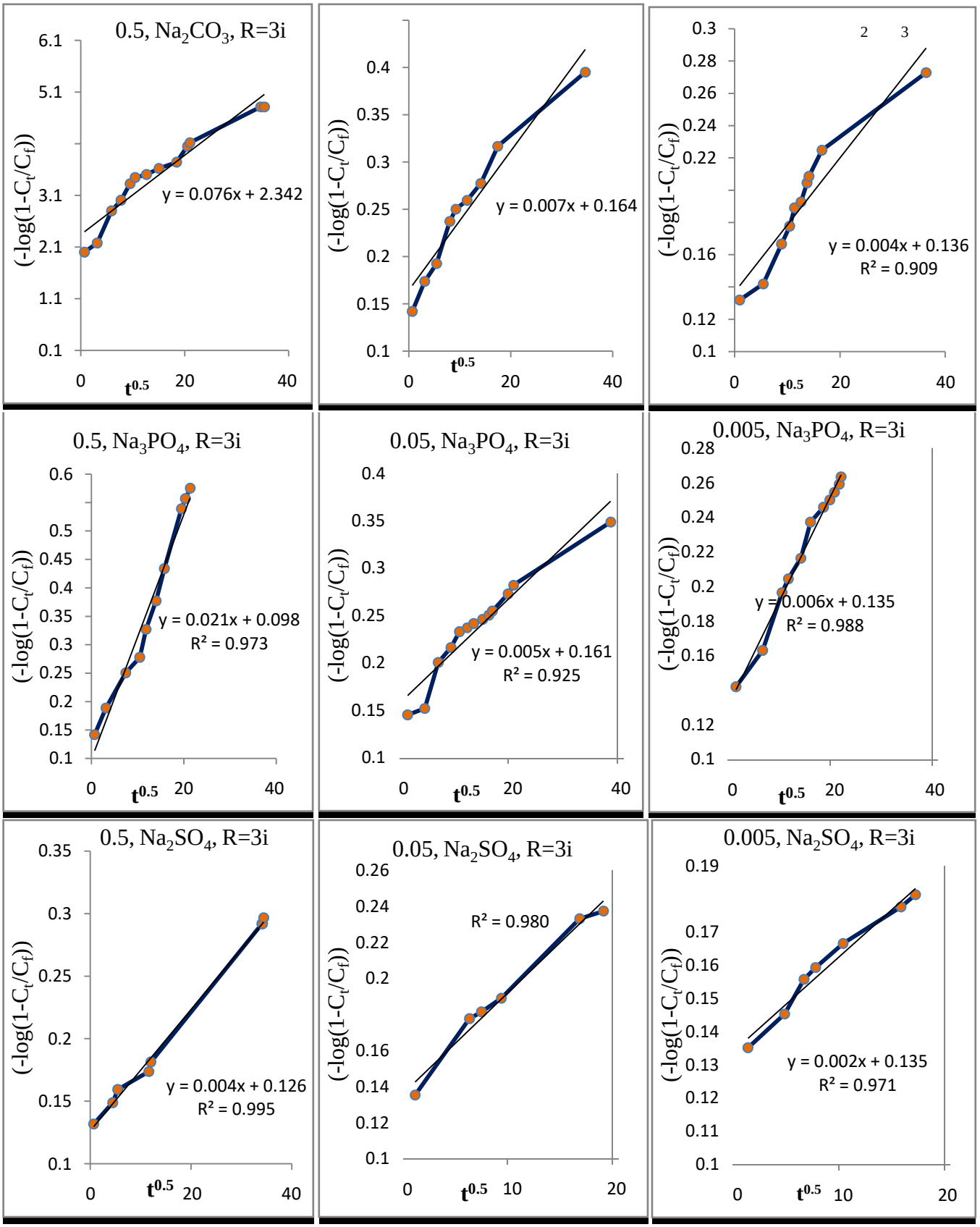

Figure 27. Fitting the data of the release of (FA) from the interlamellae of Ni-Al-FA-LDHs, the nanohybrid into various aqueous solution systems with different concentrations was containing several anions of carbonate, sulphate and phosphate using Bhaskar equation (Ni/Al=3 ion-exchange).

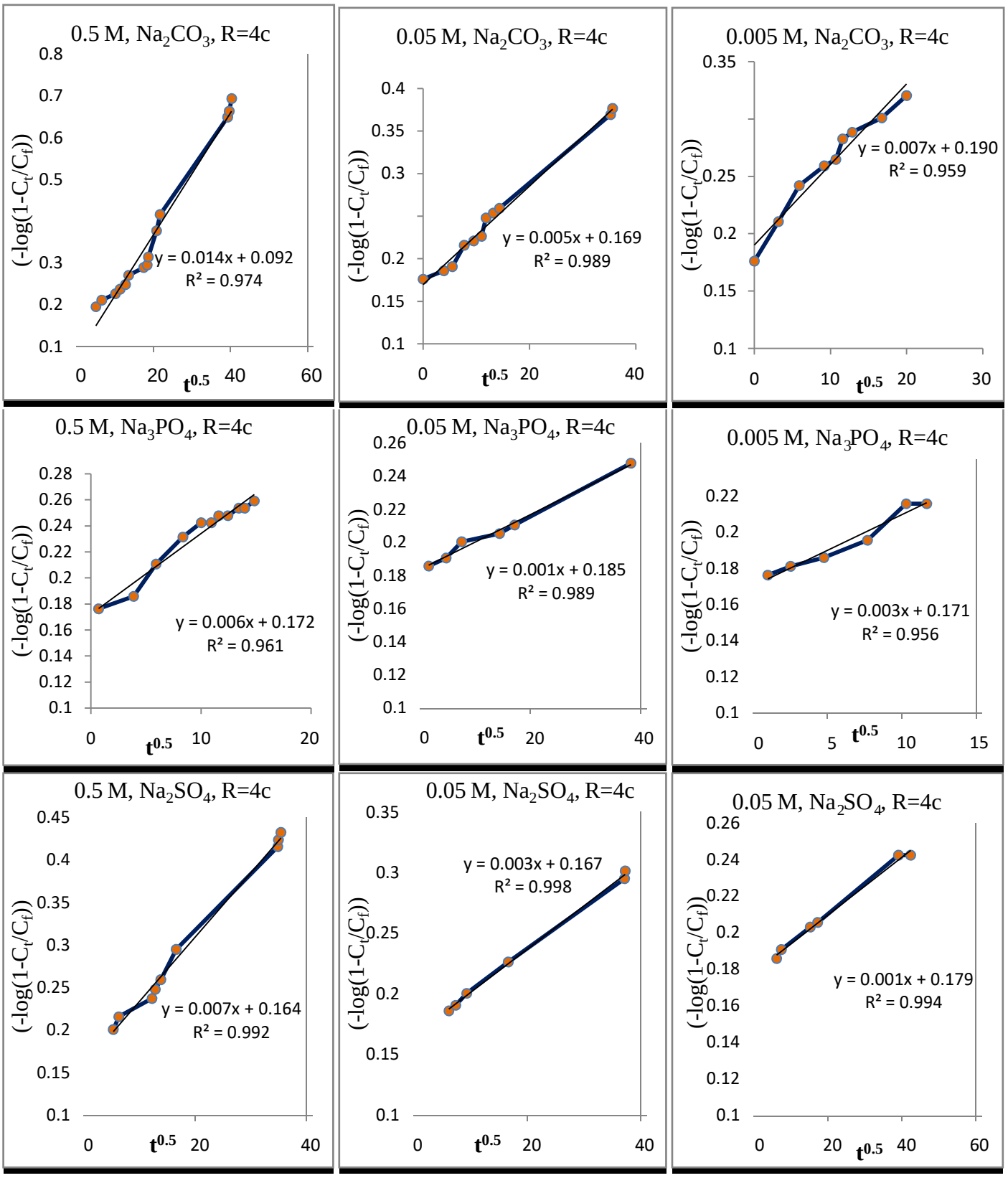

Figure 28. Fitting the data of the release of (FA) from the interlamellae of Ni-Al-FA-LDHs, the nanohybrid into various aqueous solution systems with different concentrations was containing several anions of carbonate, sulphate and phosphate using Bhaskar equation (Ni/Al=4 Co-precipitation).

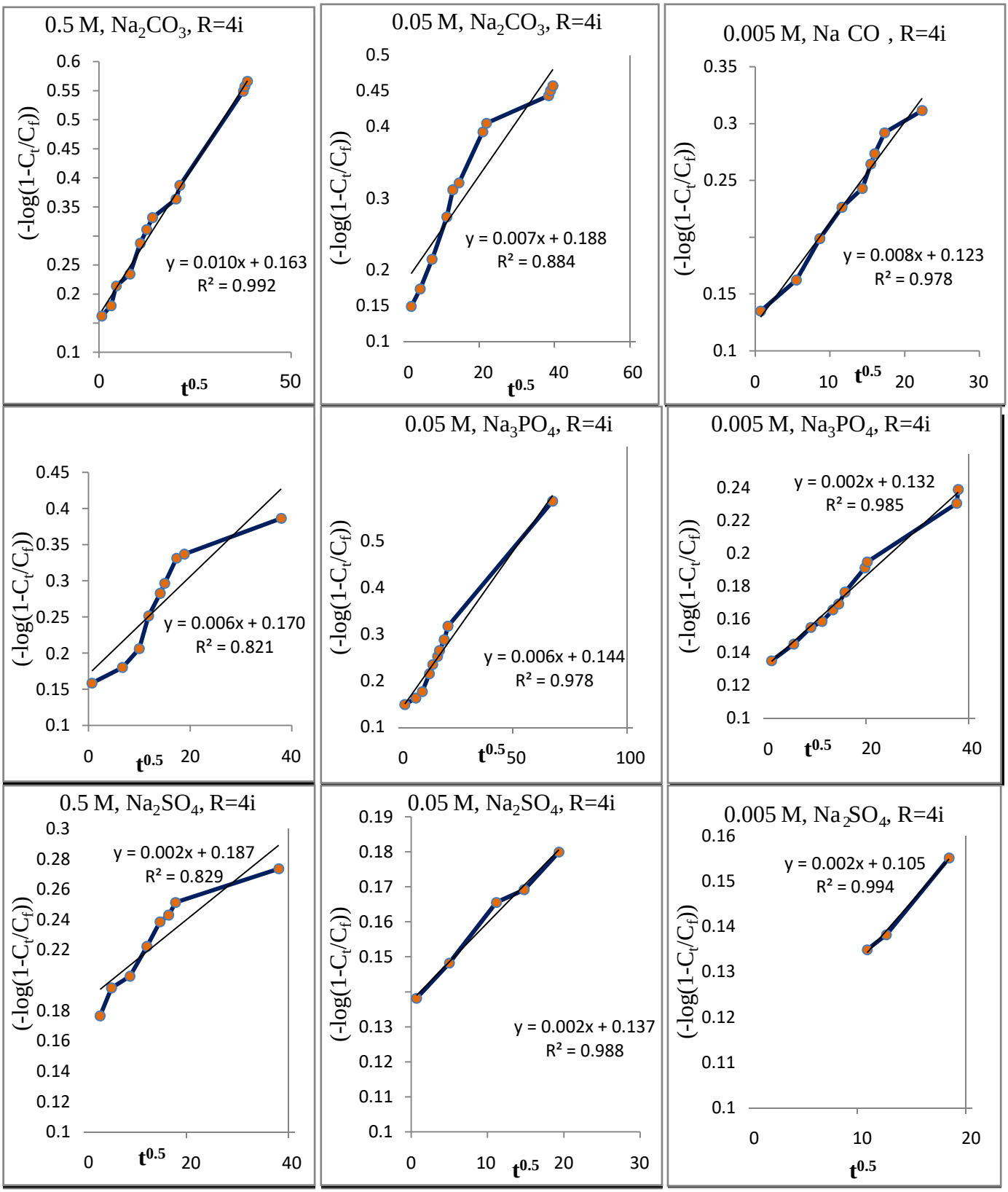

Figure 29. Fitting the data of the release of (FA) from the interlamellae of Ni-Al-FA-LDHs, the nanohybrid into various aqueous solution systems with different concentrations was containing several anions of carbonate, sulphate and phosphate using Bhaskar equation (Ni/Al=4 ion-exchange).

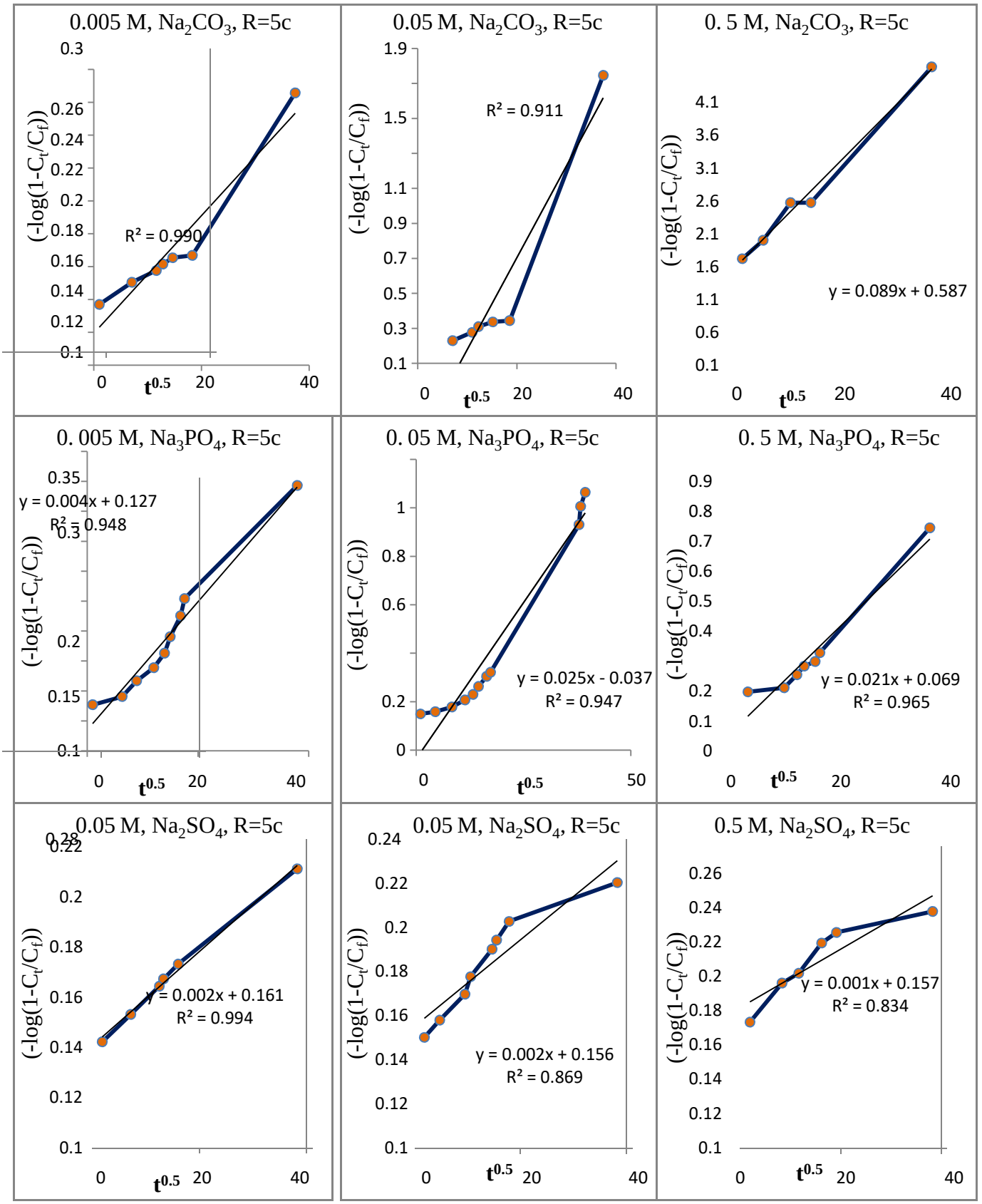

Figure 30. Fitting the data of the release of (FA) from the interlamellae of Ni-Al-FA-LDHs, the nanohybrid into various aqueous solution systems with different concentrations was containing several anions of carbonate, sulphate and phosphate using Bhaskar equation (Ni/Al=5 Co-precipitation).

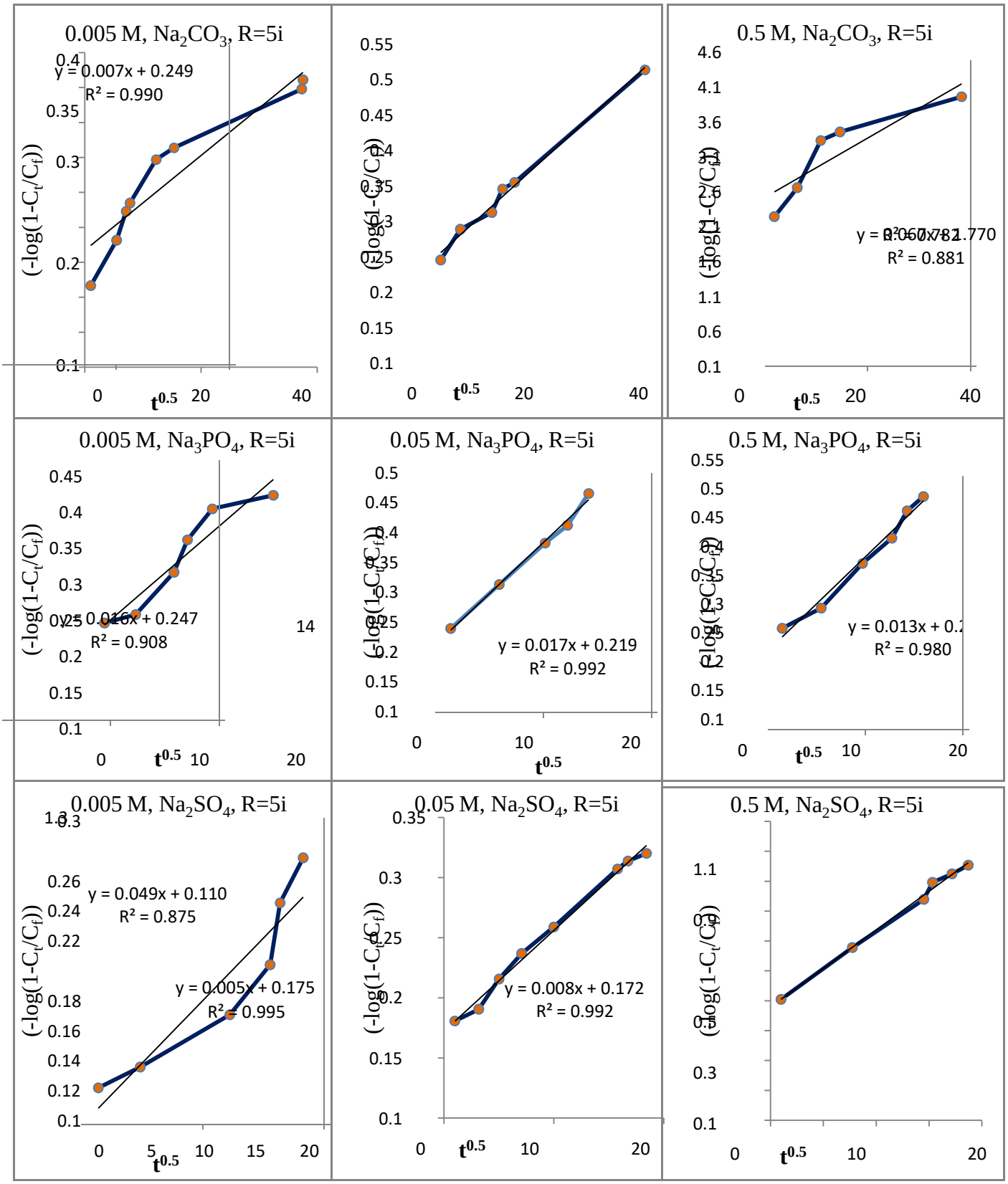

Figure 31. Fitting the data of the release of (FA) from the interlamellae of Ni-Al-FA-LDHs, the nanohybrid into various aqueous solution systems with different concentrations was containing several anions of carbonate, sulphate and phosphate using Bhaskar equation (Ni/Al=5 ion-exchange).

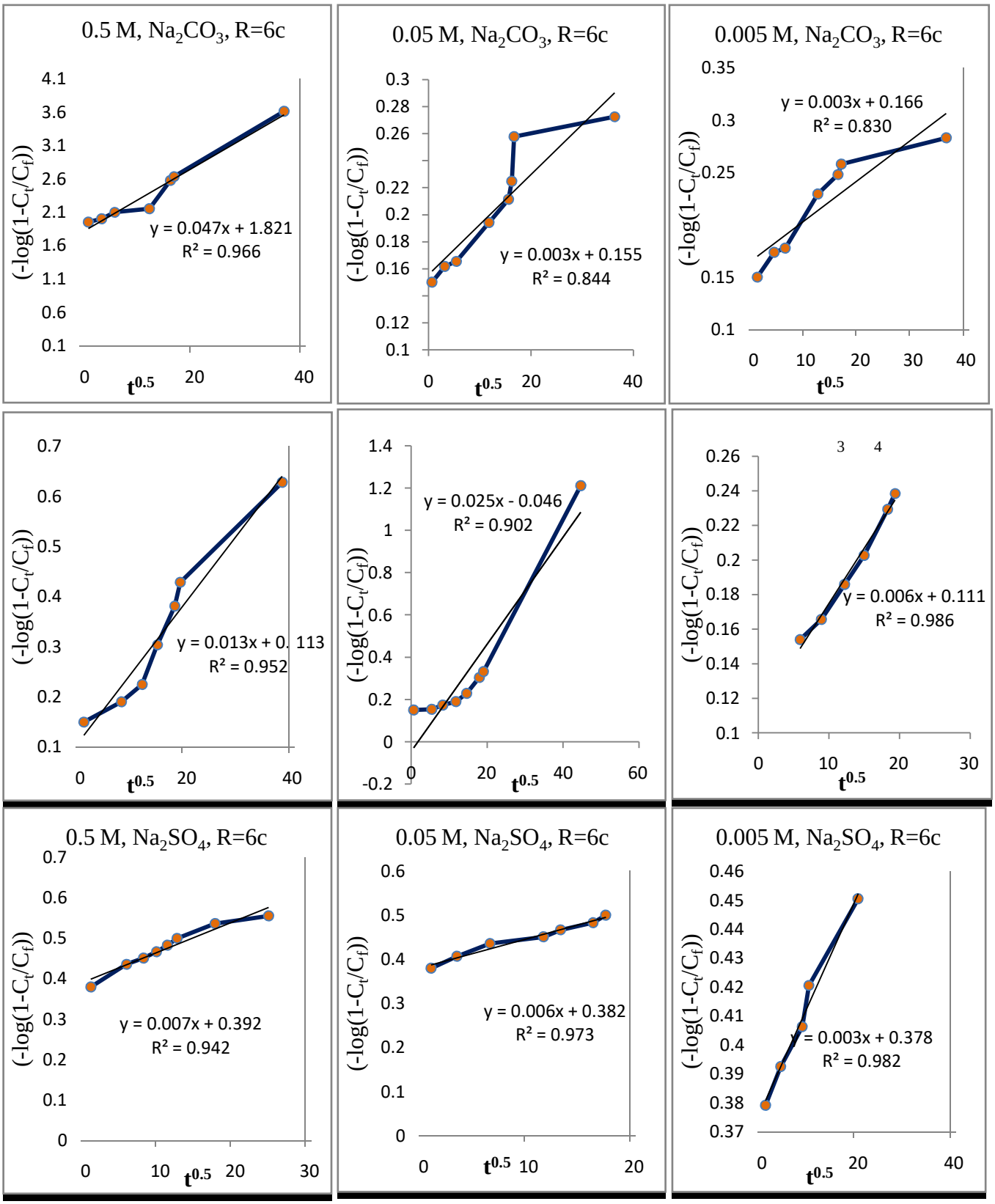

Figure 32. Fitting the data of the release of (FA) from the interlamellae of Ni-Al-FA-LDHs, the nanohybrid into various aqueous solution systems with different concentrations was containing several anions of carbonate, sulphate and phosphate using Bhaskar equation (Ni/Al=6 Co-precipitation).

An Artificial Neural Network (ANN) based on the Quick Propagation (QP) algorithm was used to predict Folic acid release from Ni-Al-FA- LDHs, by treating the entire release profile as a time-series curve, and estimating the whole profile. The controlled-release parameter vectors (concentrations and time) were employed as the input layer, and the output layer was the concentration of folic acid released. The network performance was evaluated by comparing the predicted release profiles to those obtained from experiments and theoretical models the results were more coincided "Figure 33".

It can be seen from "Figures 34 and 36 - 41" that the release profiles of FA from the interlamellae of (Ni-Al-FA) LDHs obtained from estimation method. The benefit of this method is to predict the concentration of folic acid with the time.

Comparing the data (correlation coefficient r^2 and rate constant k) (Table 1 and Table 8) those obtained from experiments and theoretical models respectively, it could be seen that the values are very close. On the other hand, the maximum release and maximum time are the same due to the maximum values of concentration and time used in learning process are taken from experimental data and this method is very convenient.

As shown in "Figure 35", the release kinetics was fitted for predicted folic acid released and it indicates that the estimation method did not affect on the reaction order.

The results obtained from this approach coincided with the experimental value and it is regarded to be more suitable.

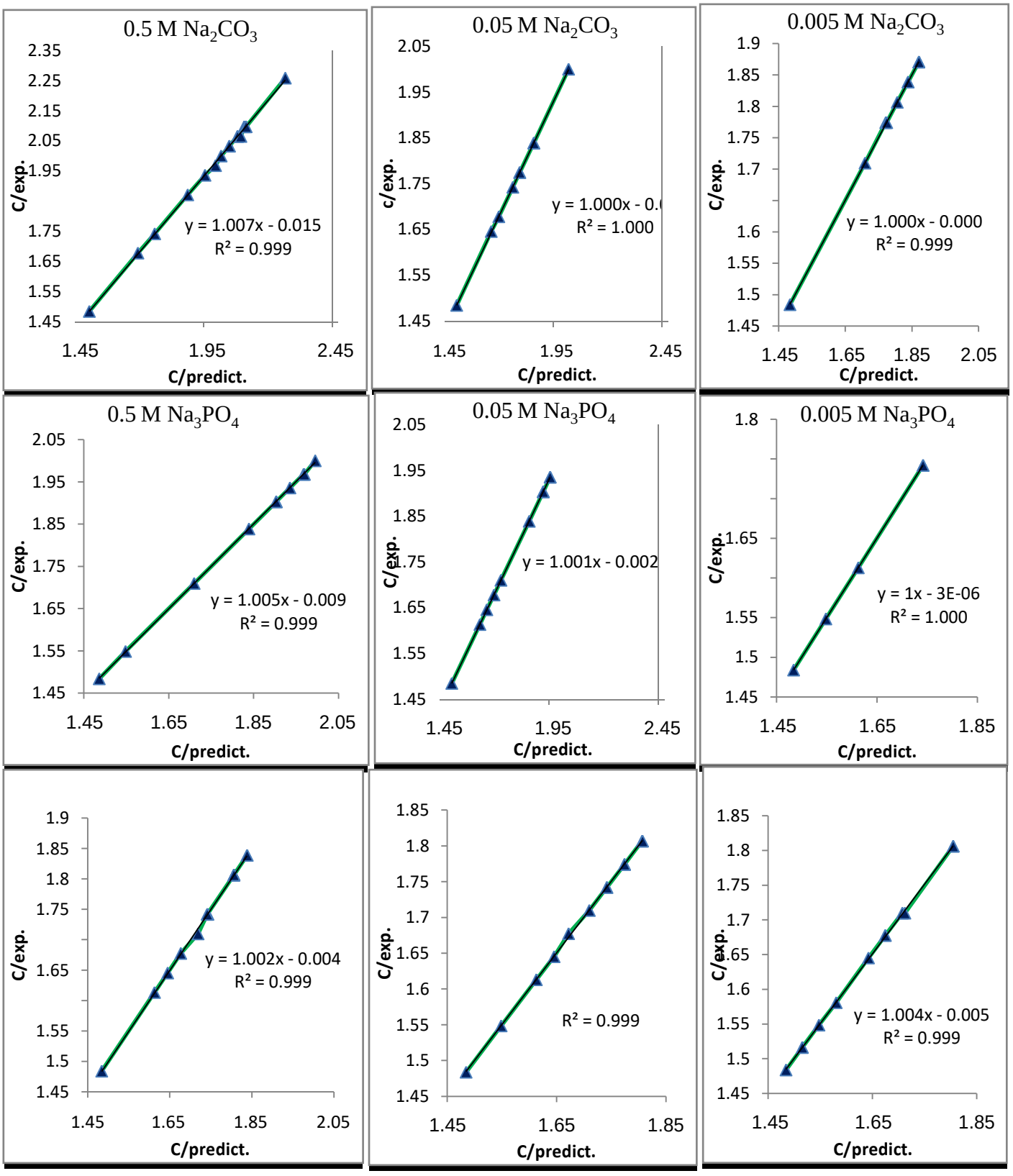

Figure 33. Experimental values of Folic acid release concentration versus predicted values (Ni/Al=3 Co-precipitation).

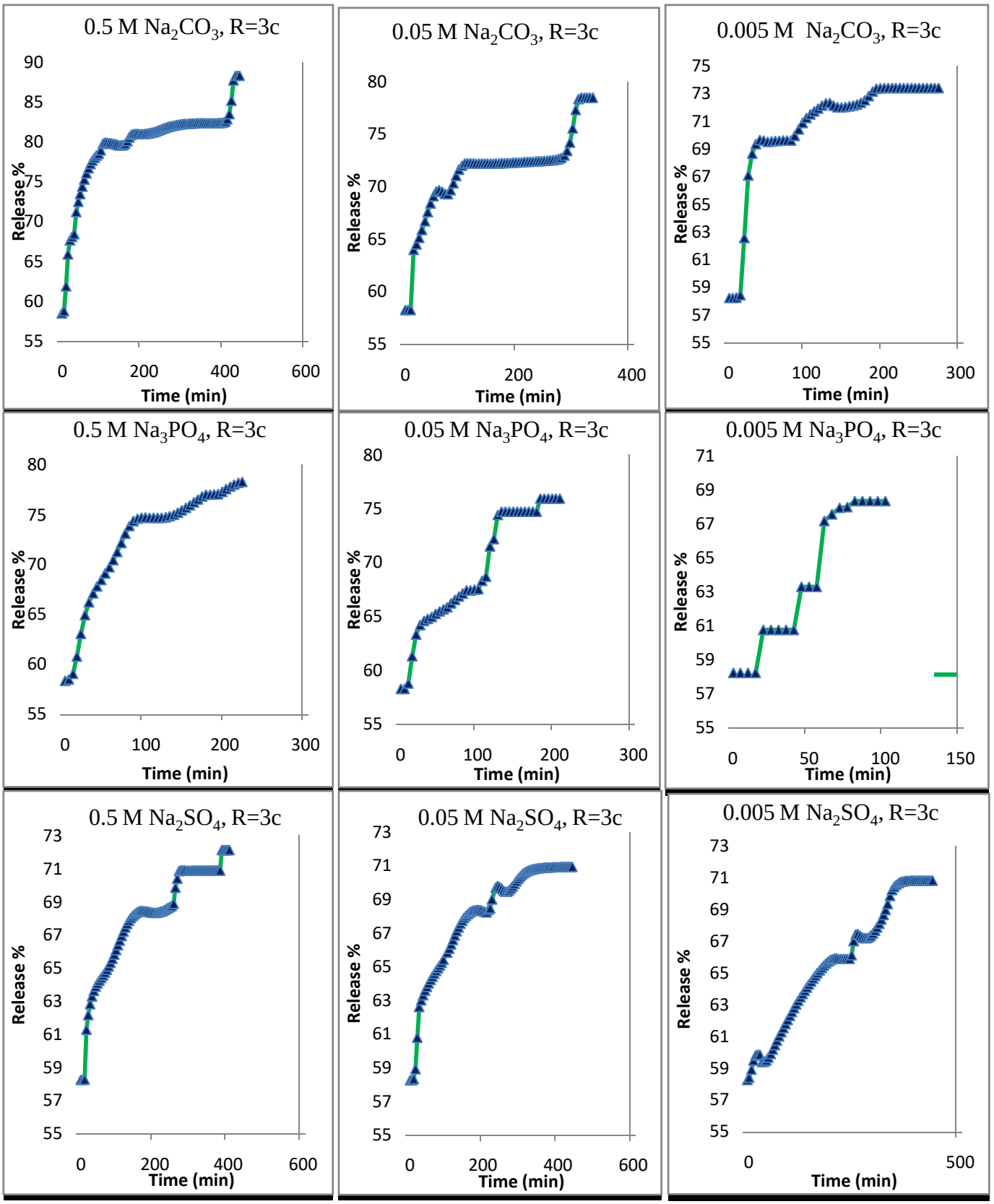

Figure 34. Release profiles of (FA) from the interlamellae of (Ni-Al-FA) LDHs that obtained from estimation method, the nanohybrid into various aqueous solution systems with different concentrations were containing several anions of carbonate, phosphate and sulphate (Ni/Al=3 Co-precipitation).

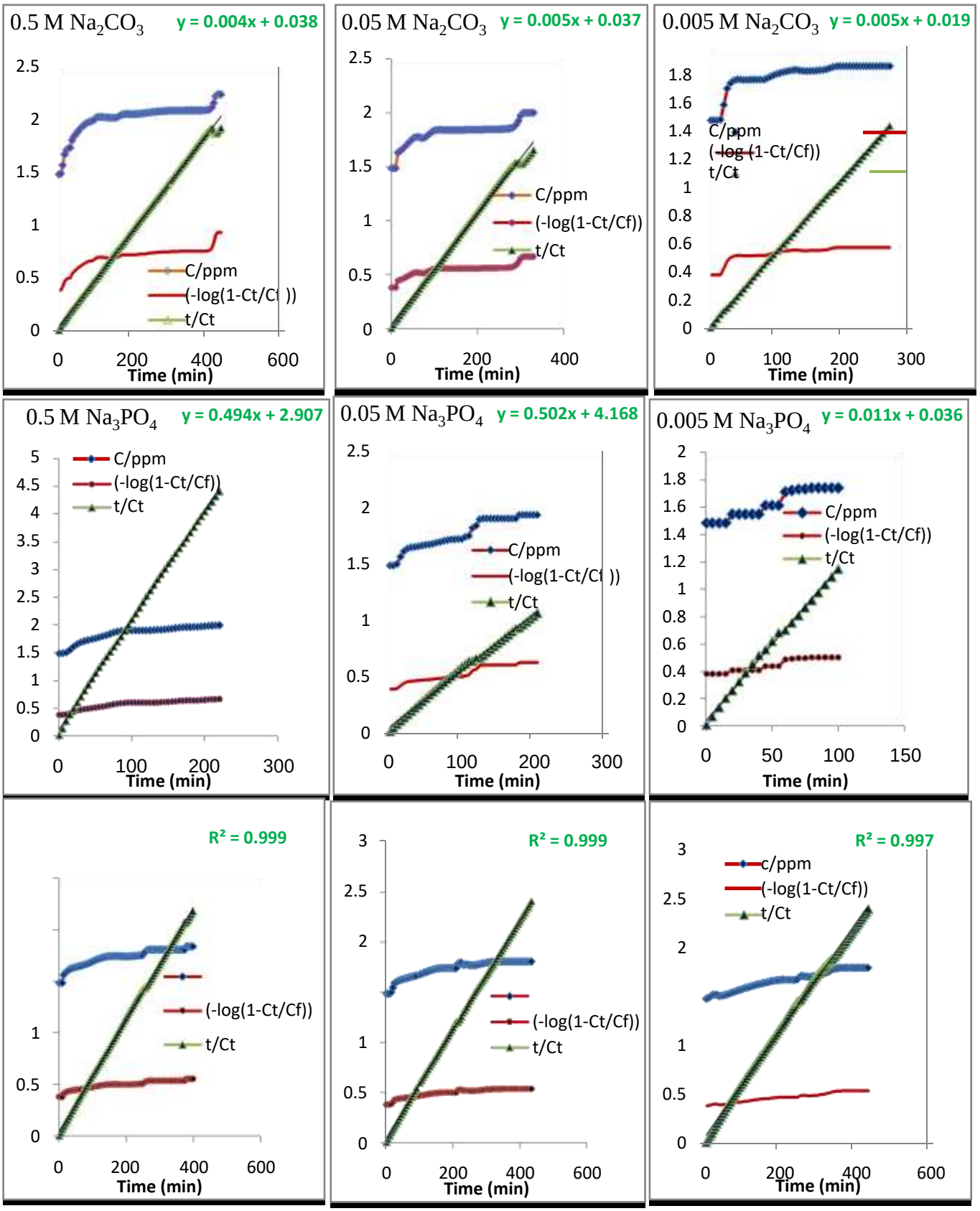

Figure 35. Fitting of the data to the zeroth, first and pseudo-second order kinetics for predicted folic acid released into different aqueous solutions (Ni/Al=3 Co-precipitation.

Table 8. Predicted values for chosen outputs of Rate Constant (k), Half Life ($t_{1/2}$) and Correlation Coefficients (r^2) obtained from Alyuda Neuro Intelligence software of the release data of (FA) from Ni-Al-FA LDH Nanohybrid into various aqueous solution (Ni/Al=3 Co-precipitation).

Aqueous solution	Concentration (mol L^{-1})	Maximum Release %	Maximum Time (min)	Zeroth order	First order	Bhaskar equation	Pseudo-second order	Other parameters for pseudo-second order	
				r^2				$K\times10^{-4}$ ($L.mg^{-1}$ min^{-1})	$t_{1/2}$ (min)
Na_2CO_3	0.500	88	435	0.618	0.713	0.828	0.998	398.000	9.857
	0.050	78	330	0.697	0.734	0.803	0.996	412.000	9.523
	0.005	73	270	0.601	0.661	0.816	0.999	800.000	4.903
Na_3PO_4	0.500	78	220	0.803	0.862	0.958	0.999	529.000	7.408
	0.050	75	205	0.929	0.938	0.919	0.996	369.000	10.621
	0.005	68	100	0.922	0.920	0.861	0.997	849.000	4.617
Na_2SO_4	0.500	72	400	0.844	0.879	0.959	0.999	367.000	10.682
	0.050	70	435	0.801	0.837	0.949	0.999	391.000	10.035
	0.005	70	435	0.974	0.979	0.953	0.997	20.000	19.513

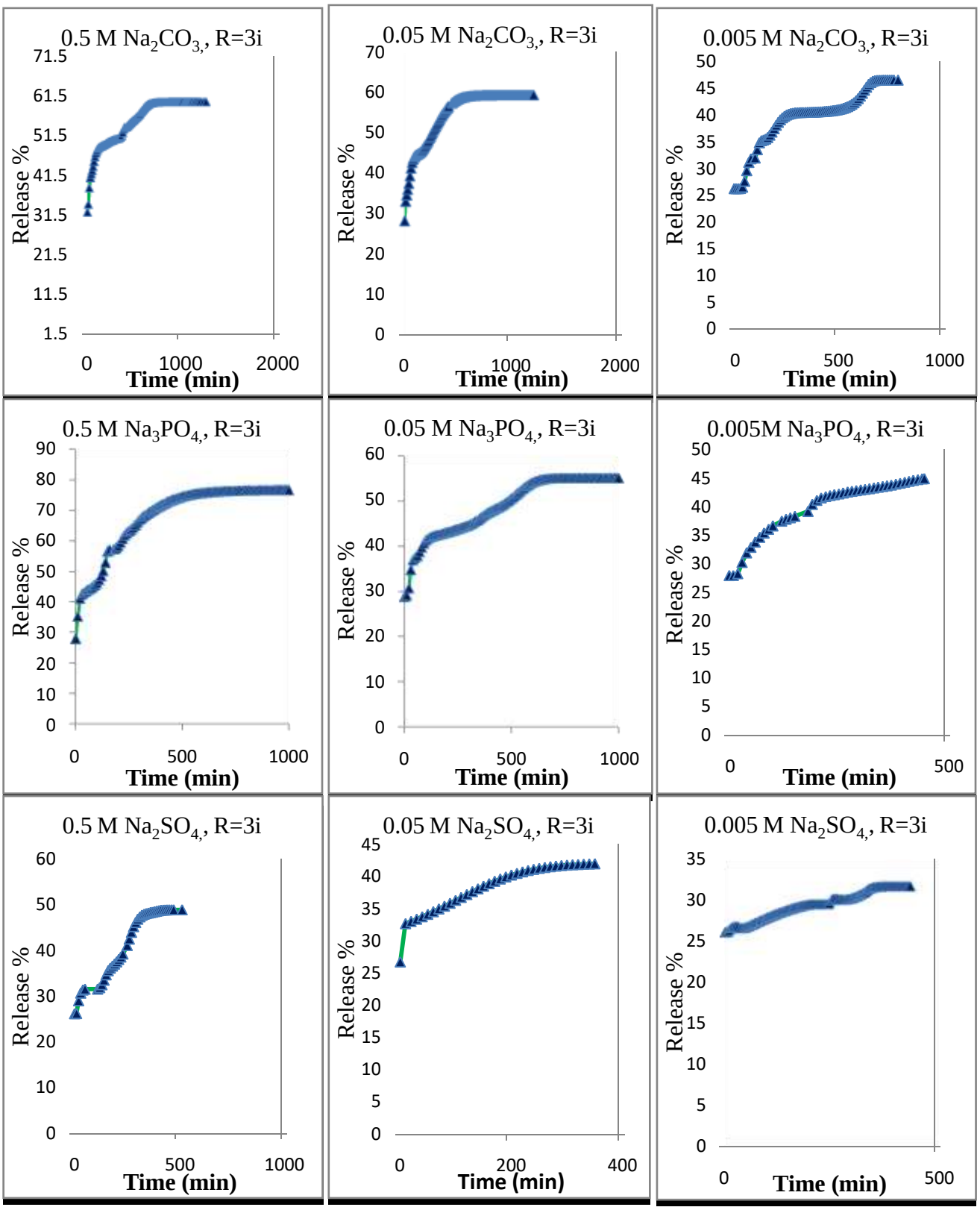

Figure 36. Release profiles of (FA) from the interlamellae of (Ni-Al-FA) LDHs that obtained from estimation method, the nanohybrid into various aqueous solution systems with different concentrations were containing several anions of carbonate, phosphate and sulphate (Ni/Al=3 ion-exchange).

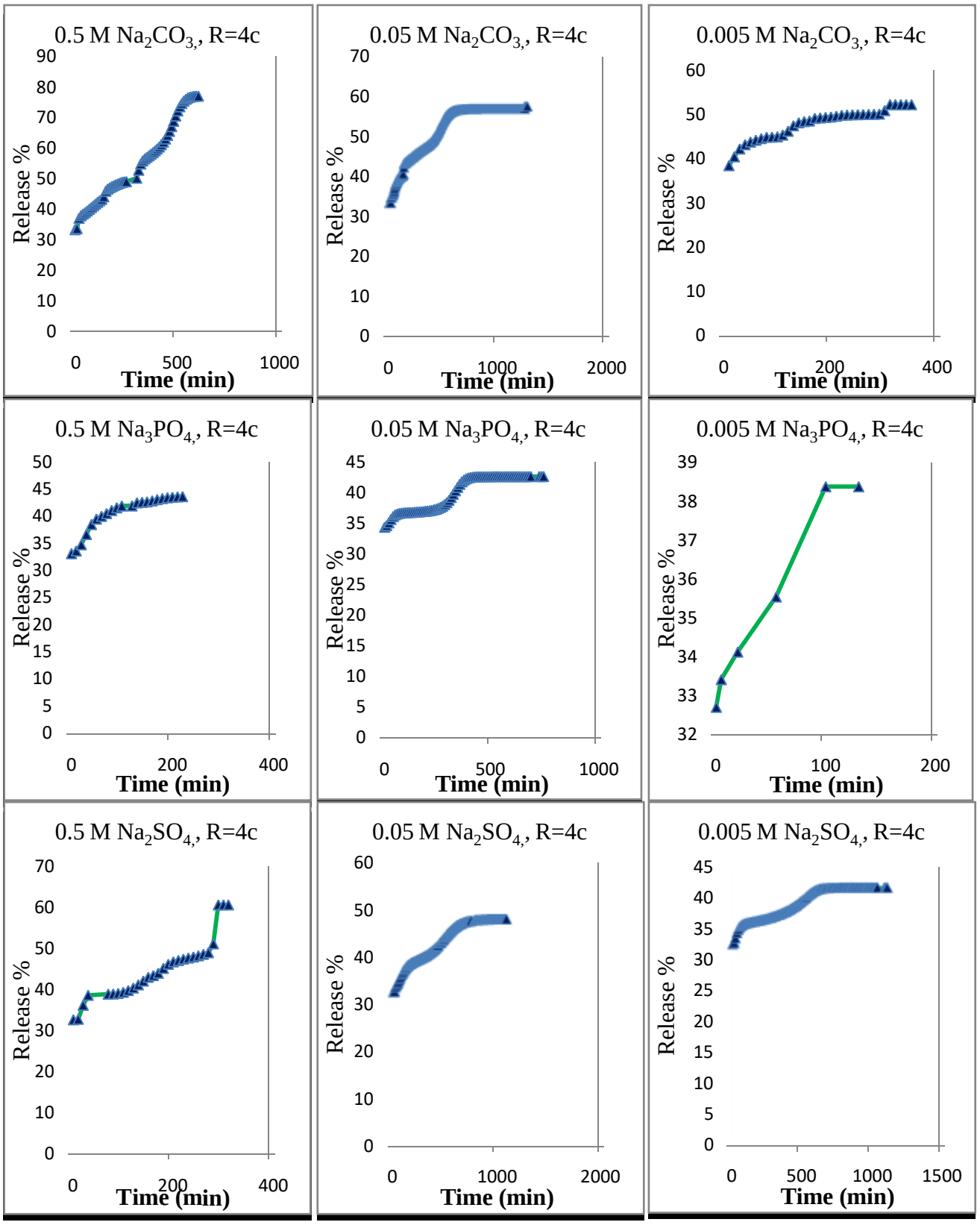

Figure 37. Release profiles of (FA) from the interlamellae of (Ni-Al-FA) LDHs that obtained from estimation method, the nanohybrid into various aqueous solution systems with different concentrations were containing several anions of carbonate, phosphate and sulphate (Ni/Al=4 Co-precipitation).

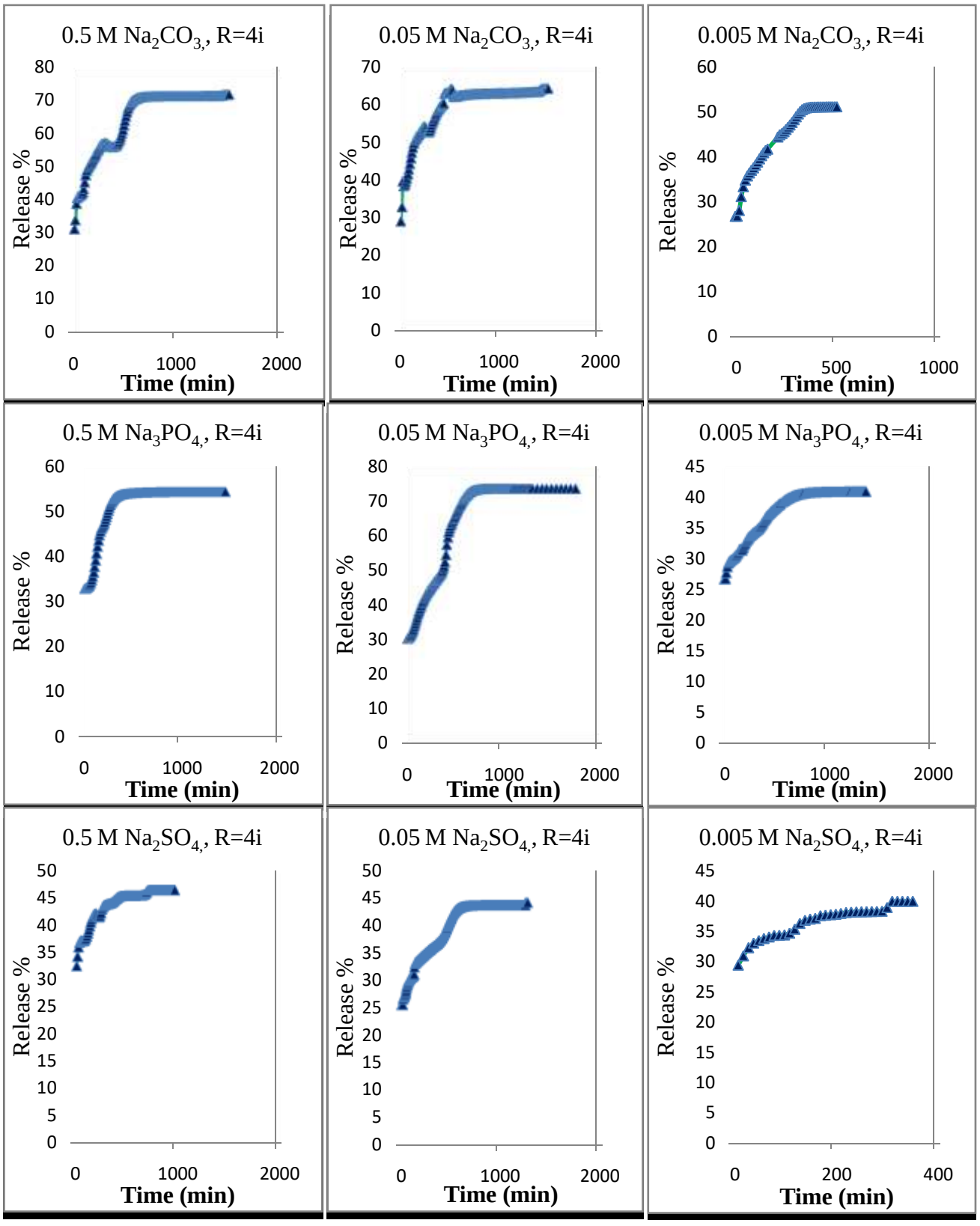

Figure 38. Release profiles of (FA) from the interlamellae of (Ni-Al-FA) LDHs that obtained from estimation method, the nanohybrid into various aqueous solution systems with different concentrations were containing several anions of carbonate, phosphate and sulphate (Ni/Al=4 ion-exchange).

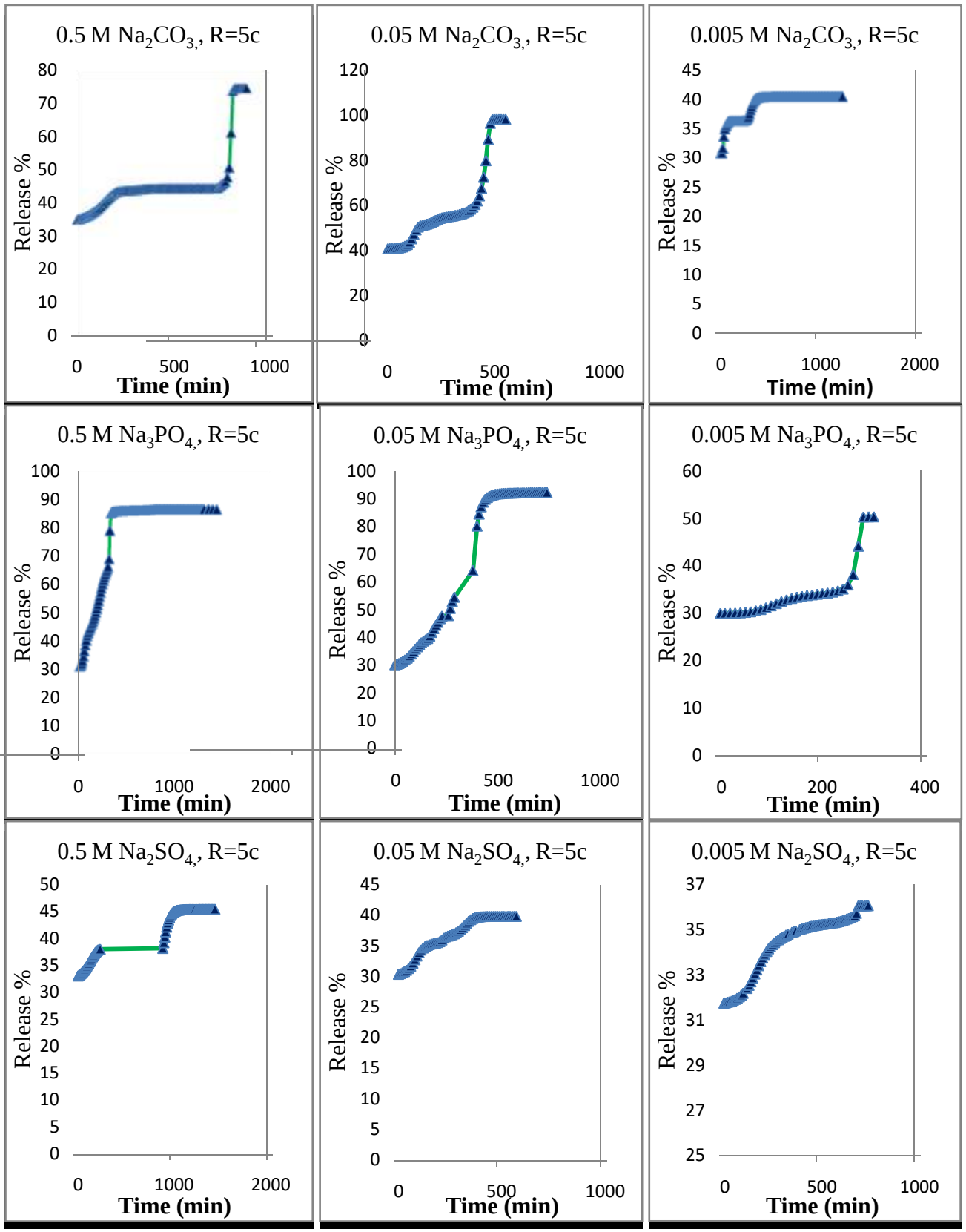

Figure 39. Release profiles of (FA) from the interlamellae of (Ni-Al-FA) LDHs that obtained from estimation method, the nanohybrid into various aqueous solution systems with different concentrations were containing several anions of carbonate, phosphate and sulphate (Ni/Al=5 Co-precipitation).

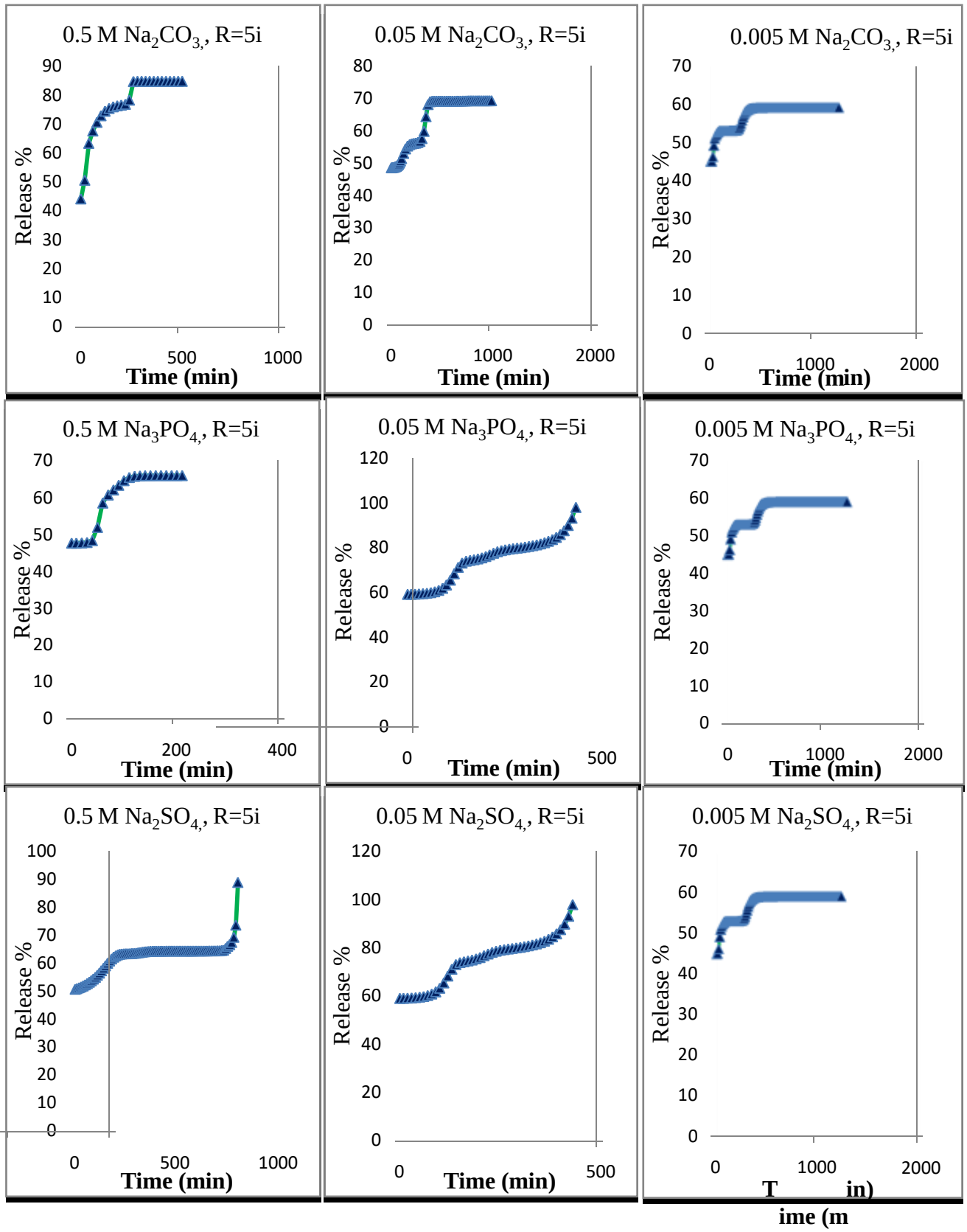

Figure 40. Release profiles of (FA) from the interlamellae of (Ni-Al-FA) LDHs that obtained from estimation method, the nanohybrid into various aqueous solution systems with different concentrations were containing several anions of carbonate, phosphate and sulphate (Ni/Al=5 ion-exchange).

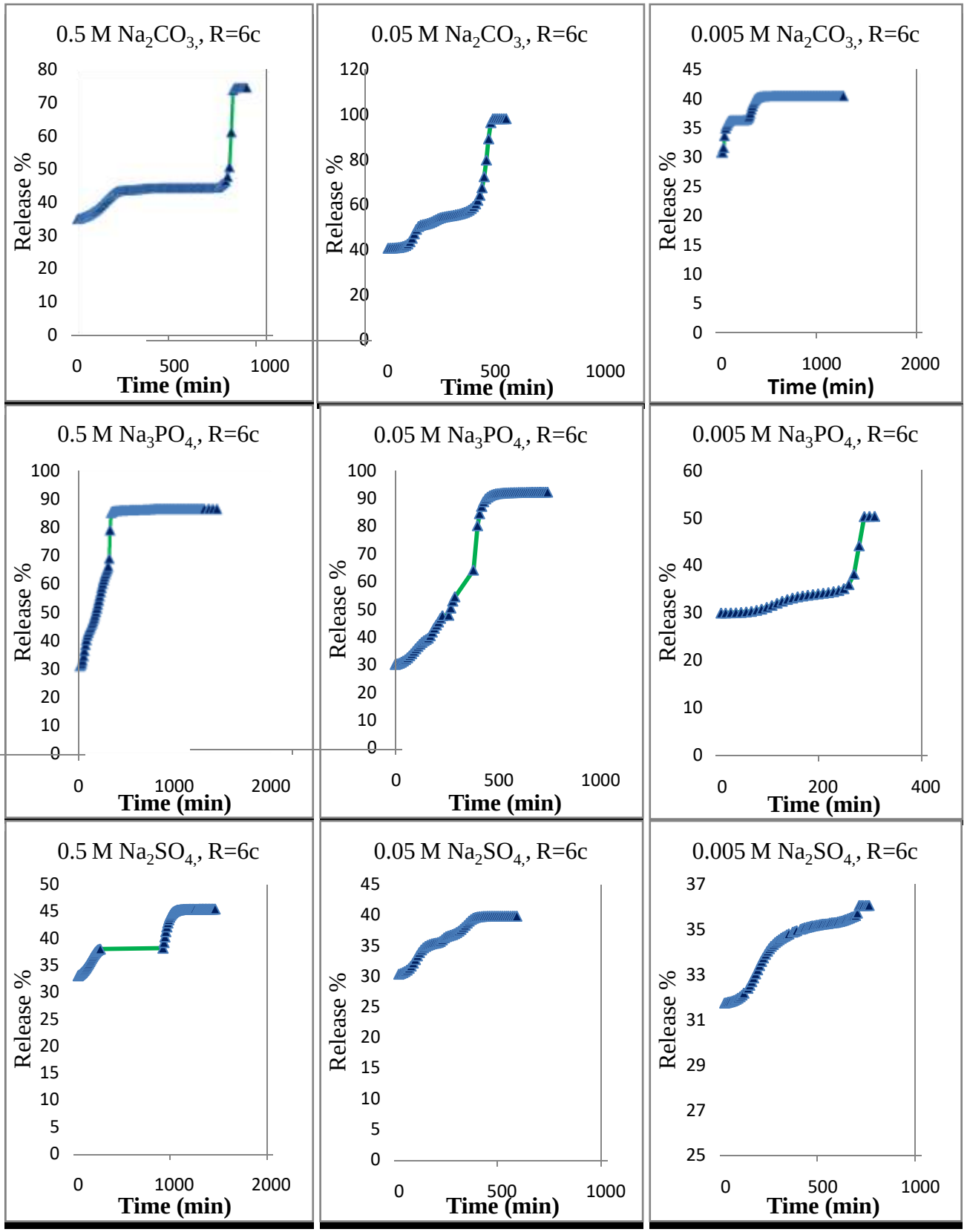

Figure 41. Release profiles of (FA) from the interlamellae of (Ni-Al-FA) LDHs that obtained from estimation method, the nanohybrid into various aqueous solution systems with different concentrations were containing several anions of carbonate, phosphate and sulphate (Ni/Al=6 Co-precipitation).

Moreover, the release of FA from the inorganic LDH interlamellae involved dissolution of the nanocomposite as well as diffusion of the intercalated anion. The dissolution phenomena take place by ion-exchange process between the intercalated anions and the incoming anion such as carbonate, phosphate and sulphate anions in the aqueous solution can be better described by pseudo-second order kinetics because the mechanism of release has been interpreted on the basis of the ion-exchange process between the drug anion intercalated in the lamella host and carbonate, phosphate, or sulphate anions in the aqueous solution i.e. depending on two factors: incoming and outgoing anion. In addition, the dissolution time will represent the total time of how long the molecule spends outside the interlamellae host as well as the pseudo-second order model will represent the dissolution as well as diffusion phenomena.

Therefore, in this study, it has been innovated novel equations to evaluate the diffusion of organic species through the LDHs nanohybrid inter particles (equation 9 and 12), "Figure 42 - 55" and (Table 9 – 15).

$$\ln\frac{C_t}{C_f^2 - C_t C_f} = \ln\frac{\mathrm{D}}{\mathrm{n}-1} + (n-1)\ln t \qquad (9)$$

$$\frac{t^m}{C_t} = \frac{m}{K C_f^2} + \frac{t^m}{C_f} \qquad (12)$$

By comparing the correlation coefficient of equation 12 (Table 9 – 15) together with Bahskar equation (Table 1 – 7) it can be seen that the equation 12 has higher values and it is the best there is. In addition, the novel equation will give us a lot of information like m value that could not be given by any other equation. Hence, as can be seen from (Table 9) the m value decreased with increased concentration and at the same time leads to increased rate constant that indicates the increased of concentration of aqueous solution causing increased rate of an ion exchange due to increased concentration leading to increased anion and that causes an increase of competitive anions incoming to the interlayer. In a word, from the results above it could be

conclude that the diffusion through the LDHs nanohybrid particles was governed by the equation 8 and this equation is the best convenient.

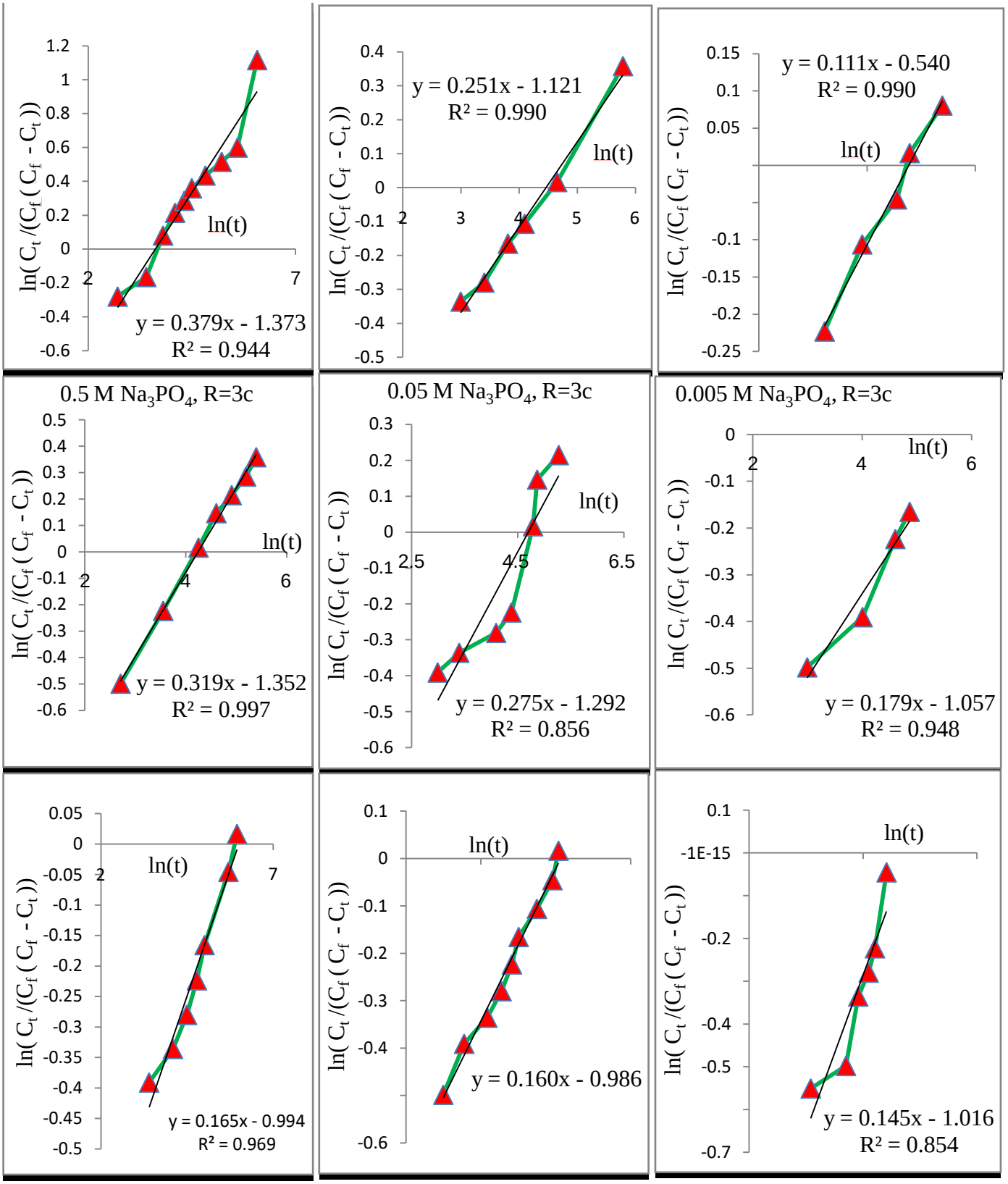

Figure 42. Plots of $\ln(C_t/((C_f - C_t) C_f))$ versus ln (t), (Ni/Al= 3 Co-precipitation).

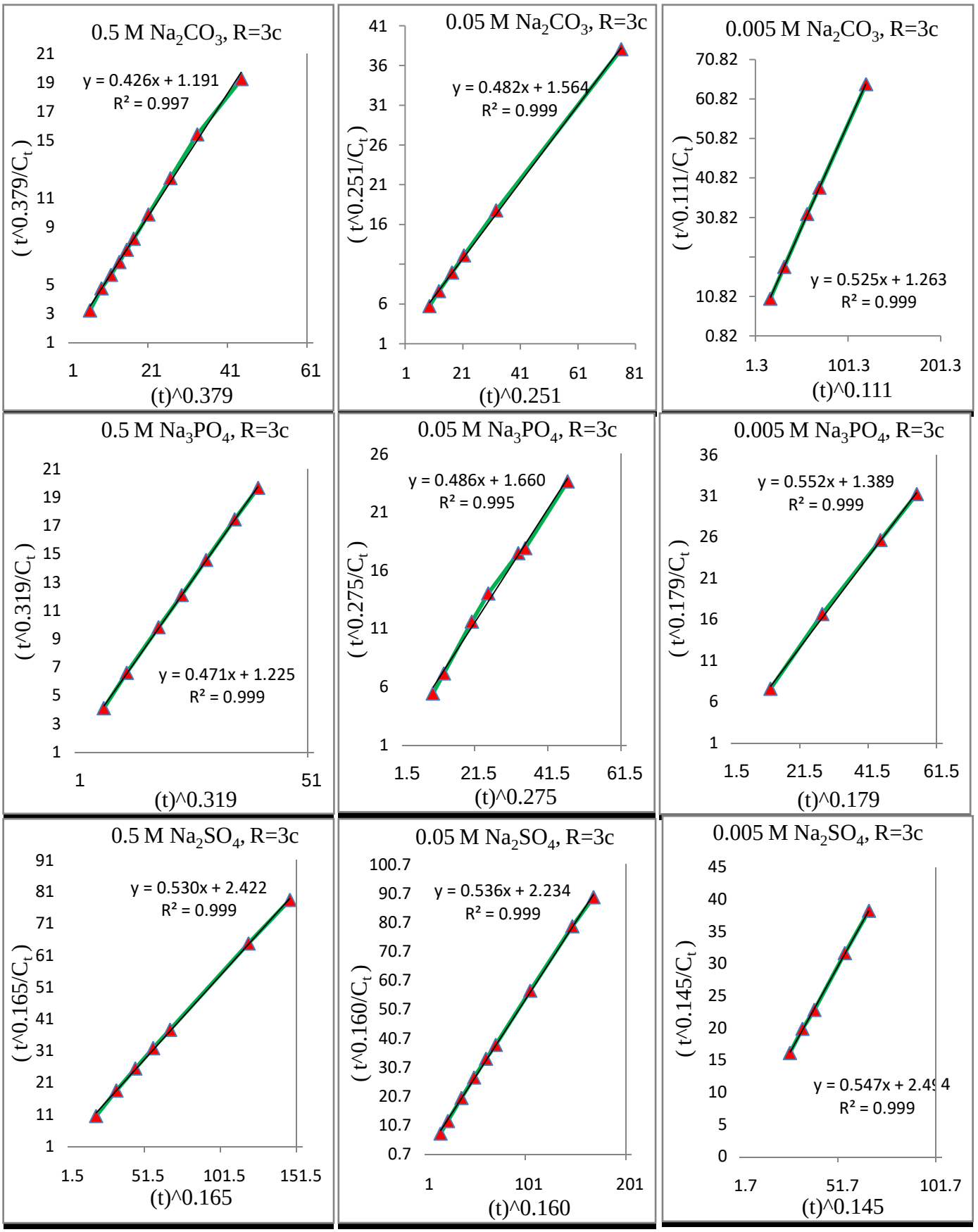

Figure 43. Plots of (t^m/C_t) versus (t^m), (Ni/Al= 3 Co-precipitation).

Table 9. Rate Constant (k), Half Life ($t_{1/2}$) and Correlation Coefficients (r^2) obtained from fitting of the release data of (FA) from Ni-Al-FA-LDH Nanohybrid into various aqueous solution by using equation 9 and 12 (Ni/Al=3 Co-precipitation).

r^2 of equation 12	m value	$t_{1/2}$ (min)	$K*10^{-4}$ ($L.mg^{-1}.min^{-1)}$	Concentration (mol L^{-1})	Aqueous solution
0.997	0.379	3.025	808.000	0.500	Na_2CO_3
0.999	0.251	3.972	742.000	0.050	
0.999	0.111	3.208	1091.000	0.005	
0.999	0.319	3.111	861.000	0.500	Na_3PO_4
0.995	0.275	4.216	676.000	0.050	
0.999	0.179	3.528	984.000	0.005	
0.999	0.165	6.151	534.000	0.500	Na_2SO_4
0.999	0.160	5.674	582.000	0.050	
0.999	0.145	6.334	470.000	0.005	

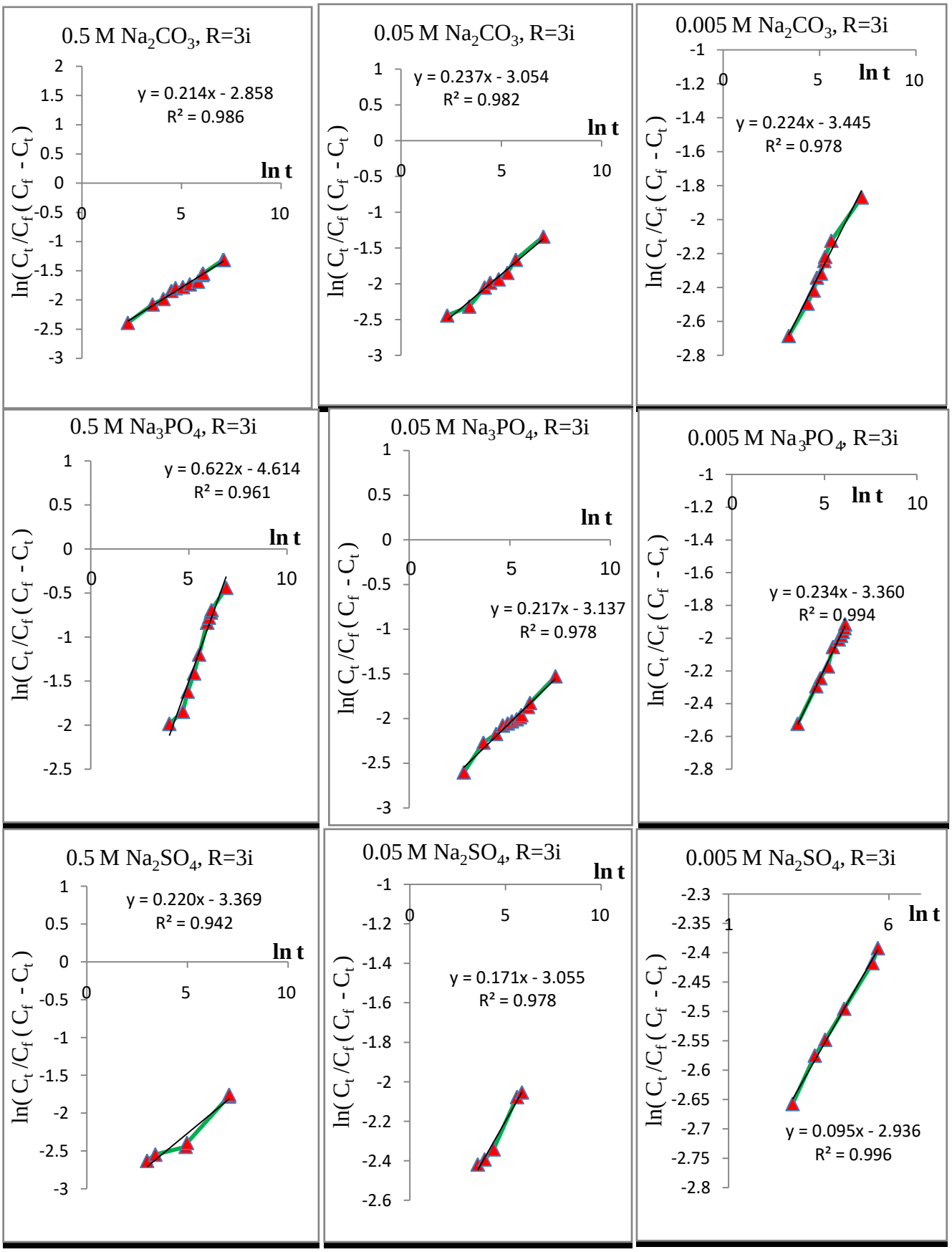

Figure 44. Plots of $\ln(C_t/((C_f - C_t) C_f))$ versus ln (t), (Ni/Al= 3 ion-exchange).

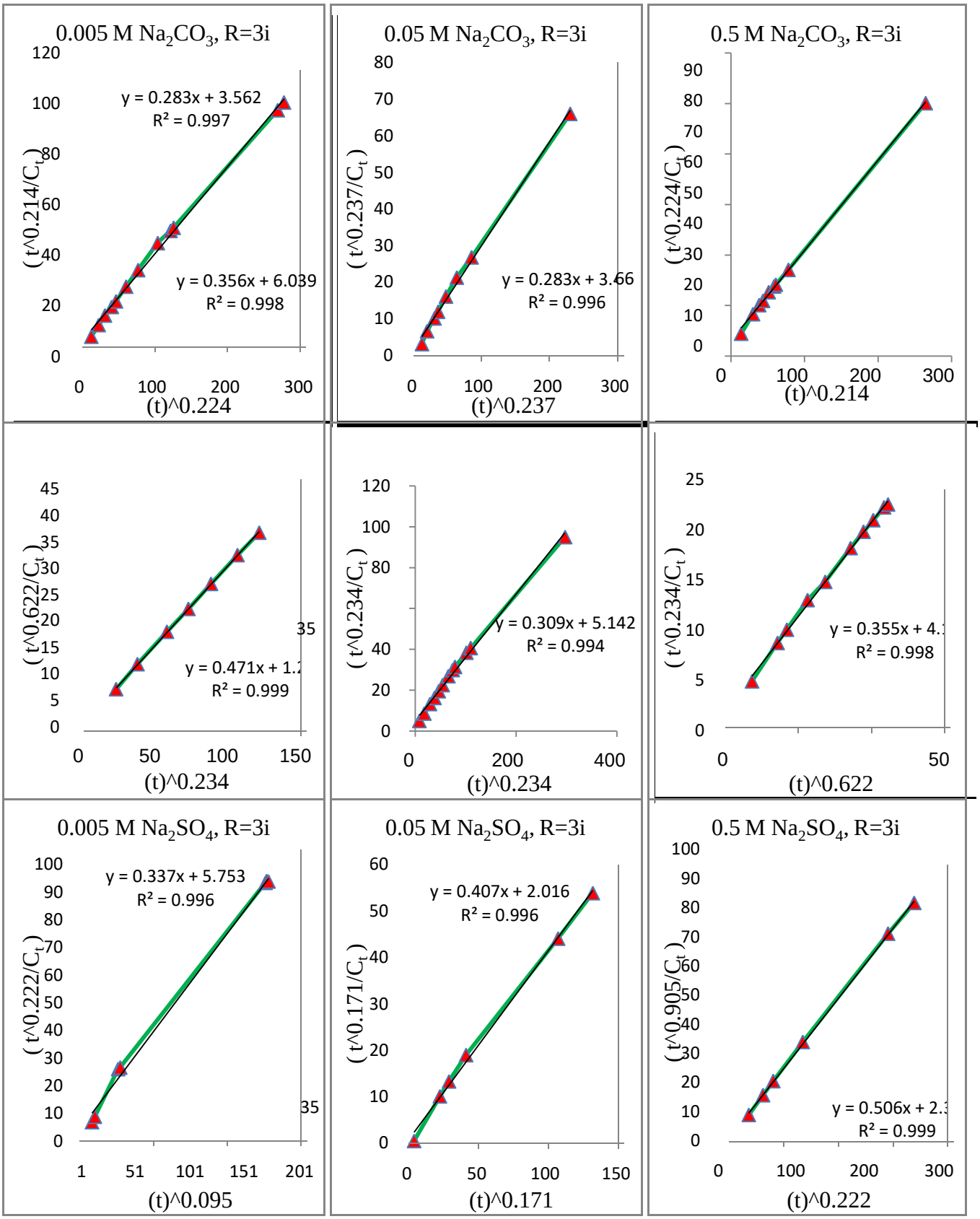

Figure 45. Plots of (t^m/C_t) versus (t^m), (Ni/Al= 3 ion-exchange).

Table 10. Rate Constant (k), Half Life ($t_{1/2}$) and Correlation Coefficients (r^2) obtained from fitting of the release data of (FA) from Ni-Al-FA-LDH Nanohybrid into various aqueous solution by using equation 9 and 12 (Ni/Al=3 ion-exchange).

Aqueous solution	Concentration (mol L^{-1})	$K*10^{-4}$ ($L.mg^{-1}.min^{-1}$)	$t_{1/2}$ (min)	m value	r^2 of equation 12
Na_2CO_3	0.500	339.000	9.077	0.214	0.997
	0.050	338.000	8.832	0.237	0.996
	0.005	197.000	15.389	0.224	0.998
Na_3PO_4	0.500	781.000	3.121	0.622	0.999
	0.050	234.000	13.103	0.234	0.994
	0.005	285.000	10.537	0.234	0.998
Na_2SO_4	0.500	210.000	14.660	0.222	0.996
	0.050	633.000	5.137	0.171	0.996
	0.005	596.000	5.950	0.095	0.999

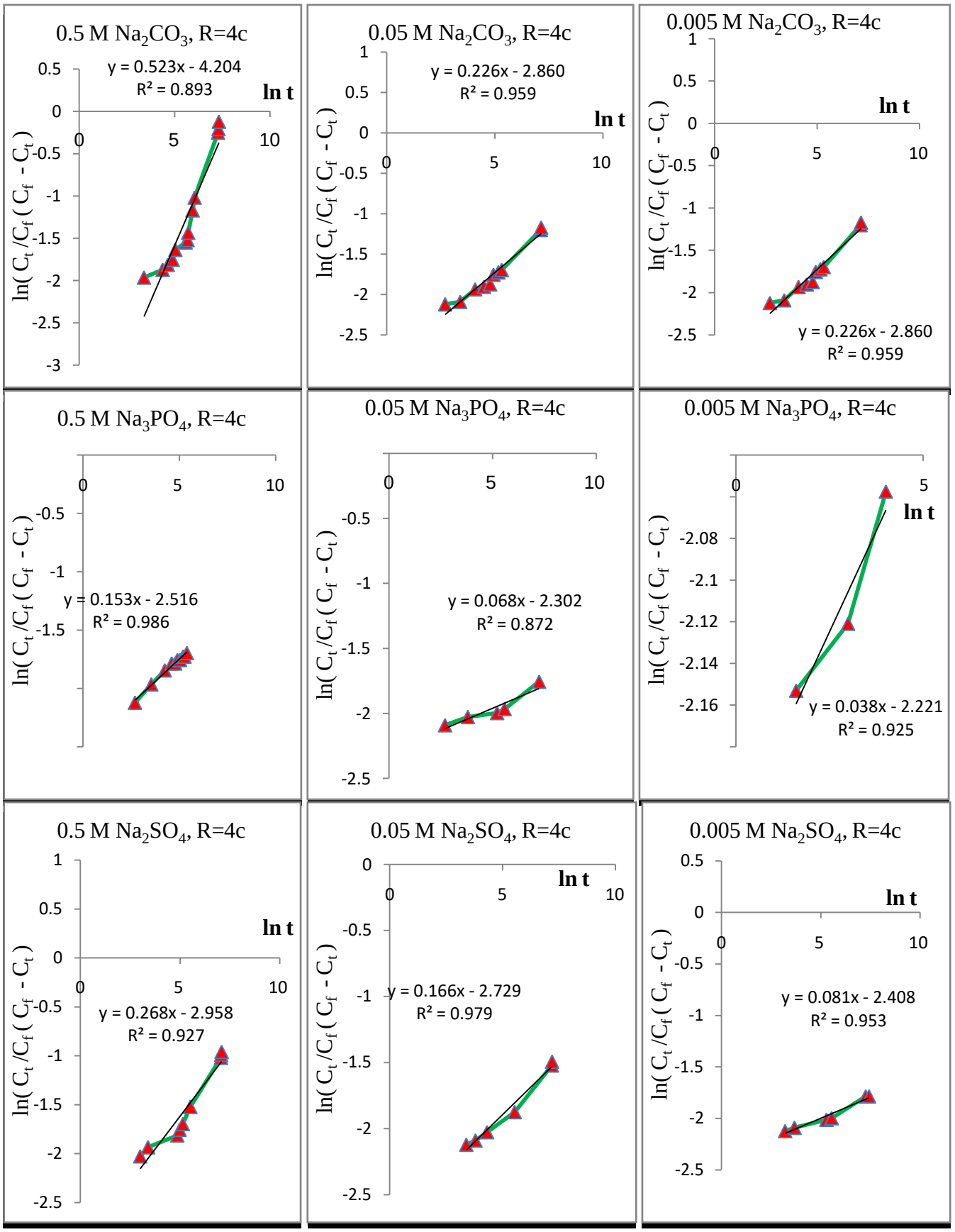

Figure 46. Plots of $\ln(C_t/((C_f - C_t)\,C_f))$ versus ln (t), (Ni/Al= 4 Co-precipitation).

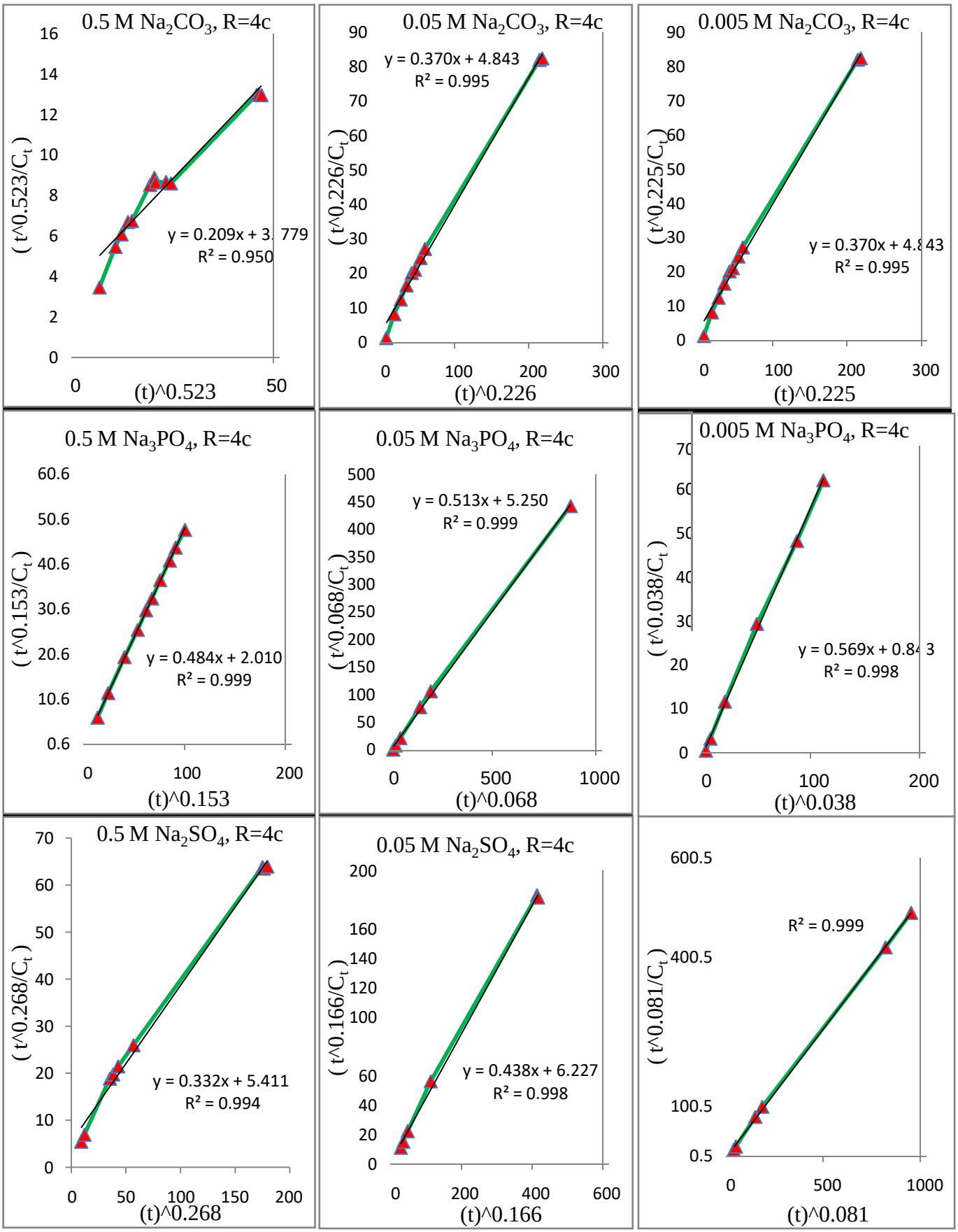

Figure 47. Plots of (t^m/C_t) versus (t^m), (Ni/Al= 4 Co-precipitation).

Table 11. Rate Constant (k), Half Life ($t_{1/2}$) and Correlation Coefficients (r^2) obtained from fitting of the release data of (FA) from Ni-Al-FA-LDH Nanohybrid into various aqueous solution by using equation 9 and 12 (Ni/Al=4 Co-precipitation).

Aqueous solution	Concentration (mol L^{-1})	$K*10^{-4}$ ($L.mg^{-1}.min^{-1}$)	$t_{1/2}$ (min)	m value	r^2 of equation 12
Na_2CO_3	0.500	59.000	16.816	0.523	0.950
	0.050	78.000	21.551	0.226	0.995
	0.005	78.000	21.551	0.225	0.995
Na_3PO_4	0.500	212.000	8.944	0.153	0.999
	0.050	89.000	23.362	0.068	0.999
	0.005	576.000	3.751	0.038	0.998
Na_2SO_4	0.500	68.000	24.078	0.268	0.994
	0.050	67.000	27.710	0.166	0.998
	0.005	66.000	31.283	0.081	0.999

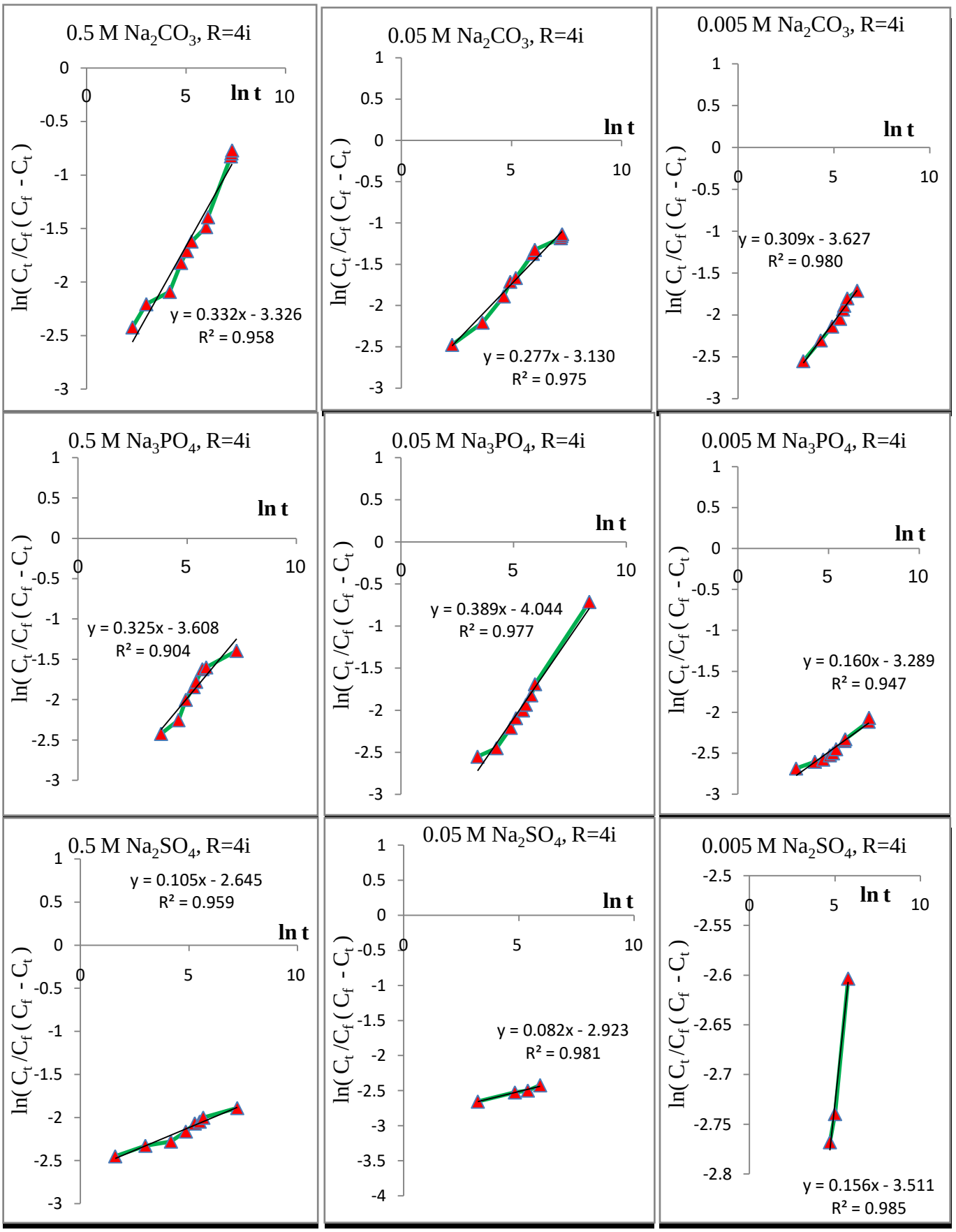

Figure 48. Plots of $\ln(C_t/((C_f - C_t) C_f))$ versus ln (t), (Ni/Al= 4 ion-exchange).

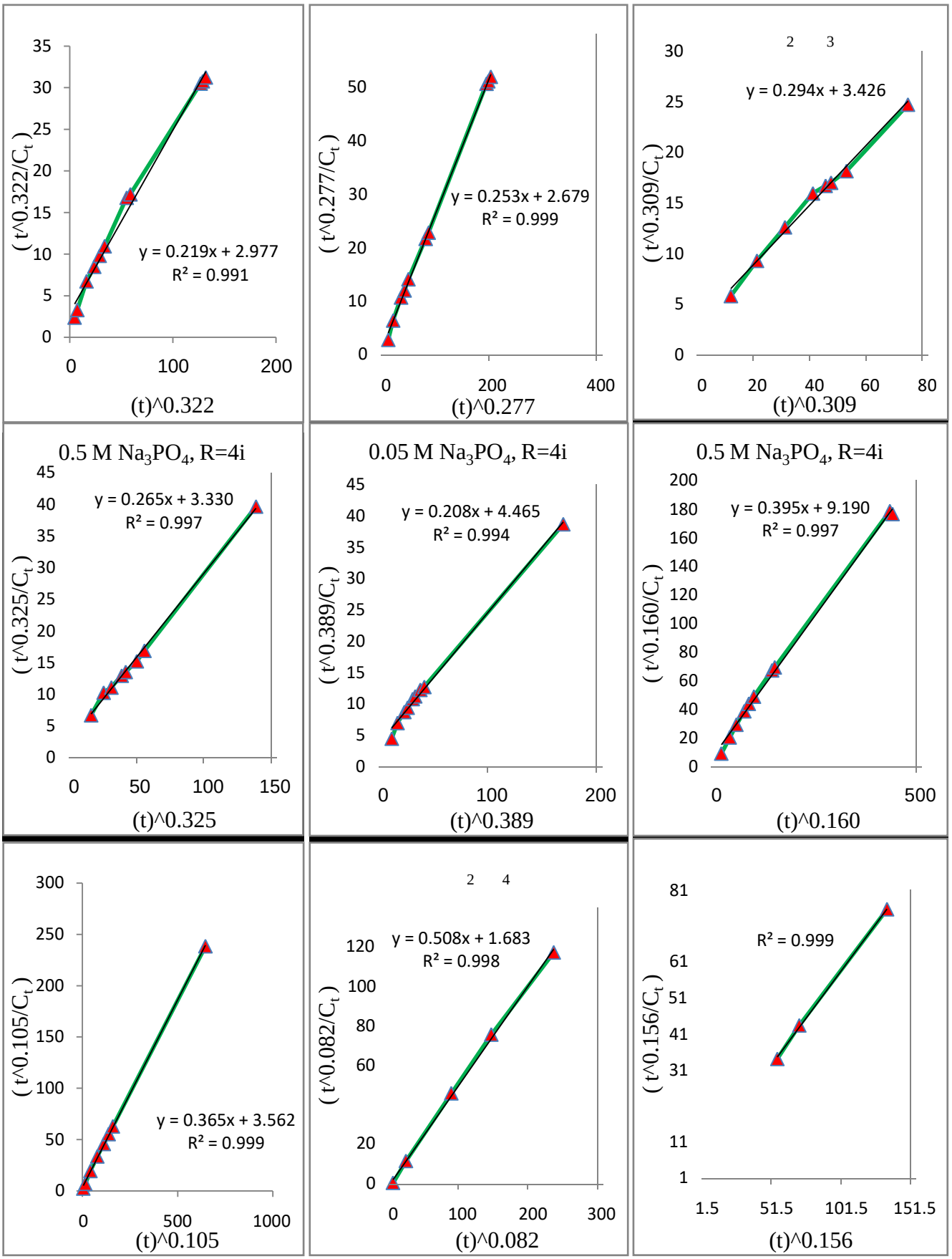

Figure 49. Plots of (t^m/C_t) versus (t^m), (Ni/Al= 4 ion-exchange).

Table 12. Rate Constant (k), Half Life ($t_{1/2}$) and Correlation Coefficients (r^2) obtained from fitting of the release data of (FA) from Ni-Al-FA-LDH Nanohybrid into various aqueous solution by using equation 9 and 12 (Ni/Al=4 ion-exchange).

Aqueous solution	Concentration (mol L^{-1})	$K*10^{-4}$ ($L.mg^{-1}.min^{-1}$)	$t_{1/2}$ (min)	m value	r^2 of equation 12
Na_2CO_3	0.500	66.000	17.266	0.322	0.991
	0.050	80.000	15.538	0.277	0.999
	0.005	59.000	19.870	0.309	0.992
Na_3PO_4	0.500	60.000	19.314	0.325	0.997
	0.050	40.000	25.897	0.389	0.994
	0.005	27.000	53.302	0.160	0.997
Na_2SO_4	0.500	74.000	20.659	0.105	0.999
	0.050	162.000	9.761	0.082	0.998
	0.005	35.000	40.797	0.156	0.999

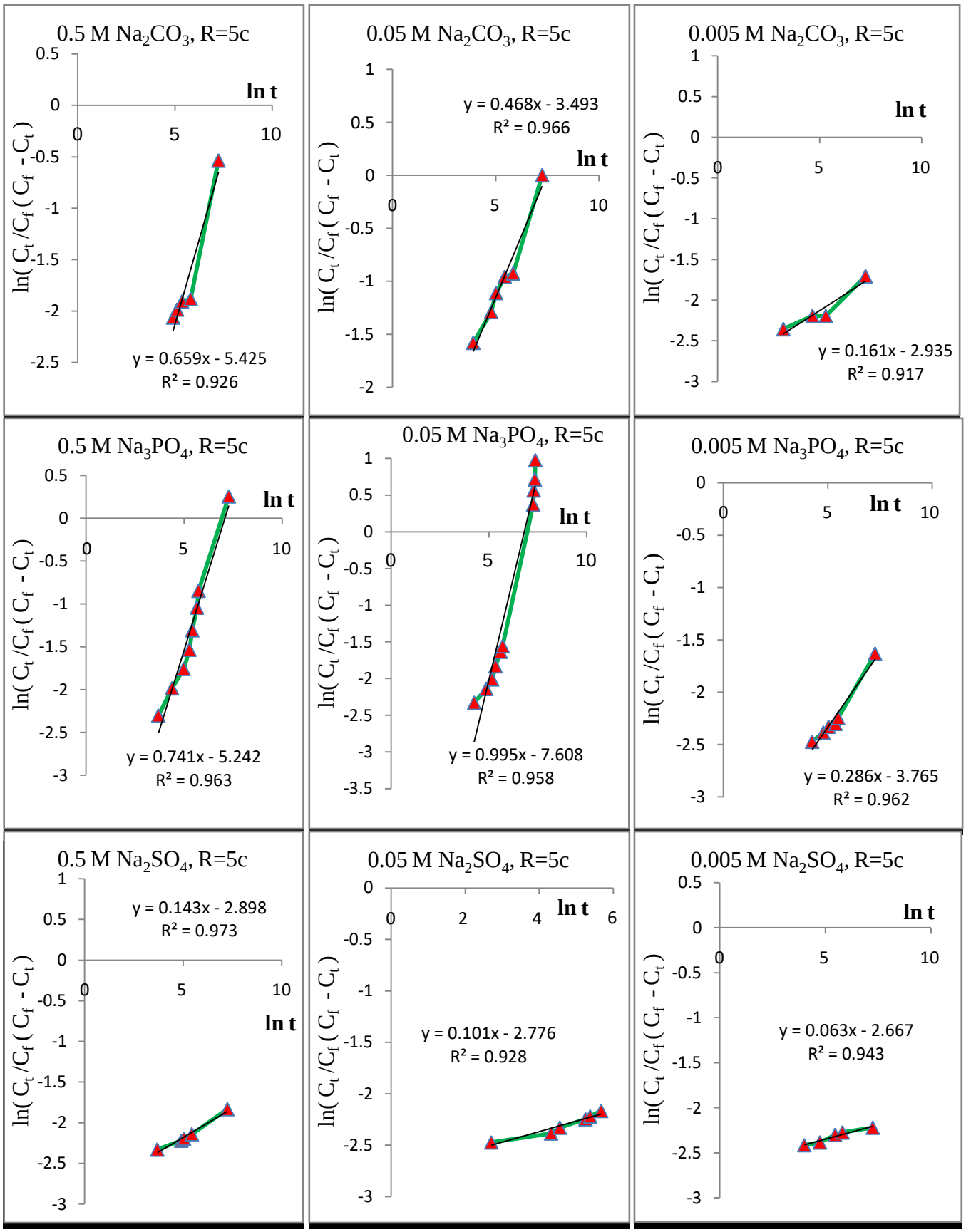

Figure 50. Plots of $\ln(C_t/((C_f - C_t)\,C_f))$ versus ln (t), (Ni/Al= 5 Co-precipitation).

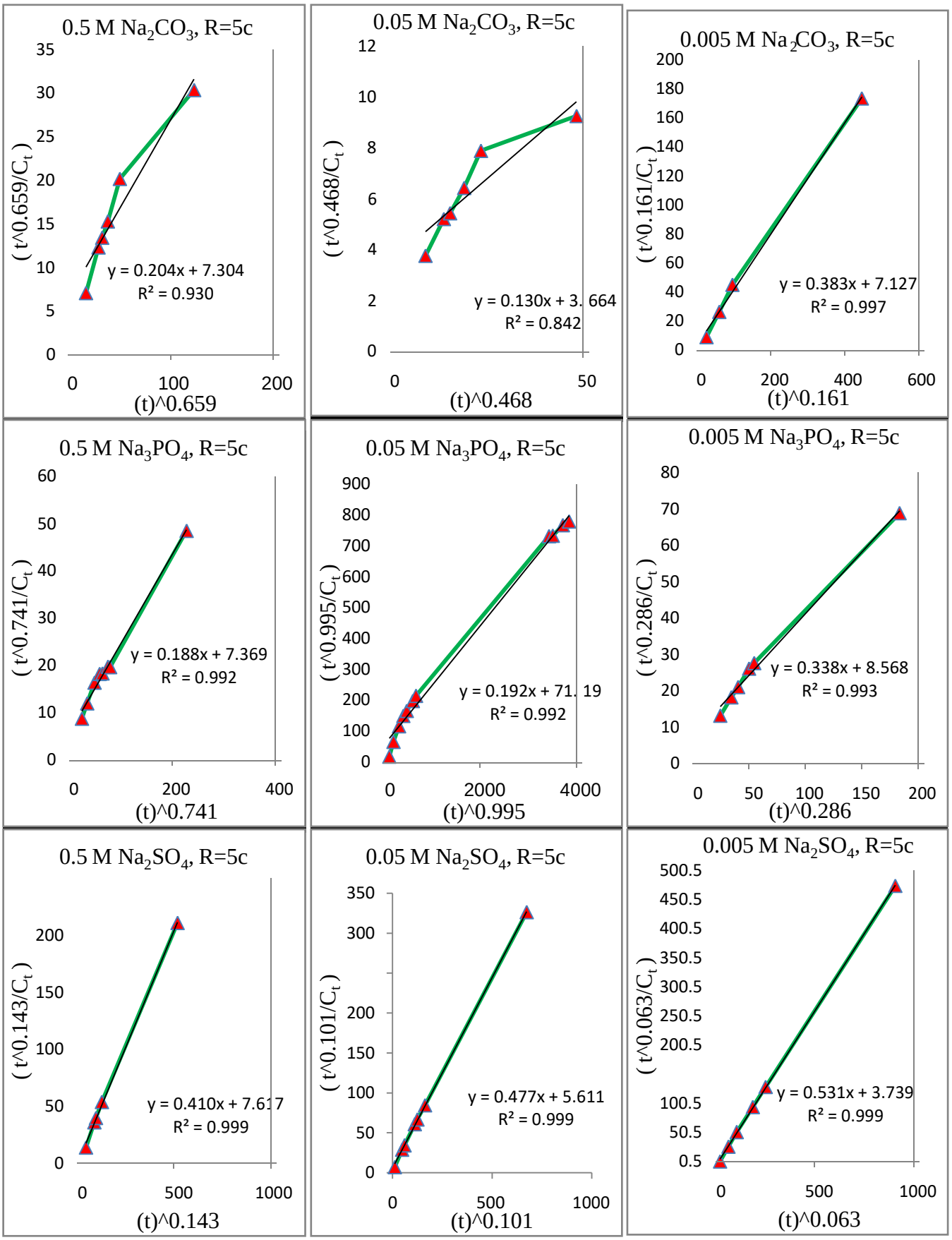

Figure 51. Plots of (t^m/C_t) versus (t^m), (Ni/Al= 5 Co-precipitation).

Table 13. Rate Constant (k), Half Life ($t_{1/2}$) and Correlation Coefficients (r^2) obtained from fitting of the release data of (FA) from Ni-Al-FA-LDH Nanohybrid into various aqueous solution by using equation 9 and 12 (Ni/Al=5 Co-precipitation).

Aqueous solution	Concentration (mol L^{-1})	$K*10^{-4}$ ($L.mg^{-1}.min^{-1}$)	$t_{1/2}$ (min)	m value	r^2 of equation 12
Na_2CO_3	0.500	33.000	37.907	0.659	0.930
	0.050	53.000	19.016	0.468	0.842
	0.005	43.000	36.989	0.161	0.997
Na_3PO_4	0.500	37.000	38.245	0.741	0.992
	0.050	5.000	369.476	0.995	0.995
	0.005	30.000	44.467	0.286	0.993
Na_2SO_4	0.500	41.000	39.532	0.143	0.999
	0.050	58.000	29.121	0.101	0.999
	0.005	93.000	19.405	0.063	0.999

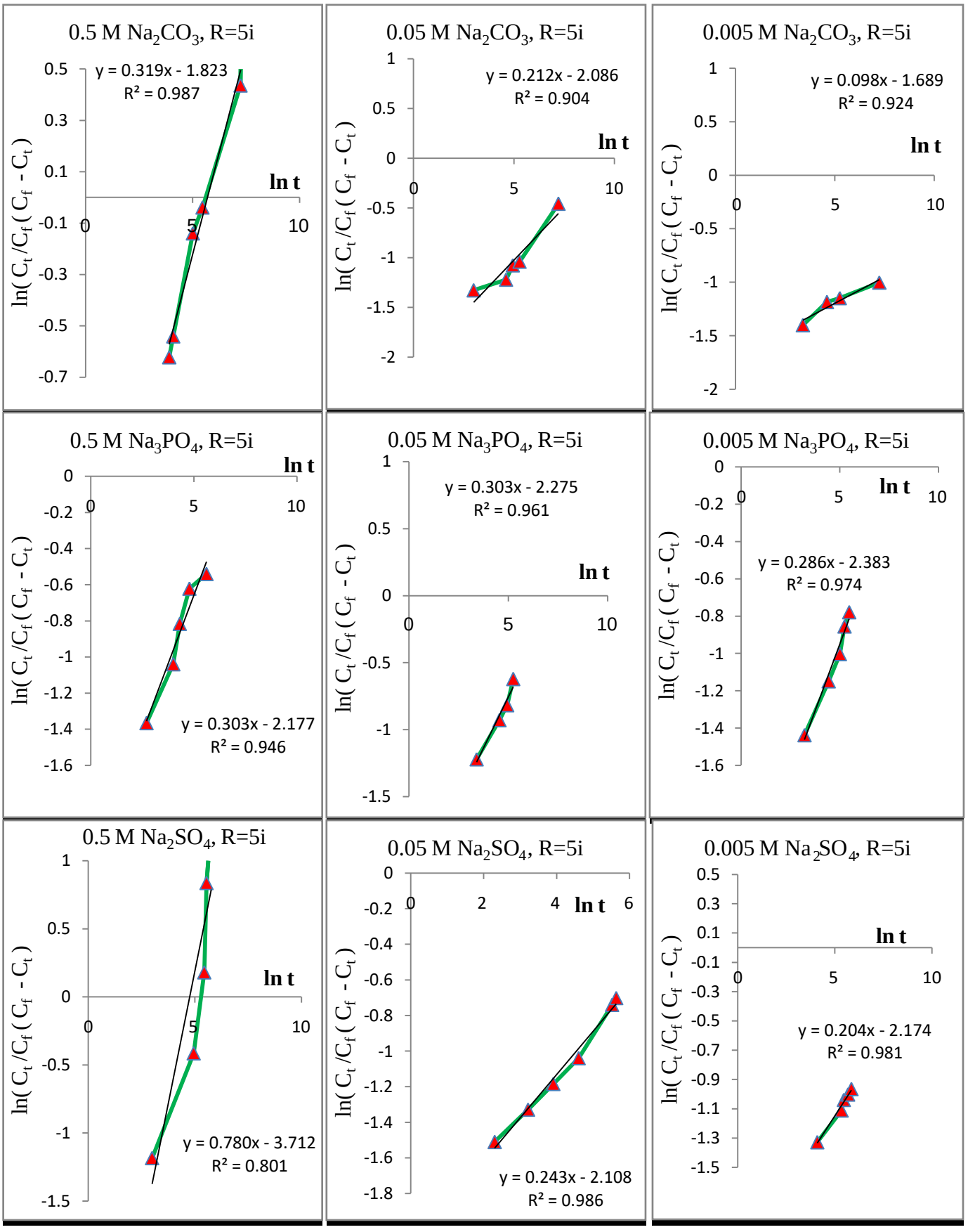

Figure 52. Plots of $\ln(C_t/((C_f - C_t) C_f))$ versus ln (t), (Ni/Al= 5 ion-exchange).

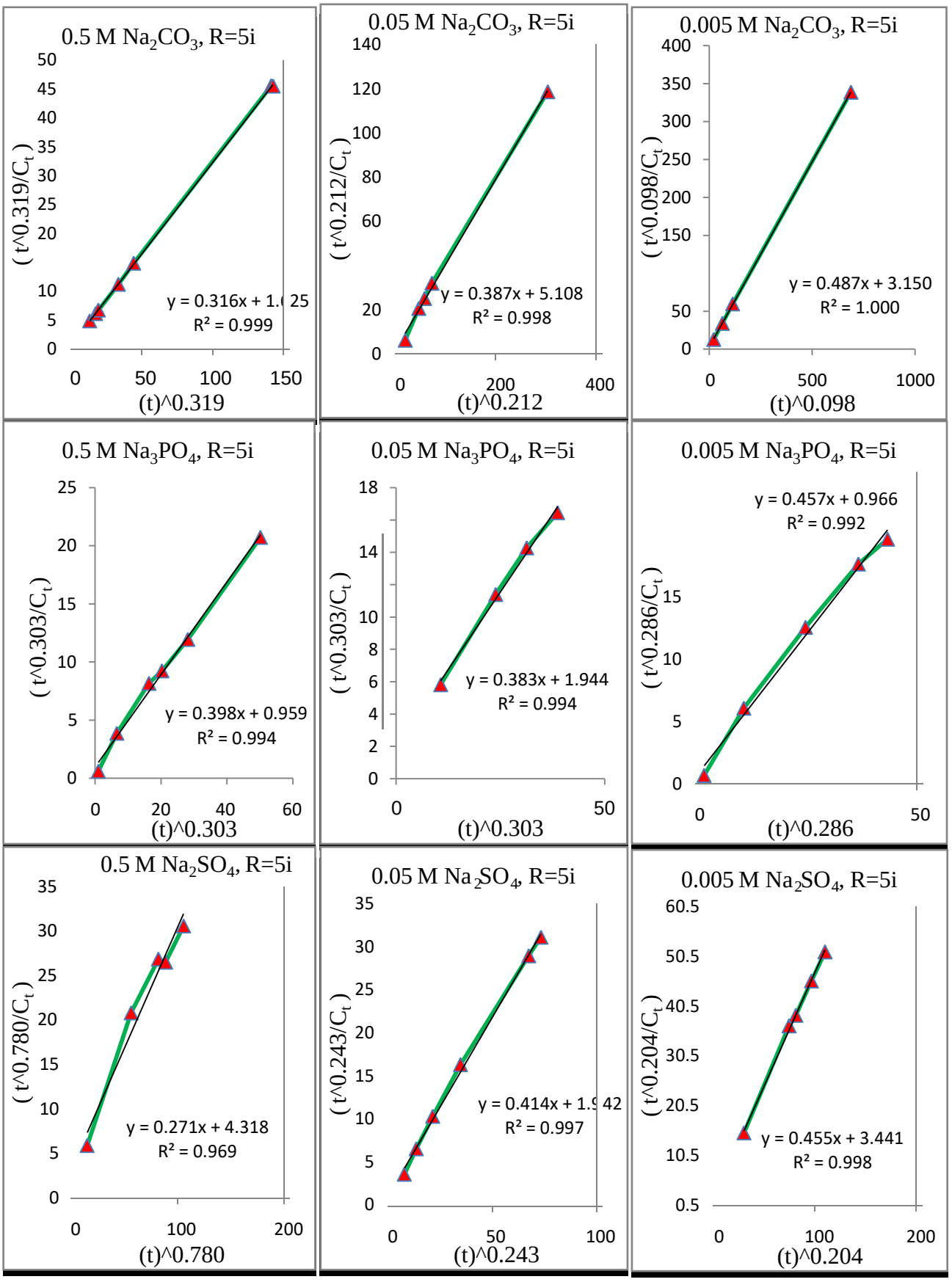

Figure 53. Plots of (t^m/C_t) versus (t^m), (Ni/Al= 5 ion-exchange).

Table 14. Rate Constant (k), Half Life ($t_{1/2}$) and Correlation Coefficients (r^2) obtained from fitting of the Release Data of (FA) from Ni-Al-FA-LDH Nanohybrid into various aqueous solution by using equation 9 and 12 (Ni/Al=5 ion-exchange).

Aqueous solution	Concentration (mol L^{-1})	$K*10^{-4}$ ($L.mg^{-1}.min^{-1)}$	$t_{1/2}$ (min)	m value	r^2 of equation 12
Na2CO3	0.500	153.000	5.817	0.319	0.999
	0.050	120.000	18.286	0.212	0.998
	0.005	223.000	11.277	0.098	1.000
Na_3PO_4	0.500	567.000	3.433	0.303	0.994
	0.050	279.000	6.959	0.303	0.994
	0.005	576.000	3.458	0.286	0.992
Na_2SO_4	0.500	140.000	15.458	0.780	0.969
	0.050	304.000	6.952	0.243	0.997
	0.005	180.000	12.318	0.204	0.998

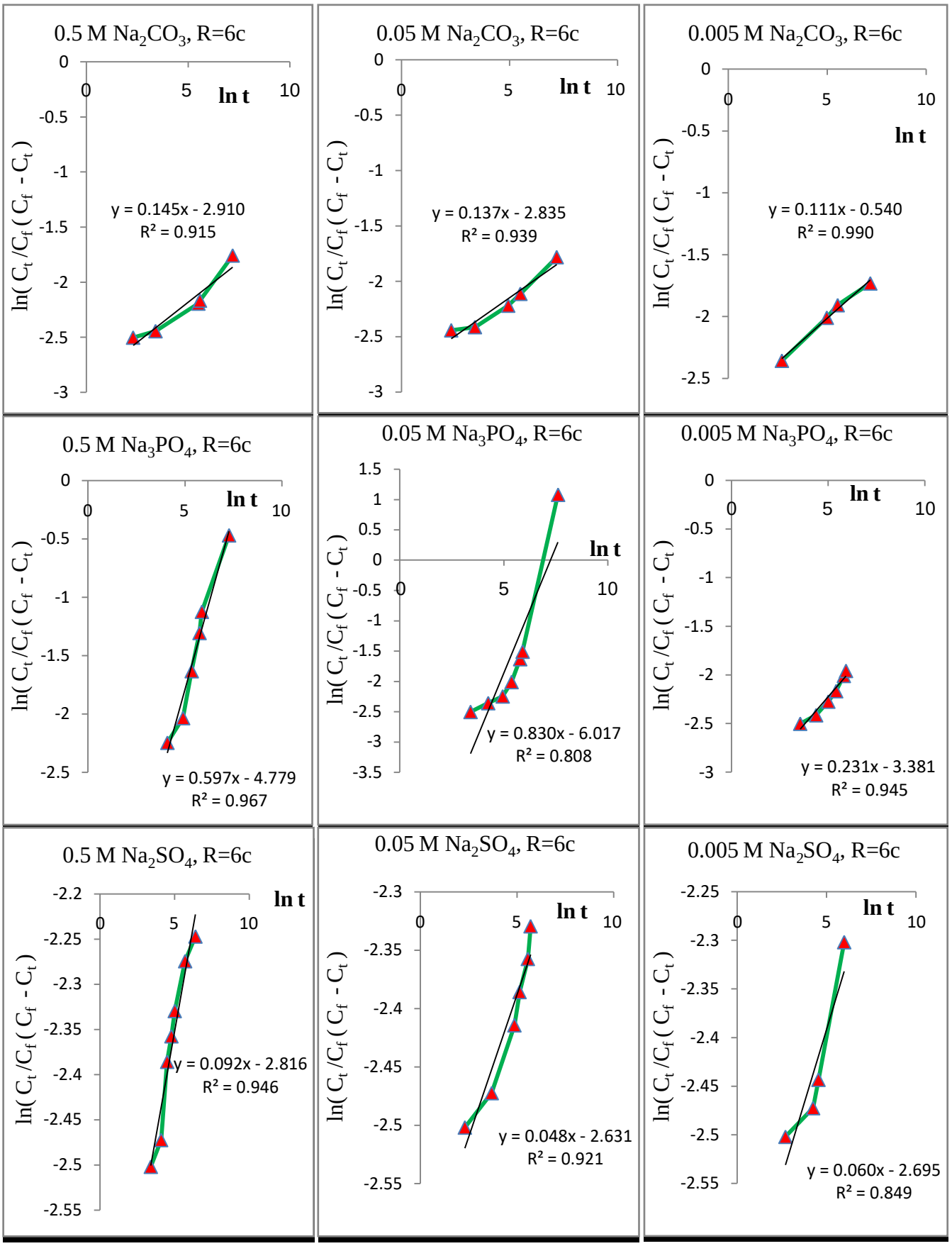

Figure 54. Plots of $\ln(C_t/((C_f - C_t)\,C_f))$ versus ln (t), (Ni/Al= 6 Co-precipitation).

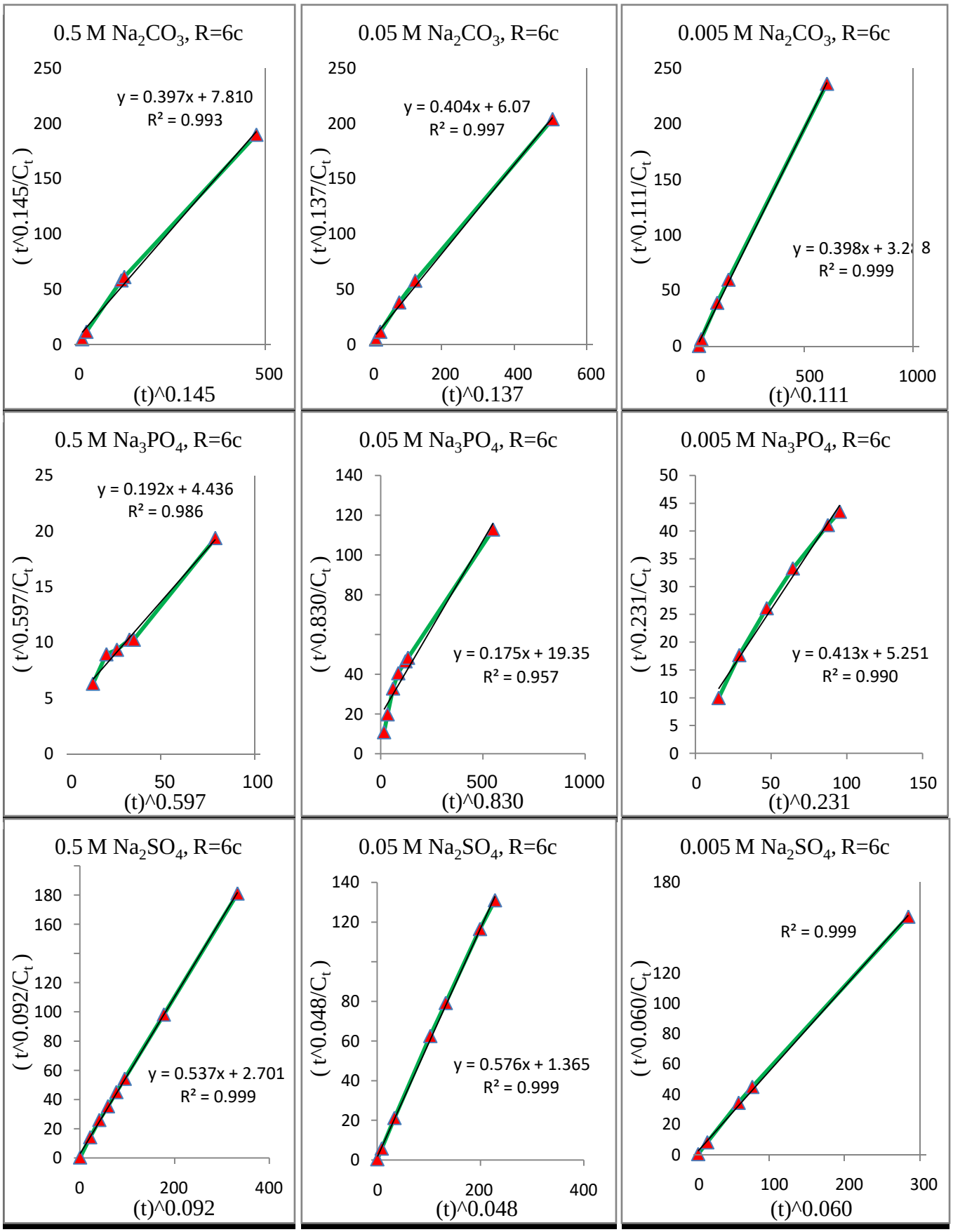

Figure 55. Plots of (t^m/C_t) versus (t^m), (Ni/Al= 6 Co-precipitation).

Table 15. Rate Constant (k), Half Life ($t_{1/2}$) and Correlation Coefficients (r^2) obtained from fitting of the release data of (FA) from Ni-Al-FA-LDH Nanohybrid into various aqueous solution by using equation 9 and 12 (Ni/Al=6 Co-precipitation).

Aqueous solution	Concentration (mol L^{-1})	$K*10^{-4}$ ($L.mg^{-1}.min^{-1}$)	$t_{1/2}$ (min)	m value	r^2 of equation 12
Na_2CO_3	0.500	40.000	40.533	0.145	0.993
	0.050	52.000	31.503	0.137	0.997
	0.005	100.000	17.064	0.111	0.999
Na_3PO_4	0.500	49.000	23.022	0.597	0.986
	0.050	15.000	100.425	0.830	0.957
	0.005	54.000	27.252	0.231	0.990
Na_2SO_4	0.500	124.000	14.018	0.092	0.999
	0.050	258.000	7.084	0.048	0.999
	0.005	160.000	11.319	0.060	0.999

3.4. Conclusions

1. PXRD pattern showed the presence of sharp and intense peaks with the d-spacing 7.9 Å which signify high crystallite size at 180˚C and it is the best synthesis temperature.
2. Intercalation of drugs was leading to a significant increase in the interlayer space and showed the presence of sharp and intense peaks with the d-spacing 17.3 Å.
3. Folic acid has been intercalated into Ni/Al Layered double hydroxide successfully.
4. Carbonate dominated the accumulated release percentage as well as nanohybrid compound is more stable in acidic media due to the lowest value of release percentages of folic acid compared with those obtain from basic media.
5. The release profiles were governed by the pseudo second order.
6. By comparing the correlation coefficient of equation 12 together with correlation coefficient of Bahskar equation, it was concluded that the equation 12 give higher values.
7. The diffusion through the LDHs nanohybrids particles was governed by the suggested equation (equation 12) and this equation is the most convenient.

References

1. K. J. Klabunde, Nanoscale materials in chemistry, John Wiley & Sons, Inc., New York, (2001), pp. 1-285.
1. N. Islam and K. Miyazaki, An empirical analysis of nanotechnology research domains, Technov., (2010), Vol. 30, pp. 229-237.
2. L. Jia and Y. Zhao, X. Liang, Fast evolving nanotechnology and relevant programs and entities in China, Nano Today, (2011), Vol. 6, pp. 6-11.
3. G. Schmid, M. Decker, H. Ernst, H. Fuchs, W. Grünwald, A. Grunwald, H. Hofmann, M. Mayor, W. Rathgeber, U. Simon and D. Wyrwa, Small dimensions and material properties a definition of nanotechnology, Eur. Akademie, (2003), pp. 1-134.
4. S. K. Sahoo, S. Parveen and J. J. Panda, The present and future of nanotechnology in human health care, Nanomed. Nanotechnol. Biol. Med., (2007), Vol. 3, pp. 20-31.
5. M. Fiedler and I. M. Welpe, Antecedents of cooperative commercialisation strategies of nanotechnology firms, Research Policy, (2010), Vol. 39, pp. 400–410.
6. C. O'Connor, H. Hayden, Contextualising nanotechnology in chemistry education, Chem. Educ. Res. Pract., (2008), Vol. 9, pp. 35–42.
7. P. J. Borm, D. Robbins, S. Haubold, T. Kuhlbusch, H. Fissan, K. Donaldson, R. Schins, V. Stone, W. Kreyling, J. Lademann, J. Krutmann, D. Warheit and E. Oberdorster, The potential risks of nanomaterials: a review carried out for ECETOC, Part. Fibre Toxicol., (2006), Vol. 3, pp. 11-46.
8. S. C. Tjong and H. Chen, Nanocrystalline materials and coatings, Mater. Sci. Eng., R, (2004), Vol. 45, pp. 1–88.
9. U. D. Sharma and M. Kumar, Analysis of equation of state for nanomaterials, Physica. B, (2011), Vol. 406, pp. 794–800.

10. M. Sharpe (Contributing News Editor), Small wonders, big future: the development of environmental nanotechnology (focus), J. Environ. Monit., (2006), Vol. 8, pp. 235–239.
11. T. Yokoyama, Nanoparticle technology handbook, K. Nogi (Director), First edition, (2007), pp. 1-622.
12. B. I. Kharisov, O. V. Kharissova, J. J. R. Vald´es and V. M. J. P´erez, Coordination and organometallic nanomaterials: a microreview, Synth. React. Inorg. Met.-Org. Chem., (2010), Vol. 40, pp. 640-650.
13. P. Pandey, M. Datta and B. D. Malhotra, Prospects of nanomaterials in biosensors, Anal. Lett., (2008), Vol. 41, pp. 159-209.
14. J. Xiao and Y. Huang, Towards nanomaterial design automation: hierarchical computational architecture development, Comput. Aided Chem. Eng., (2009), Vol. 26, pp. 81-86.
15. S. Kaluza, J. k. Balderhaar, B. Orthen, B. f. A. Arbeitsmedizin, B. Honnert, E. Jankowska, P. Pietrowski, M. G. Rosell, C. Tanarro, J. Tejedor and A. Zugasti, Workplace exposure to nanoparticles, J. Kosk-Bienko (Editor), EU-OSHA, Literature Review, (2010), pp. 1-89.
16. Nanoscience and nanotechnologies: opportunities and uncertainties, The Royal Society and The Royal Academy of Engineering, report, (2004), pp. 1-116.
17. L. Williams and W. Adams, Nanotechnology demystified, McGraw-Hill Comp., (2007), pp. 1-343.
18. J. K. Oh and J. M. Park, Iron oxide-based superparamagnetic polymeric nanomaterials: Design, preparation, and biomedical application, Prog. Polym. Sci., (2011), Vol. 36, pp. 168–189.
19. T. Masciangioli and W. Zhang, Environmental technologies at the nanoscale, Environ. Sci. Technol., (2003), Vol. 37, pp. 102A-108A.
20. M. Y. Ghotbi, Synthesis, modification and characterization of layered hydroxides and magnetite and their nanohybrids with D-gluconate and gallate anions, University Putra Malaysia, 2009.

21. M. H. B. Abdul Razak, Synthesis of organic-inorganic hybrid nanocomposite material 9-Hydroxy-9-fluorenecarboxylic acid intercalated into zinc-aluminum layered double hydroxide, Universiti Teknologi MARA, 2009.
22. E. Ruiz-hitzky and A. V. Meerbeek, Handbook of clay science, , Chapter 10.3, F. Bergaya, B.K.G. Theng, G. Lagaly (Editors), Elsevier, Dev. Clay Sci., (2006), Vol. 1, p. 584.
23. N. Hüsing and S. Hartmann, Hybrid nanocomposites for nanotechnology Electronic, Optical, Magnetic and Biomedical Applications, L. Merhari (Editor), Spring**Error! Hyperlink reference not valid.** p. 142.
24. E. Ruiz-Hitzky, Functionalizing inorganic solids: towards organic-inorganic nanostructured materials for intelligent and bio-inspired systems. Chem. Rec., (2003), Vol. 3, pp. 88–100.
25. A. D. Pomogailo and V. N. Kestelman, Metallopolymer nanocomposites, Springer, (2005), p. 3.
26. A. Vaccari, Preparation and catalytic properties of cationic and anionic clays, Catal. Today, (1998), Vol. 41, pp. 53-71.
27. M. Zammarano, S. Bellayer, J. W. Gilman, M. Franceschi, F. L. Beyer, R. H. Harris and S. Meriani, Delamination of organo-modified layered double hydroxides in polyamide 6 by melt processing, Polym., (2006), Vol. 47, pp. 652–662.
28. F. Cavani, F. Trifirb and A.Vaccari, Hydrotalcite-type anionic clays: preparation, properties and applications, Catal. Today, (1991), Vol. 11, pp. 173-301.
29. J. Choy, S. Choi, J. Oh and T. Park, Clay minerals and layered double hydroxides for novel biological applications, Appl. Clay Sci., (2007), Vol. 36, pp. 122–132.
30. M. I. Carretero, Clay minerals and their beneficial effects upon human health. A review, Appl. Clay Sci., (2002), Vol. 21, pp. 155–163.
31. J. Bouzaid and R. L. Frost, Thermal decomposition of stichite, J. Therm. Anal. Calorim. (2007), Vol. 89, pp. 133–135.

32. R. L. Frost, S. J. Palmer and L. M. Grand, Synthesis and thermal analysis of indium-based hydrotalcites of formula $Mg_6In_2(CO_3)(OH)_{16}.4H_2O$. J. Therm. Anal. Calorim., (2010), Vol. 101, pp. 859–863.
33. S. Gago, M. Pilinger, T. M. Santos and I. S. Goncalves, Zn-Al Layered double hydroxide pillared by different dicarboxylate anions, J. Ceram.-Silik., (2004), Vol. 4, pp. 155-158.
34. K. H. Bakon, S. J. Palme and R. L. Frost, Thermal analysis of synthetic reevesite and cobalt substituted reevesite $(Ni,Co)_6Fe_2(OH)_{16}(CO_3).4H_2O$, J. Therm. Anal. Calorim., (2010), Vol. 100, pp.125–131.
35. T. Lopez, E. Ramos, P. Bosch, M. Asomoza and R. Gomez, DTA and TGA characterization of sol-gel hydrotalcites, Mater. Lett., (1998), Vol. 30, pp. 279-282.
36. Z. Liu, R. Ma, M. Osada, N. Iye, Y. Ebina, K. Takada and T. Sasaki, Synthesis, anion exchange, and delamination of Co-Al layered double hydroxide: assembly of the exfoliated nanosheet/polyanion composite films and magneto-optical studies, J. Am. Chem. Soc., (2006), Vol. 128, pp. 4872-4880.
37. A. Violante, M. Pucci, V. Cozzolino, J. Zhua and M. Pigna, Sorption/desorption of arsenate on/from Mg–Al layered double hydroxides: influence of phosphate, J. Colloid Interface Sci., (2009), Vol. 333, pp. 63-70.
38. F. Costa, Mg-Al layered double hydroxide: a potential nanofiller and flame-retardant for polyethylene, Von der Fakult¨at Maschinenwesen der Technischen Universit¨at Dresden, (2007).
39. L. Hickey, J. T. Kloprogge and R. L. Frost, The effects of various hydrothermal treatments on magnesium-aluminium hydrotalcites, J. Mater. Sci., (2000), Vol. 35, pp. 4347-4355.
40. O. Altuntasoglu, Y. Matsuda, S. Ida and Y. Matsumoto, Syntheses of Zinc Oxide and Zinc Hydroxide Single Nanosheets, Chem. Mater., (2010), Vol. 22, pp. 3158-3164.

41. F. Geng, R. Ma and T. Sasaki, Anion-exchangeable layered materials based on rare-earth phosphors: unique combination of rare-earth host and exchangeable anions, Acc. Chem. Res., (2010), Vol. 43, pp. 1177-1185.
42. A. Bhattacharyya, D. B. Hall and T. J. Barnes, Novel oligovanadate-pillared hydrotalcites, Appl. Clay Sci., (1995), Vol. 10, pp. 57-67.
43. M. Baki, Molecular Simulation, Application, Synthesis and Characterization of Layered Double Hydroxide in search of anionic clays, University of Texas, 2008.
44. A. I. Khan and D. O'Hare, Intercalation chemistry of layered double hydroxides: recent developments and applications, J. Mater. Chem., (2002), Vol. 12, pp. 3191-3198.
45. X. Duan and D. G. Evans, Layered Double Hydroxides, Springer, (2005), p. 12.
46. K. Goh, T. Lim and Z. Dong, Application of layered double hydroxides for removal of oxyanions: A review, Water Res., (2008), Vol. 42, pp. 1343-1368.
47. R. L. Goswamee, P. Sengupta, K. G. Bhattacharyya and D. K. Dutta., Adsorption of Cr(VI) in layered double hydroxides, Appl. Clay Sci., (1998), Vol. 13, pp. 21-34.
48. Y. You, G. F. Vance and H. Zhao, Selenium adsorption on Mg–Al and Zn–Al layered double hydroxides, App. Clay Sci., (2001), Vol. 20, pp. 13-25.
49. M. del Arco, S. Gutierrez, C. Martin, V. Rives and J. Rocha, Effect of the Mg:Al ratio on borate(or silicate)/nitrate exchange in hydrotalcite. J. Sol. Stat. Chem., (2000), Vol. 151, pp. 272-280.
50. R. L. Frost and A. W. Musumeci, Nitrate adsorption through hydrotalcite reformation, J. Coll. Int. Sci., (2006), Vol. 302, pp. 203-206.
51. N. N. Das, J. Konar, M. K. Mohanta and S. C. Srivastava, Adsorption of Cr(VI) and Se(IV) from their aqueous solutions onto Zr^{4+}-substituted ZnAl/MgAl-layered double hydroxides: effect of Zr^{4+} substitution in the layer. J. Coll. Int. Sci., (2004), Vol. 270, pp. 1-8.
52. S. Wang, C. H. Liu, M. K. Wang, Y. H. Chuang and P. N. Chiang, Arsenate adsorption by Mg/Al–NO3layered double hydroxides with varying the Mg/Al ratio, App. Clay Sci., (2009), Vol. 43, pp. 79-85.

53. M. Islam and R. Patel, Nitrate sorption by thermally activated Mg/Al chloride hydrotalcite-like compound, J. Haza. Mat., (2009), Vol. 169, pp. 524-531.
54. M. Thyveetil, P. V. Coveney, H. C. Greenwell and J. L. Suter, Computer Simulation Study of the Structural Stability and Materials Properties of DNA-Intercalated Layered Double Hydroxides, J. Am. Chem. Soc., 2008, Vol. 130, pp. 4742–4756.
55. Z. P. Xu, T. L. Walker, K. Liu, H. M. Cooper,G. M. Lu and P. F. Bartlett, Layered double hydroxide nanoparticles as cellular delivery vectors of supercoiled plasmid DNA, Int. J. Nanomed.,(2007), Vol. 2, pp. 163–174.
56. J. Oh, S. Kwak and J. Choy, Intracrystalline structure of DNA molecules stabilized in the layered double hydroxide, J. Phys. Chem. Sol., (2006), Vol. 67, pp. 1028–1031.
57. S. P. Newman, T. D. Cristina and P. V. Coveney, Molecular dynamics simulation of cationic and anionic clays containing amino acids, Langmuir, (2002), Vol. 18, pp. 2933–2939.
58. T. Hibino, Delamination of layered double hydroxides containing amino acids, Chem. Mater., (2004), Vol. 16, pp. 5482–5488.
59. S. Aisawa, S. Takahashi, W. Ogasawara, Y. Umetsu and E. Narita, Direct intercalation of amino acids into layered double hydroxides by coprecipitation, J. Sol. Stat. Chem., (2001), Vol. 162, pp. 52-62.
60. H. Nakayama, N. Wada and M. Tsuhako, Intercalation of amino acids and peptides into Mg–Al layered double hydroxide by reconstruction method, Int. J. Pharm., (2004), Vol. 269, pp. 469–478.
61. S. Aisawa, N. Higashiyama, S. Takahashi, H. Hirahara, D. Ikematsu, H. Kondo, H. Nakayama and E. Narita, Intercalation behavior of L-ascorbic acid into layered double hydroxides, Appl. Clay Sci., (2007), Vol. 35, pp. 146-154.
62. M. S. Gasser, Inorganic layered double hydroxides as ascorbic acid (vitamin c) delivery system-Intercalation and their controlled release properties, Colloids Surf., B, (2009), Vol. 73, pp. 103-109.

63. N. Das and R. Das, Insertion of chromium(III) ascorbate complex into layered double hydroxide through reduction of intercalated chromate by ascorbic acid, Appl. Clay Sci., (2008), Vol. 42, pp. 90-94.
64. C. Bolognesi, Genotoxicity of pesticides: a review of human biomonitoring studies, Mutation Research, (2003), Vol. 543, pp. 251-272.
65. J. Gong, L. Wang, D. Song, X. Zhu and L. Zhang, Stripping voltammetric analysis of organophosphate pesticides using Ni/Al layered double hydroxides as solid-phase extraction, Biosens. Bioelectron., (2009), Vol. 25, pp. 493-496.
66. M. Z. Hussein, A. M. Jaafar, A.H. Yahaya and Z. Zainal, The effect of single, binary and ternaryanions of chloride, carbonate and phosphate on the release of 2,4-Dichlorophenoxyacetate intercalation into the Zn-Al-layered double hydroxide nanohybride, Nanosc. Res. Lett., (2009), Vol. 4, pp. 1351-1357.
67. J. Gong, L. Wang, X. Miao, L. Zhang, Efficient stripping voltammetric detection of organophosphate pesticides using NanoPt intercalated Ni/Al layered double hydroxides as solid-phase extraction, Electrochem. Commun., (2010), Vol. 12, pp. 1658–1661.
68. D. Chaara, I. Pavlovic, F. Bruna, M. A. Ulibarri, K. Draoui and C. Barriga, Removal of nitrophenol pesticides from aqueous solutions by layered double hydroxides and their calcined products, App. Clay Sci., (2010), Vol. 50, pp. 292–298.
69. M. Z. Hussein, Z. Zainal, A. H. Yahaya and D. W. V. Foo, Controlled release of a plant growth regulator, a-naphthaleneacetate from the lamella of Zn–Al-layered double hydroxide nanocomposite, J. Controlled Release, (2002), Vol. 82, pp.417–427.
70. J. Wang, Q. Liu, G. Zhang, Z. Li, P. Yang, X. Jing, M. Zhang, T. Liu and Z. Jiang, Synthesis, sustained release properties of magnetically functionalized organic-inorganic materials: Amoxicillin anions intercalated magnetic layered double hydroxides via calcined precursors at room temperature, J. Sol. State Sci., (2009), Vol. 11, pp. 1597-1601.

71. L. Qin, S. Wang, R. Zhang, R. Zhu, X. Sun and S. Yao, Two different approaches to synthesizing Mg–Al-layered double hydroxides as folic acid carriers, J. Phys. Chem. Sol., (2008), Vol. 69, pp. 2779–2784.
72. H. Rachmawati, D. H. Rasaputri and S. Tarini, Preparation and characterization of folic acid-encapsulated solid lipid nanoparticle, J. Nanosain. Nanotek., (2010), Vol. 3, pp.37-40.
73. Z. Zhu, L. Qu, Y. Guo, Y. Zeng, W. Sun and X. Huang, Electrochemical detection of dopamine on a Ni/Al layered double hydroxide modified carbon ionic liquid electrode , Sens. Actuators, B, (2010), Vol. 151, pp. 146-152.
74. L. Jiang, L. Gao and Y. Liu, Adsorption of salicylic acid, 5-sulfosalicylic acid and tiron at the alumina-water interface, Colloids Surf., A, (2002), Vol. 211, pp. 165-172.
75. J. Choy, J. Jung, J. Oh, M. Park, J. Jeong, Y. Kang and O. Han, Layered double hydroxide as an efficient drug reservoir for folate derivatives, Biomater., (2004), Vol.25, pp. 3059-3064.
76. R. Xiao, W. Wang, L. Pan, R. Zhu, Y. Yu, H. Li, H. Liu and S. Wang, A sustained folic acid release system based on ternary magnesium/zinc/aluminum layered double hydroxides, J. Mater. Sci., (2011), Vol. 46, pp. 2635-2643.
77. M. R. Wright, An introduction to chemical kinetics, John Wiley and Sons, Ltd., England, (2004), p. 2.
78. E. T. Denisov, O. M. Sarkisov and G. I. Likhtenshtein, Chemical kinetics Fundamentals and new developments, Elsevier, (2003), p. 1-3.
79. L. Arnaut, S. Formosinho and H. Burrows, Chemical kinetics, from molecular structure to chemical reactivity, Elsevier, (2006), p. xvii, xviii.
80. D. L. Sparks, New frontiers in elucidating the kinetics and mechanisms of metal and oxyanion sorptionat the soil mineral/water interface, J. Plant Nutr. Soil Sci., (2000), Vol. 163, pp. 563-570.
81. H. Zhang, K. Zou, S. Guo and X. Duan, Nanostructural drug-inorganic clay composites: Structure, thermal property and in vitro release of captopril-intercalated

Mg–Al-layered double hydroxides," J. Solid State Chem., (2006), Vol. 179, pp. 1792–1801.

82. D. Pan, H. Zhang, T. Zhang and X. Duan, A novel organic–inorganic microhybrids containing anticancer agent doxifluridine and layered double hydroxides: Structure and controlled release properties, Chem. Eng. Sci., (2010), Vol. 65, pp. 3762-3771.
83. Y. N. Abd AL-Ameer, Synthesis and characterization of nano hybrid compounds orgnanic-inorganic and kinetic controlled release study of 2,4-Dicloro and 4-Chloro phenoxy acetate from Zinc/Aluminum layered double hydroxide by direct ion exchange method, M.Sc. Thesis, University of Karbala, (2011).
84. R. Bhaskar, R. S. R. Murthy, B. D. Miglani and K. Viswanathan, "Novel method to evaluate diffusion controlled release of drug from resinate," Int. J. Pharm., (1986), Vol. 28, pp. 59-66.
85. S. Agatonovic-Kustrin and R. Beresford, Basic concepts of artificial neural network (ANN) modeling and its application in pharmaceutical research, Review, J. Pharm. Biomed. Anal., (2000), Vol. 22, pp. 717-727.
86. M. G. Moghaddam, F. H. Ahmad, M. Basri and M. B. Abdul Rahman, Artificial neural network modeling studies to predict the yield of enzymatic synthesis of betulinic acid ester, Electron. J. Biotechnol., (2010), Vol. 13, pp. 1-12.
87. P. J. Lisboa and A. F. G. Taktak, The use of artificial neural networks in decision support in cancer: A systematic review, Neural Networks, (2006), Vol. 19, pp. 408-415.
88. S. Mandal, P. V. Sivaprasad, S. Venugopal and K. P. N. Murthy, Artificial neural network modeling to evaluate and predict the deformation behavior of stainless steel type AISI 304L during hot torsion, Appl. Soft Comput., (2009), Vol. 9, pp. 237-244.
89. Y. Chena, T. W. McCall, A. R. Baichwal and M. C. Meyer, The application of an artificial neural network and pharmacokinetic simulations in the design of controlled-release dosage forms, J. Controlled Release, (1999), Vol. 59, pp. 33-41.

90. C. Modrogan, E. Diacon, O. D. Orbulet and A. R. Miron, Forecasting study for nitrate ion removal using reactive barriers, REV. CHIM. (Bucharest), (2010), Vol. 61, pp. 580-584.
91. H. R. F. Masoumi, A. Kassim, M. Basri, D. K. Abdullah and M. J. Haron, Multivariate optimization in the biosynthesis of a triethanolamine (TEA)-based esterquat cationic surfactant using an artificial neural network, Mol. (2011), Vol. 16, pp. 5538-5549.

الخلاصة

يعتبر حامض الفوليك من المركبات ذات الاهمية الكبيرة والضرورية لجسم الانسان , ونظراً لكونه غير مستقر ويحتوي على الكثير من المساوئ مثل الذوبانية القليلة في الماء وكذلك الزيادة او النقص منه يسبب اثار سلبية على الجسم لذلك ولغرض الحد من هذه المساوئ وجدت هذه الدراسة والتي تضمنت تحضير مجموعة من مركبات النيكل/المنيوم-حامض الفوليك النانوية الهجينة وبنسب مولية مختلفة (R=3, 4, 5 and 6) باستخدام الطريقة المباشرة وغير المباشرة باستخدام المعالجة الحرارية وبثلاث درجات حرارية مختلفة.

بينت دراسات حيود الاشعة السينية (XRD) بان افضل درجة حرارية لتحضير هذه المركبات عند 180°C لظهور قمة ذات شدة عالية والتي تشير الى ان البلورة اكثر انتظاماً. اضافة الى ذلك, بينت اطياف حيود الاشعة السينية اقحام حامض الفوليك بين طبقات النيكل/المنيوم بنجاح من خلال المقارنة بين قيم سمك الطبقة بعد وقبل الاقحام. كذلك تم تشخيص المركبات النانوية الهجينة باستخدام اطياف الاشعة تحت الحمراء (FTIR).

اضافة الى ذلك, تم دراسة حركيات التحرر لحامض الفوليك الى اوساط مائية مختلفة مثل الكربونات , الفوسفات والكبريتات وبتراكيز مختلفة باستخدام معادلات الرتبة الصفرية, الاولى والثانية الكاذبة بالاضافة الى استخدام معادلة Bhaskar والتي تمثل انتشار الحامض من بين التجمعات الجزيئية وقد بينت هذه الدراسة بأن حركية التحرر تخضع للرتبة الثانية الكاذبة.

اضافة الى ذلك, في هذه الدراسة تم ابتكار معادلات لتحليل انتشار الجزيئات او الايونات من بين تجمعات المركبات النانوية الهجينة ودراسة حركيات انتشار حامض الفوليك من بين هذه التجمعات خلال اوساط مائية مختلفة مثل الكربونات والفوسفات والكبريتات وبتراكيز مختلفة.

بينت هذه الدراسة ان المعادلات المبتكرة هي الاكثر ملائمة لتحليل انتشار الجزيئات او الايونات من بين التجمعات الجزيئية للمركبات النانوية الهجينة مقارنة بمثيلاتها من المعادلات المستخدمة سابقاً.

في هذه الدراسة تم استخدام الشبكات العصبية الصناعية (Artificial Neural Network (ANN)) والتي تعتمد على فكرة الذكاء الاصطناعي باستخدام برنامج حاسوبي Alyuda Neuro Intelligence لغرض تخمين تراكيز حامض الفوليك المتحرر مع الزمن باستخدام خوارزمية الانتشار السريع , وجد بان هذه الطريقة هي الاكثر دقة لحساب تراكيز حامض الفوليك.

جمهورية العراق
وزارة التعليم العالي والبحث العلمي
جامعة كربلاء/كلية العلوم
قسم الكيمياء

تحضير وتشخيص مركبات النيكل/المنيوم النانويةالهجينةمع حامض الفوليك واقتراح معادلات لتحليل انتشار الحامض بين التجمعات الجزيئية

رسالة مقدمة إلى
مجلس كلية العلوم-جامعة كربلاء
وهي جزء من متطلبات نيل درجة الماجستير في الكيمياء

من قبل
محمد عدنان مزعل
بكالوريوس علوم كيمياء (٢٠٠٩) جامعة كربلاء

بإشراف

أ.د. صالح مهدي حداوي أ.م. د. عباس مطرود باشي

1433 هـ *2012* م